AD-A033 580 COAST GUARD RESEARCH AND DEVELOPMENT CENTER GROTON CONN F/G 8/3
MOVEMENT OF SPILLED OIL OVER THE BEAUFORT SEA SHELF - A FORECAS--ETC(U)
JUN 76 G L HUFFORD, I M LISSAUER, J P WELSH

UNCLASSIFIED CGR/DC-12/76 USCG-D-101-76 NL

| OF |
AD A033580

END

DATE FILMED
2-77

Report No. CG-D-101-76
Task No. 764244

1 14 B.S.

MOVEMENT OF SPILLED OIL OVER THE BEAUFORT SEA SHELF - A FORECAST

G.L. Hufford
I.M. Lissauer
J.P. Welsh

U.S. Coast Guard Research and Development Center
Avery Point, Groton, CT 06340

June 1976

Final Report

Prepared for

U.S. DEPARTMENT OF TRANSPORTATION
UNITED STATES COAST GUARD
Office of Research and Development
Washington, D.C. 20590

U.S. DEPARTMENT OF INTERIOR
BUREAU OF LAND MANAGEMENT
Office of Environmental Studies
Washington, D.C. 20242

NOTICE

This document is disseminated under the sponsorship of the Department of Transportation in the interest of information exchange. The United States Government assumes no liability for its contents or use thereof.

The contents of this report reflect the views of the U.S. Coast Guard Research and Development Center, which is responsible for the facts and accuracy of data presented. This report does not constitute a standard, specification or regulation.

Technical Report Documentation Page

1. Report No.	2. Government Accession No.	3. Recipient's Catalog No.
US CG-D-101-76		

4. Title and Subtitle	5. Report Date
MOVEMENT OF SPILLED OIL OVER THE BEAUFORT SEA SHELF - A FORECAST.	June 1976
	6. Performing Organization Code

7. Author(s)	8. Performing Organization Report No.
G.L. HUFFORD, I.M. LISSAUER and J.P. WELSH	CGR/DC-12/76

9. Performing Organization Name and Address	10. Work Unit No. (TRAIS)
US Coast Guard Research and Development Center Avery Point Groton, CT 06340 (12) 90p.	764244
	11. Contract or Grant No. RD0002-R7120815 2517

12. Sponsoring Agency Name and Address	13. Type of Report and Period Covered
Department of Interior Bureau of Land Management Office of Environmental Studies Washington, DC 20242	Final Report.
	14. Sponsoring Agency Code

15. Supplementary Notes

This study was prepared for both the US Coast Guard Office of Research and Development and The Dept. of Interior Bureau of Land Management to assist both agencies. Funding for the study was made available by the Bureau of Land Management.

16. Abstract

Projections of the movement of oil slicks and their impact location along the north Alaskan coast are determined from fifteen potential oil drilling sites. Two approaches are implemented to determine impact locations. The first is a description of the environment with emphasis on the meteorology and water movement in the area. The second considers the interactions of the environmental processes in forecasting the potential paths of spilled oil and their impact location on the shoreline.

17. Key Words	18. Distribution Statement
Oil spill movement Impact assessment Environmental studies Alaska	Document is available to the public thru the National Technical Information Service, Springfield, VA 22161

19. Security Classif. (of this report)	20. Security Classif. (of this page)	21. No. of Pages	22. Price
Unclassified	Unclassified	87	

Form DOT F 1700.7 (8-72) Reproduction of completed page authorized

408730 AB

TABLE OF CONTENTS

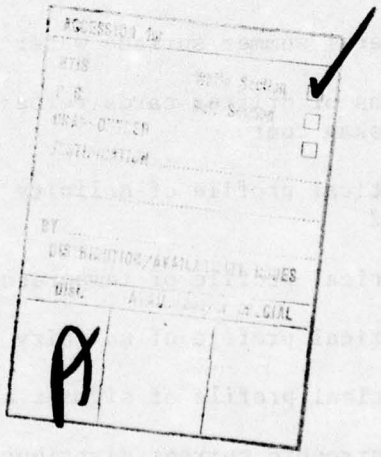

LIST OF ILLUSTRATIONS

LIST OF ILLUSTRATIONS (cont.)

LIST OF ILLUSTRATIONS (cont.)

LIST OF ILLUSTRATIONS (cont.)

LIST OF TABLES

1.0 SUMMARY

1.1 Purpose and Scope

Offshore oil drilling along the north Alaskan coast is certain to be undertaken within the next few years. To understand the ecological and economic implications of an oil spill from offshore, projections of the movement of oil slicks and their impact location along the shoreline must be determined.

The trajectory of spilled oil over a continental shelf depends primarily on the temporal and spatial variability of three factors: the thermohaline structure of the waters, the circulation of the waters, and the winds. Existing data about the three factors is analyzed for summer conditions (ice is ignored) along the Alaskan north coast. The environmental data along with a storm model is used to predict the paths of oil slicks from fifteen potential sites.

1.2 Conclusions

The greatest danger of an oil spill impacting the shoreline occurs when the wind direction varies between east and northeast. These wind directions are the dominant winds along the coast over the entire summer.

An equation, $y = -6.54 + 4.81x - 0.10x^2$ (where x is distance offshore and y is impact time), has been developed to predict the minimum impact time on the shore for an oil spill originating along the Beaufort Sea coast. Using the equation, minimum impact time for an oil spill occurring 1 nm off the coastline is 3.5 hours; minimum impact time for an oil spill occurring 20 nm off the coastline is about 60 hours.

Fifteen potential oil spill sites were chosen to develop graphs of impact probability versus distance offshore. The graphs are very useful as a management tool for predicting probability of oil spill impact on shore for the potential offshore spill sites.

A "typical" low pressure storm moving along the primary storm track will cause an oil spill 5 nm offshore to impact the coastline in less than 8 hours.

1.3 Recommendations

Wind and current data along the Beaufort Sea coast are sparse. In order to offset the uncertainties due to these factors, the oil spill trajectories were enveloped rather than given a single path for each spill.

The study results should be treated as a preliminary cut and best estimate based on limited data. The probabilities should be treated simply as tools used by management in assessing the environmental risk of a spill at different locations along the coast.

An ambitious research program is being conducted along the north Alaskan coast as part of the BLM/NOAA Outer Continental Shelf Environmental Assessment. These data as they become available will be used to refine, modify and hopefully verify the oil spill model.

2.0 INTRODUCTION

The discovery of oil reserves along the Beaufort Sea coast has brought development and exploitation onshore, with offshore drilling on the continental shelf certain to be undertaken within the next few years. Because even the best of planning and the most modern of safety techniques cannot insure that accidental oil spills will not occur, there is a definite need for an oil spill drift forecasting model for the Beaufort Sea shelf waters.

The path of spilled oil over a continental shelf depends primarily on the temporal and spatial variability of three factors: the thermohaline structure of the water, the circulation of the water, and the winds. This study considers the existing data in relation to these three factors along the Beaufort Sea coast and incorporates the data into a risk analysis model. The model is appropriate for summer coastal conditions when the area is essentially ice free. Future work will consider the effect of isolated ice fragments and the presence of an ice edge within the area.

3.0 DESCRIPTION OF STUDY AREA

Oceanographically, the Beaufort Sea is an integral part of the Arctic Ocean (Coachman and Barnes, 1961, and Coachman, 1963). The area of specific interest in this report is bounded by Point Barrow (156°30'W) to the west, Demarcation Point (141°10'W) to the east, and the shelf break to the north (Figure 1).

The bathymetry of the Beaufort Sea continental shelf has been discussed by Carsola (1954) and Carsola, et. al (1961). The shelf is very shallow with a well-defined shelf break at about 65 m depth. The width of the shelf is variable, ranging from 55 km at Demarcation Point to 110 km at Cape Halkett (153°W) and 20 km at Point Barrow. The shelf is essentially flat except for a very few topographic highs believed to be extensions of the low barrier islands that exist along the coast (Reimnitz, et. al, 1972).

3.1 Thermohaline Structure

Numerous hydrographic measurements have been taken on the Beaufort Sea continental shelf since 1950. The majority of these observations were taken between late July and the end of September (Table 1), i.e., the ice-free season. The observations were scattered, making temporal and spatial interpretation of the data difficult. The scatter is caused by two factors. The first factor is the heavy polar pack which is never far from the coast in the summer and can advance onto the shore at any time. The location of many offshore observations usually reflect this limitation due to the ice cover. Second, because of the draft of the icebreakers from which most data have been obtained, few measurements have been taken shoreward of the 20 m depth contour.

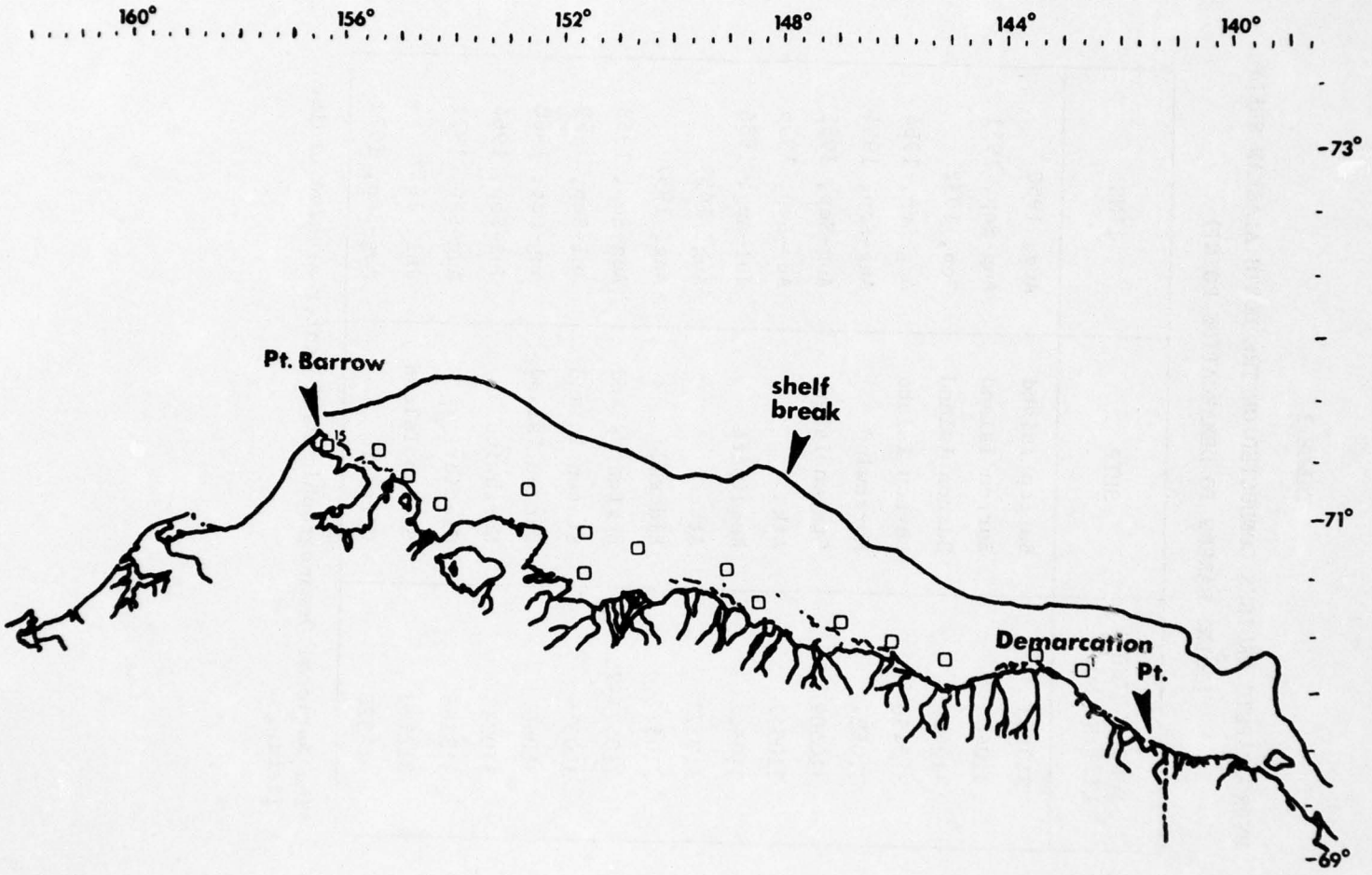

Figure 1. Location of study area along north Alaskan coast.

TABLE 1

HYDROGRAPHIC CRUISES CONDUCTED ON THE NORTH ALASKAN SHELF

(POINT BARROW TO DEMARCATION POINT)

NODC CRUISE LISTING NO.*	SHIP	TIME
310153	Burton Island	Aug, 1950
310400	Burton Island	Aug-Sep, 1951
310400	Burton Island	Sep, 1952
310456	Burton Island	Aug-Sep, 1954
310457	Northwind	Aug-Sep, 1954
310509	Staten Island	Aug-Sep, 1955
310547	Atka	Aug-Sep, 1956
310548	Requisite	Jul-Aug, 1956
310571	Atka	Aug, 1957
310572	Eldorado	Aug, 1957
310574-75	Burton Island	Aug-Sep, 1958
310636	Staten Island	Jul-Sep, 1959
310667	Burton Island	Aug-Oct, 1960
310238	Northwind	Jul-Sep, 1964
318286	Glacier	Aug-Sep, 1971
312183	Staten Island	Jul, 1972
318328	Glacier	Aug-Sep, 1972

*The National Oceanographic Data Center archive cruise listings.

There are four summers (1950, 1951, 1971, and 1972) where the temporal and spatial distribution of hydrographic measurements on the shelf are sufficient to permit detailed analysis. Data from the 1950-51 cruises are discussed by the U. S. Navy Hydrographic Office (1954). The 1971-72 data is discussed by Hufford, et. al (1974). Results from these four summers show that the shelf water has wide variations in temperature and salinity.

The extreme variability observed in the summer surface water temperatures (-1.4 to 6.0°C) and salinities (3 to 30 o/oo) is the result of the interaction of solar radiation, irregularity of ice cover, ice melt, freshening and warming by local runoff, and wind-induced water movement (mixing). Generally, the very low surface temperatures (< 0°C) are found offshore near the pack ice edge. All the low temperatures observed at or near the surface during the four summers were at least 0.2°C above the water's freezing point. Sea surface temperatures in the open water areas are more dependent on direct heating from the sun, river runoff, and advection. West of 150°W a large body of relatively warm water (0 to 7°C) is often found on the shelf from the surface to the bottom (Figure 2, map view; Figure 3, profile) (Hufford, 1973). Cursory analysis of past data from Table 1 indicates that the warm water layer was present during the summer in 10 of 16 years. This warm body of water extends from the 25 m isobath northward to at least 71°41'N. The core of the layer parallels the continental shelf edge. The eastward extension of the warm layer along the shelf appears to vary from year to year. The salinity of the warm layer (28.0 to 31.9 o/oo) does not differ from adjacent waters. Hufford (1973) suggests that the origin of the warm water is the Bering Sea.

Volume transport estimates of the warm intrusion on the shelf can be made using data from a line of hydrographic stations along 148°30'W during 1971 and 1972. The eastward transport of water with temperatures greater than 0°C is estimated to be 0.9 Sv in 1971 and 1.0 Sv in 1972 (one Sv is equal to 1×10^6 m^3 sec^{-1}). An eastward velocity of 40 cm sec^{-1} was used in the calculation. These estimates of transport are about 66 percent of the volume of the water that flows through the Bering Strait to the north (Coachman, et. al, 1975). This suggests that the majority of the warm water flowing northward through the Chukchi Sea toward the Arctic Ocean turns eastward along the Alaskan shelf. The effect of this warm layer on the Beaufort Sea shelf region will be discussed in detail in the section on circulation.

Salinity of the surface water on the outer shelf is influenced by the proximity and concentration of ice and ice melt. Salinity values between 4 o/oo and 20 o/oo are found in areas of heavy ice (6 to 8 oktas) while areas with ice concentrations of less than 3 oktas usually are associated with surface salinities of 20 o/oo to 26 o/oo.

River runoff in the summer near the coast decreases surface salinities to as low as 3 o/oo and adds heat that is important in reducing nearshore ice cover. The majority of freshwater flow occurs in late May

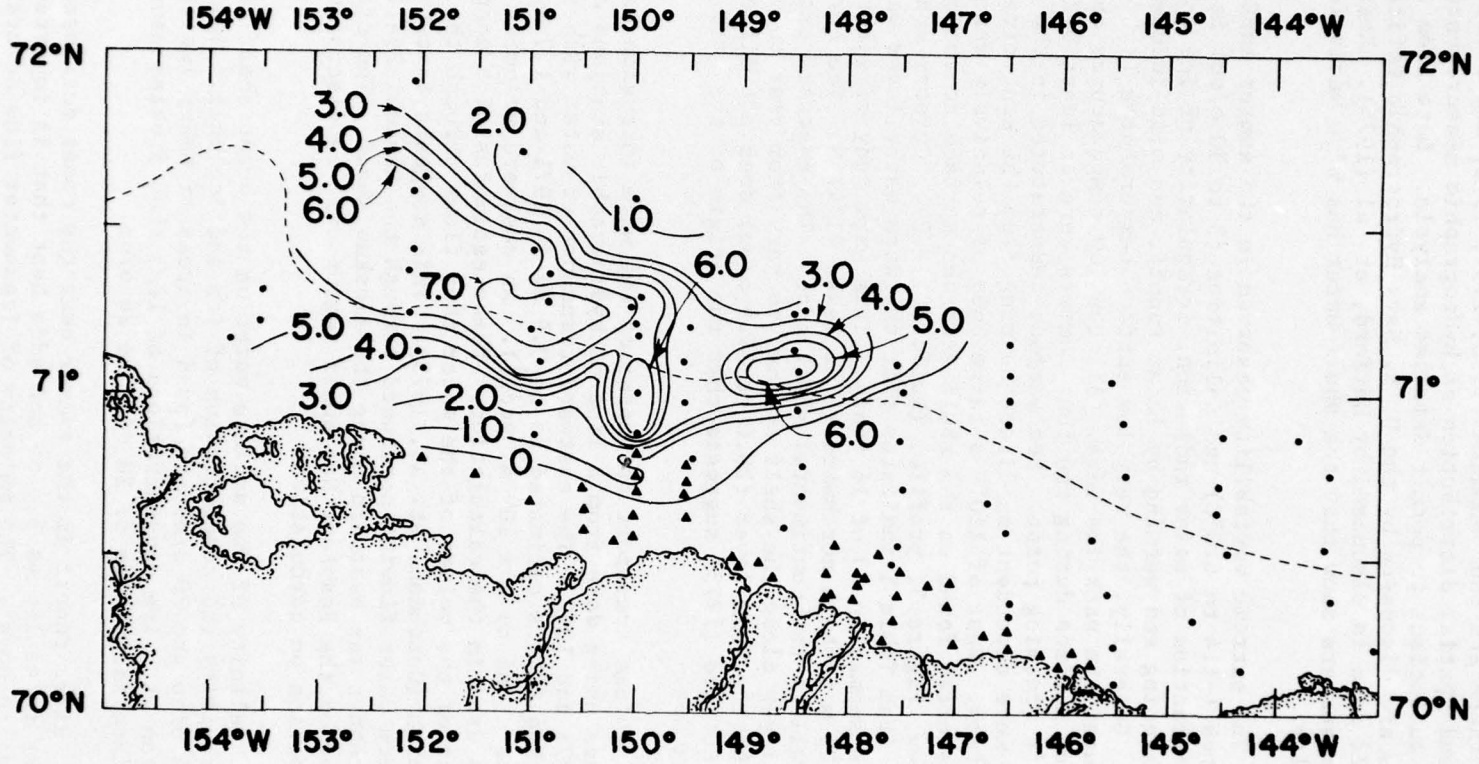

Figure 2. Horizontal distribution of maximum core temperature (°C) of Bering Sea water on the north Alaskan shelf.

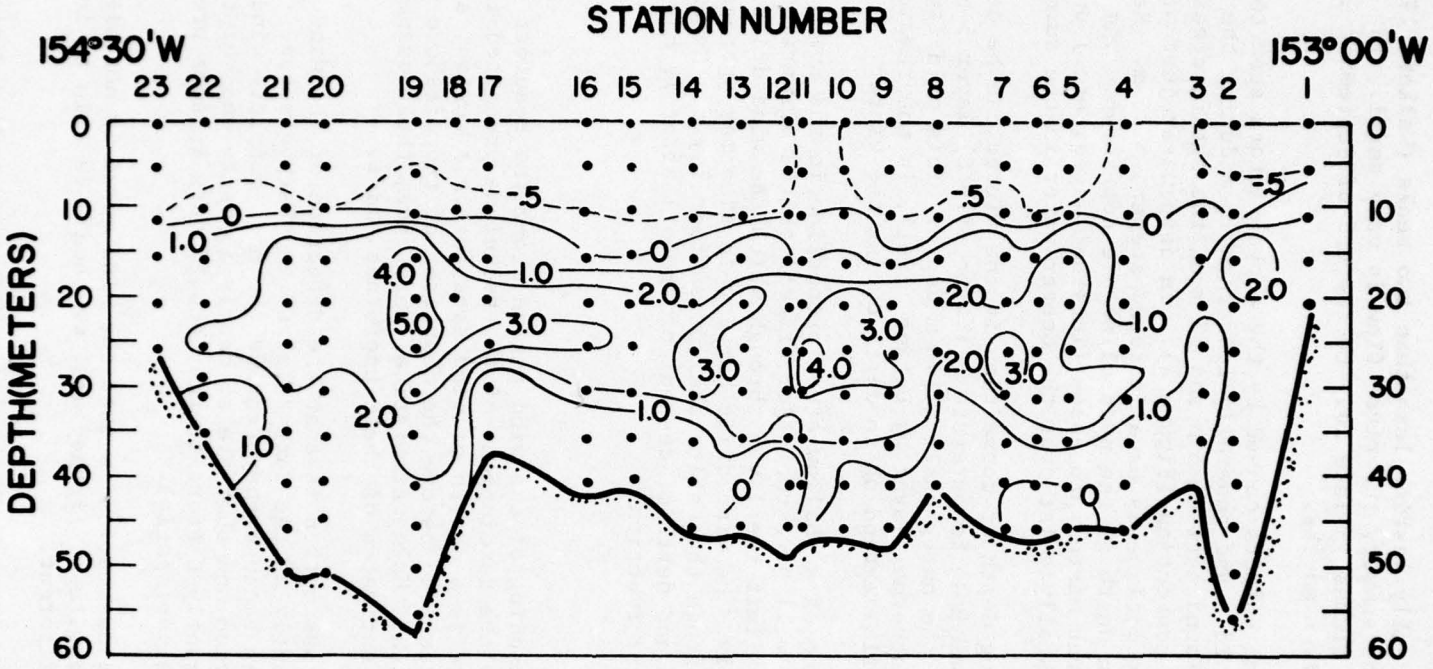

Figure 3. Vertical profile of temperature (°C) along an XBT (expendable bathythermograph) section form 153°00'W to 154°30"W, September 1971.

with intense flow normally lasting less than two weeks (Walker, 1974). During the rest of the summer, the river flow is very small. The extent of most of the river plumes in late July to the end of September is less than 5 km from the river mouths.

The vertical effects caused by the above factors seem to be limited to the upper 25 m and generally less than 15 m during the summer. A pycnocline can be found between 5 m and 15 m on the shelf, creating a dynamic barrier to convection (Figure 4). In deep water just off the shelf (> 60 m) the pycnocline is usually found deeper, $\sim$ 25 m. Reasons for the difference in depth of the pycnocline are not known. The difference may be due to different mixing processes (internal waves, etc.) under the ice cover that usually exist over the deeper water in the summer.

The limiting depth of convection in the winter can be determined by observation of a minimum temperature (-1.4 to -1.6°C) layer 5 m thick which is centered on the outer shelf at 40 m depth. This cold layer, referred to as a dicothermal layer by Defant (1961), is the remainder of the convectional flux extending to depth during the winter.

The presence of a shallow steep pycnocline in the north Alaskan coastal water column will have two major effects on the dispersion of oil. First, it will limit the layer through which the wind drift current can act. Consequently, the wind drift current in time may approach a constant velocity through the entire shallow surface layer. Second, it will affect the rate and depth of descent of the oil after it has lost its volatile and light fractions.

3.2 Winds

An understanding of the wind regime along the Beaufort coast is very important to the development of the technique presented in this paper. Because there is a dearth of wind data for this region, a number of assumptions are required before the character of the offshore wind field can be predicted. Using statistical inference, these assumptions can be examined and estimates of their usefulness made.

The first assumption is that the direction of the wind does not differ significantly at the Barter Island and Barrow sites. These two sites were chosen because they provide the most complete wind records available in the region and they are at nearly opposite ends of the coast. If they are significantly different, they should vary in some predictable way, either temporal or spatial.

The second assumption is that the wind speed is not significantly different at the two sites. If they are, we should be able to infer the way that they are different.

The third assumption is that if wind speed and/or direction do differ for the two sites then we can objectively determine how they differ and use the information as a basis for predicting the general wind field offshore along the Beaufort Sea coast.

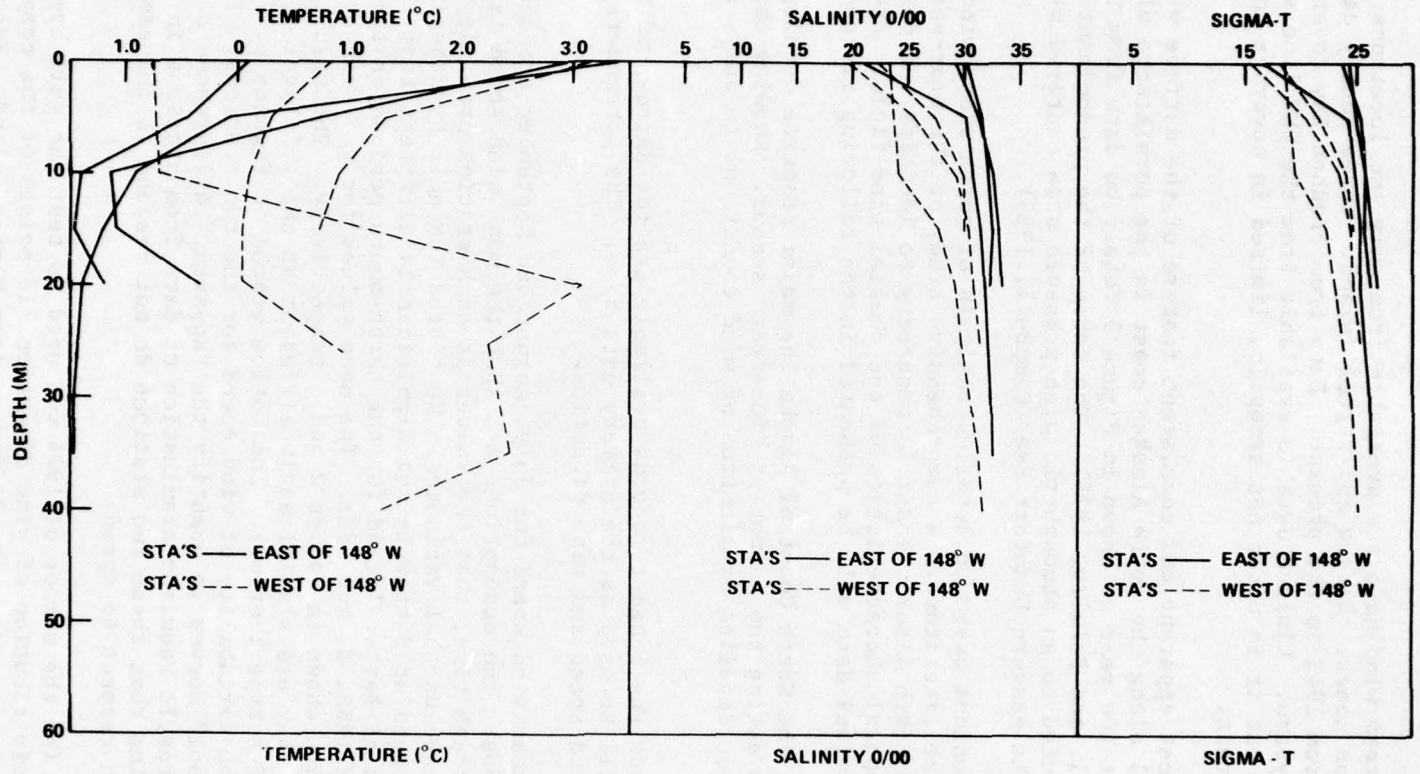

Figure 4. Vertical distribution of temperature (°C), salinity (o/oo) and sigma-t at select stations from 1971-72 Beaufort Sea cruises.

Long-term wind data are available from only two locations along the north Alaskan coast: Barrow and Barter Island. Three hourly data are available from 1942 to the present. Data from Prudhoe Bay cover only the last eight years. Limited data is available from the DEW line sites along the coast but it is often not synoptic, limited in coverage and difficult to obtain.

The most apparent and consistent feature of the surface winds (10 m elevation) along the north Alaskan coast is the persistence of easterly winds throughout the year as shown in Figure 5 (based on data from Searby and Hunter, 1971, and Belello, 1973). The cause of the predominant easterly winds is attributed to an atmospheric high pressure area centered over the Arctic in the eastern Beaufort Sea (Campbell, 1965).

Conclusions based on detailed analysis of north slope winds are sparse in the literature. A comprehensive study of the near-surface winds along the north Alaskan coast is necessary to identify and describe spatial and temporal characteristics of the coastal wind field. Preliminary analysis of previous data will be presented in the following discussion.

Along the North Coast of Alaska the major resource development activity occurs during the summer or "ice-free" season. Knowing this, we restricted our detailed examination of wind conditions to July, August and September.

Because the longest records available are for Barrow and Barter Island, they will be used as the primary data base. The parameters of interest are wind speed and wind direction.

The mean wind speed for July, August and September are compared for both stations. The assumptions are that the mean wind speed is normally distributed through time, that the values at each station are independent and that they have unequal variances. We tested the null hypothesis that the mean wind speed at Barrow is not significantly different from the mean wind speed at Barter Island for the three-month period for the dominant wind directions (ENE, E, and ESE). The mean values for the year by month and direction are shown in Tables 2 and 3 respectively. The results of the test are: they are significantly different at the .05 level of α (probability of a type I error). The bottom graphs on Figures 6, 7 and 8 illustrate the variability of wind speed for the two stations. The statistical "tool" serves to quantify the "apparent" differences on the graphs. This result requires examination of data from stations in between and by suggesting that these two stations do not respond to the same general wind field with respect to speed.

Data for the summer of 1974 was used to test the null hypothesis; the frequency distribution of wind direction (16 points of the compass) for Barrow is not significantly different from Barter Island. Examination of the top graphs on Figures 7 and 8 suggest that there may be significant differences. Using a goodness of fit technique, the two distributions were compared to test the null hypothesis. The result: the two frequency distributions are significantly different at the .05 level of α.

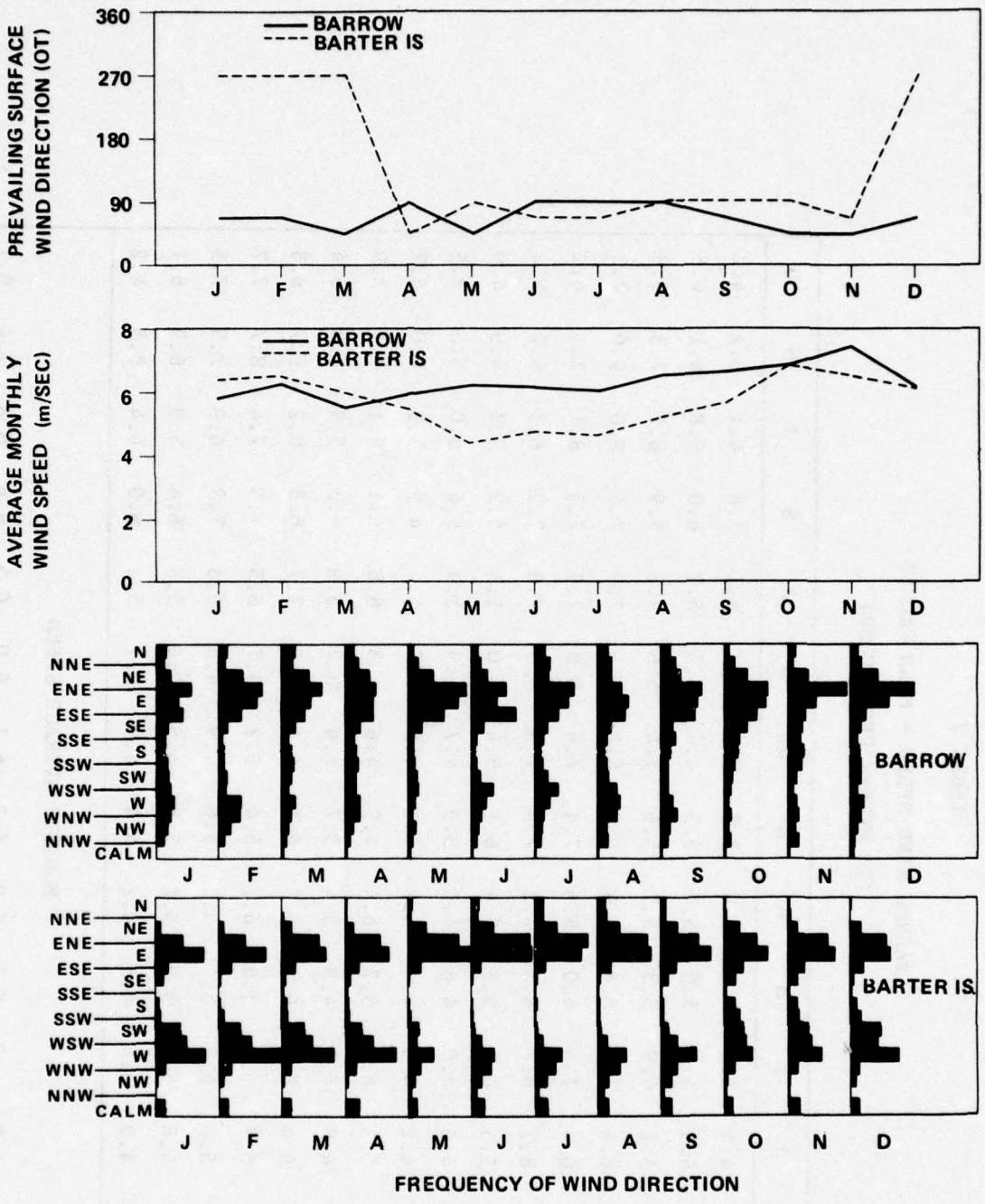

Figure 5. Characteristics of the wind at Barrow and Barter Island, Alaska.

TABLE 2

BARROW WIND SPEED - MEAN VALUES

(IN METERS PER SECOND)

	J	F	M	A	M	J	J	A	S	O	N	D
N	4.4	3.8	4.6	4.6	3.7	3.8	3.7	4.1	5.6	6.1	6.1	4.2
NNE	4.3	4.1	5.8	5.4	5.3	4.4	4.4	5.3	6.0	6.8	6.1	4.8
NE	5.1	4.9	5.3	5.2	5.6	5.4	5.6	5.3	5.9	6.7	7.3	5.8
ENE	6.4	7.2	6.4	6.4	6.8	6.8	7.4	7.9	7.4	8.0	9.0	7.3
E	6.4	7.5	6.0	6.6	7.4	7.6	6.8	7.9	7.5	8.1	7.5	6.2
ESE	8.1	6.7	6.4	7.2	7.0	7.3	6.9	7.0	7.2	6.3	6.2	5.4
SE	5.5	4.2	5.3	5.4	6.1	5.4	6.0	5.4	5.2	5.2	4.9	4.0
SSE	4.5	4.0	4.6	4.9	3.9	4.7	5.9	5.3	5.6	5.0	5.6	3.5
S	4.2	4.5	4.4	5.2	4.1	4.6	5.7	5.2	4.9	5.9	6.0	4.2
SSW	5.3	6.2	5.2	6.4	4.9	4.6	6.3	6.8	6.1	6.1	7.5	5.9
SW	4.8	6.1	4.8	5.4	5.7	5.4	6.2	5.9	6.3	5.9	7.8	5.4
WSW	6.4	8.1	6.5	6.5	6.1	6.4	6.5	7.7	6.6	8.2	9.7	6.3
W	6.9	6.7	5.6	6.1	5.4	5.2	5.7	6.5	7.5	7.4	8.7	7.7
WNW	5.6	6.4	5.4	6.5	5.6	4.9	4.6	6.3	7.8	6.9	7.3	7.5
NW	4.8	5.5	3.9	5.2	3.8	4.5	4.4	5.8	6.4	5.9	6.9	6.1
NNW	4.9	4.6	4.3	4.2	4.4	4.3	4.1	5.4	6.0	6.4	6.5	4.2
MONTHLY AVERAGE SPEED												
	5.8	6.2	5.5	5.9	6.2	6.1	6.0	6.5	6.6	6.8	7.4	6.1

TABLE 3

BARTER ISLAND WIND SPEED - MEAN VALUES

(IN METERS PER SECOND)

	J	F	M	A	M	J	J	A	S	O	N	D
N	2.7	2.9	2.2	2.4	2.4	2.3	2.5	2.6	3.2	3.8	2.6	2.5
NNE	3.0	2.5	2.9	2.9	2.6	2.7	2.7	2.9	3.2	4.2	3.2	2.9
NE	3.8	3.9	3.9	4.2	4.1	3.4	4.0	4.2	4.9	7.4	5.9	4.2
ENE	6.4	6.0	7.1	6.3	5.8	5.7	5.4	6.4	6.6	9.0	7.7	6.6
E	6.9	6.6	6.8	6.5	7.0	6.2	5.7	7.0	7.1	10.0	8.7	7.7
ESE	4.5	5.1	5.0	4.9	5.2	5.2	4.7	4.8	5.5	5.9	7.3	5.0
SE	4.2	3.0	3.3	3.7	3.2	3.7	3.2	3.5	4.4	4.2	3.6	3.3
SSE	5.0	2.9	3.0	3.5	2.6	2.9	3.3	3.0	3.1	3.0	2.8	3.1
S	3.6	3.2	3.1	3.4	3.3	2.6	3.2	3.1	3.2	3.5	3.3	3.4
SSW	3.2	3.2	2.9	3.0	2.8	2.7	3.3	3.3	3.3	3.6	3.6	3.5
SW	3.9	3.9	3.8	3.7	3.8	3.3	3.8	4.3	4.1	4.2	4.1	4.4
WSW	8.0	6.2	5.2	4.9	4.4	5.1	5.6	5.9	6.3	6.9	6.0	6.1
W	9.7	10.0	8.5	7.9	6.3	5.4	5.7	5.7	7.2	8.7	8.1	8.6
WNW	7.7	9.1	7.1	6.9	5.5	4.6	5.0	4.9	5.4	7.1	6.9	7.3
NW	4.0	4.3	3.1	3.5	3.0	3.1	3.2	3.3	3.9	5.2	4.8	4.8
NNW	3.7	2.5	2.8	2.6	2.9	2.6	2.7	2.8	3.2	4.1	2.8	3.0
MONTHLY AVERAGE SPEED												
	6.4	6.5	6.0	5.5	4.4	4.7	4.6	5.2	5.6	6.8	6.5	6.1

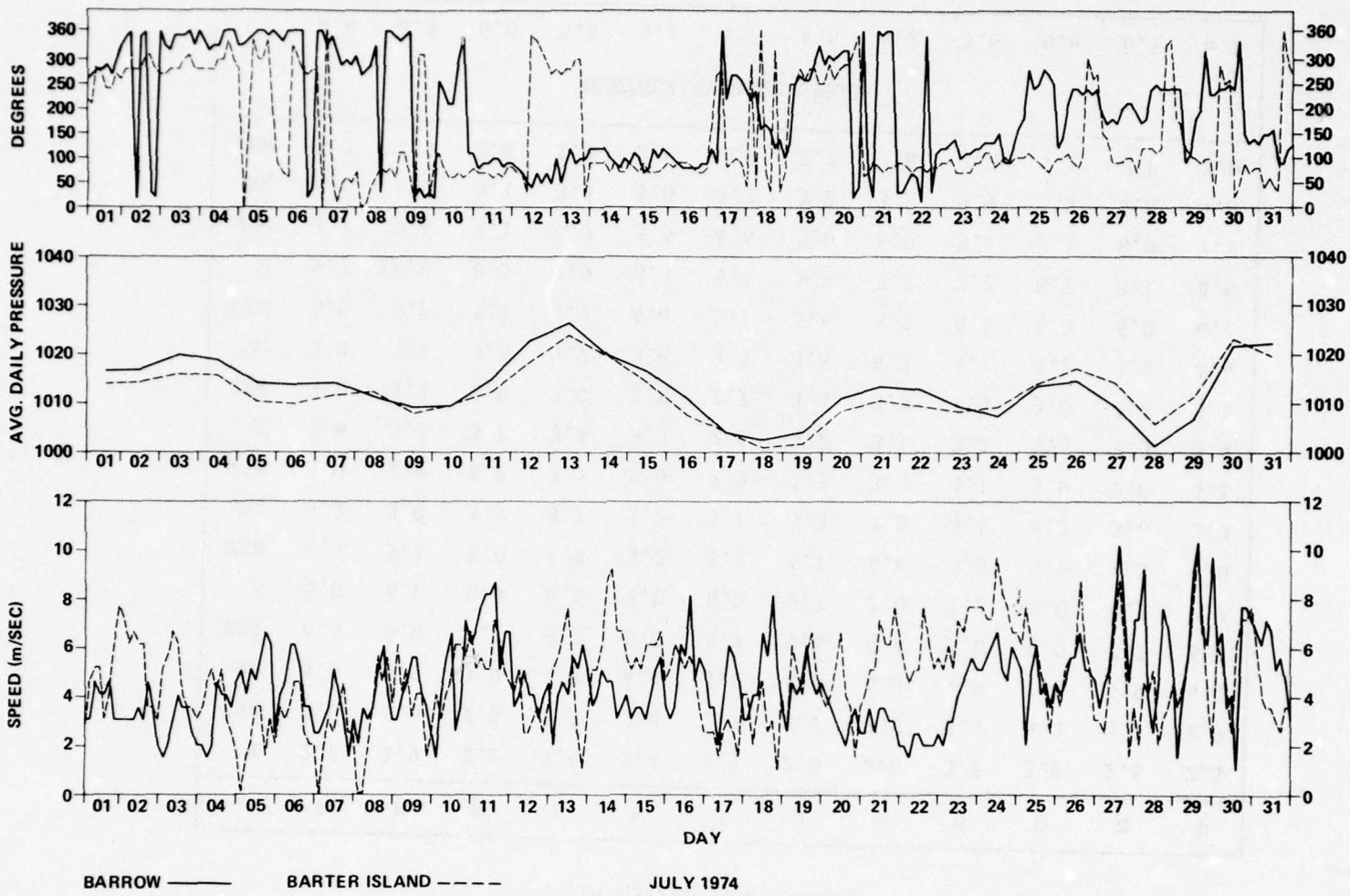

Figure 6. Meteorological record for Barrow and Barter Island, July 1974: wind direction (°T), barometric pressure (mb), and wind speed (m/sec).

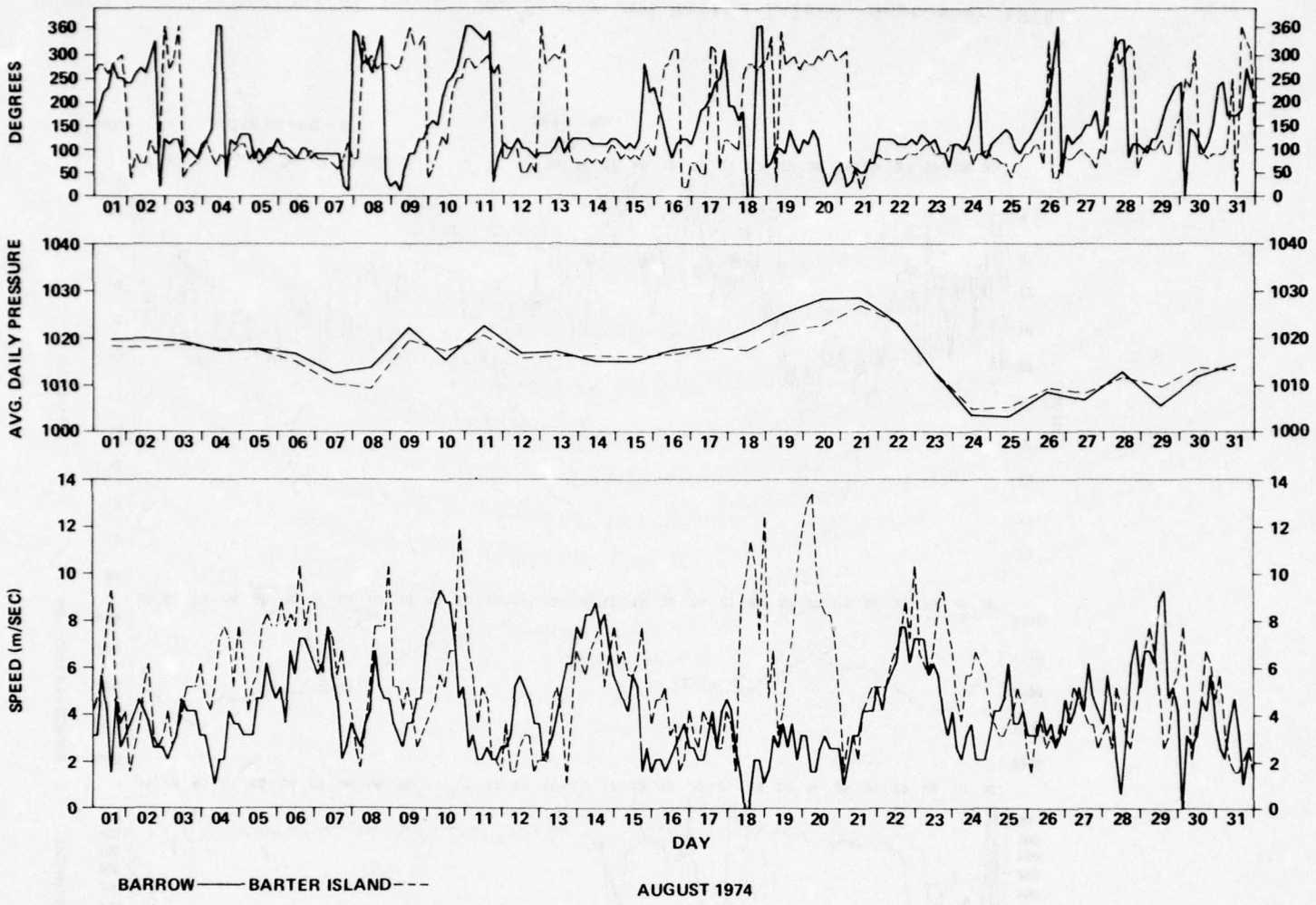

Figure 7. Meteorological record for Barrow and Barter Island, August 1974: wind direction (°T), barometric pressure (mb), and wind speed (m/sec).

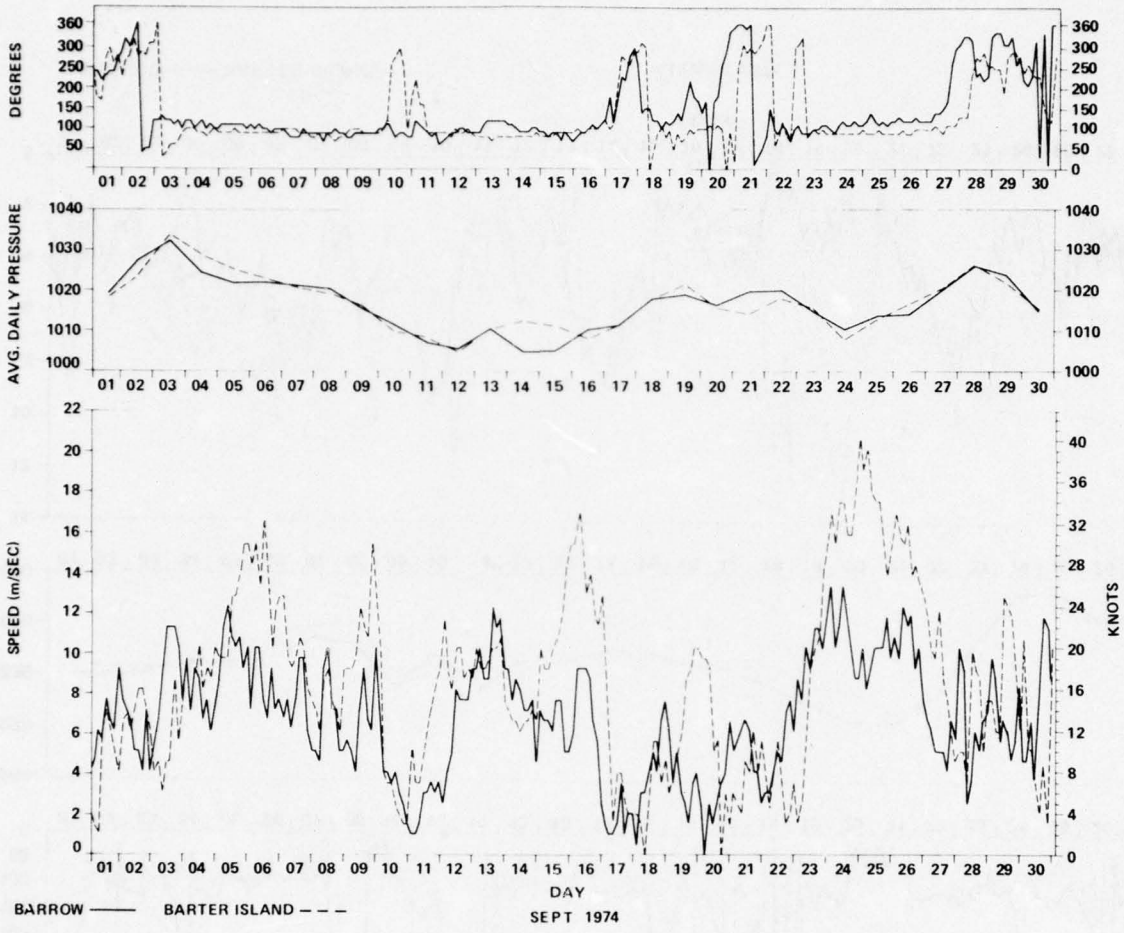

Figure 8. Meteorological record for Barrow and Barter Island, September 1974: wind direction (°T), barometric pressure (mb), and wind speed (m/sec).

The results for the wind speed and wind direction comparisons suggest that data from stations in between must be examined. The purpose is to determine at least qualitatively the scale of application of the longest and most complete data sources, Barrow and Barter Island. For this purpose the remainder of the discussion on winds will consider two provinces; the eastern north coast winds and the western north coast winds.

Eastern North Coast Winds

Examination of past data from Barter Island show that the wind field is characterized by a bimodal distribution (Figure 5).

Dickey (1961) studied the topographic effect of the Brooks Range on strong (> 11 m sec^{-1}) surface winds at Barter Island. The Brooks Range is located about 90 to 110 km south of Barter Island. Dickey expressed the following points about the winds at and around Barter Island:

1. When winds are westerly or southwesterly along the coast to the west at Barter Island, they become due west at Barter Island and shift to the northwest east of Barter Island. When winds are easterly to the east of Barter Island, they are from due east at Barter Island and remain easterly to the west of the island.

2. Wind speeds increase steadily from the west of Barter Island to a maximum some 150 km to the east of Barter Island.

3. Winds increase toward the Brooks Range to the south of Barter Island and decrease off the coast to the north. During high winds the topographic effect can be felt as far north as 120 km from Barter Island.

Dickey found that the behavior of the winds at Barter Island, 140 km west (Prudhoe Bay) and 150 km east (Komakuk) of the island can be explained by substituting a "simple physical model barrier" representing the knob of the Brooks Range and specifying the flow of air to be horizontal and irrotational. Ratios of wind speed along the coast to the wind speed at Barter Island were computed from actual data and from the model. These ratios are given in Table 4.

TABLE 4

RATIOS OF WIND SPEED ALONG THE COAST TO THE WIND SPEED AT BARTER ISLAND (FROM DICKEY, 1961 - >11 m sec^{-1})

LOCATION	OBSERVED	MODEL
Prudhoe Bay/Barter Island	0.72	0.77
Komakuk/Barter Island	1.28	1.17

Dickey's results are based on approximately three years of data. Using Dickey's technique we computed the ratios of wind speed between Prudhoe Bay and Barter Island for wind speeds greater than 6 m sec^{-1} (6 m sec^{-1} because we are interested in a broader range for prediction). We used a larger data base from 1970-1975. The ratios are shown in Table 5.

TABLE 5

COMPUTED RATIOS OF WIND SPEED AT
PRUDHOE BAY TO THE WIND SPEED OF BARTER ISLAND
(FOR WINDS GREATER THAN 6 m sec^{-1})

WIND DIRECTION	MEAN RATIO	STANDARD DEVIATION
West Winds	0.97	0.29
East Winds	1.04	0.17

We assumed the wind speed ratios are normally distributed, the two populations are independent and they have unequal variances. We tested the null hypothesis that the wind speed ratios are not significantly different for east and west winds. The result: they are not significantly different at the .05 level of α. This result supports the inference that the wind speed for the coastal area from Prudhoe Bay to Barter Island is not significantly different for the dominant wind directions. The importance of this inference is that we can consider the data (at least for the dominant directions and speeds above 6 m sec^{-1}) as representative and therefore useful for predicting the character of the immediate offshore wind field.

We were not able to test the frequencies of the dominant wind directions at Komakuk and Barter Island because of insufficient data. However, general observations show that the direction at Komakuk varies by about 25° from Barter Island; westerly winds at Barter Island are northwesterly at Komakuk, easterly winds at Barter Island are southeasterly at Komakuk.

Western North Coast Winds

The predominant wind direction at Barrow is easterly although again reference to Figure 5 shows a bimodal distribution. The mode for westerly winds is not as strongly displayed in the Barrow data as it is in the Barter Island data (Figure 5). The westerly wind directions are attributed to a high pressure cell in the interior of Alaska and the Yukon and the eastward movement of low pressure systems over the Arctic.

Again using Dickey's technique, the wind speed at Barrow was ratioed to Prudhoe Bay for east and west winds. The same assumptions apply and the same null hypothesis was tested. The ratios are shown in Table 6. The result: the mean ratio for east wind speeds and west wind speeds is significantly different for Barrow/Prudhoe Bay. This result

suggests that we cannot infer a consistent wind field for this province based on the ratio technique of Dickey. In this case we cannot infer that the two stations provide us with a representative picture for the purpose of prediction.

TABLE 6

COMPUTED RATIOS OF WIND SPEED AT
BARROW TO THE WIND SPEED AT PRUDHOE BAY
(FOR WINDS GREATER THAN 6 m sec^{-1})

WIND DIRECTION	MEAN RATIO	STANDARD DEVIATION
West Winds	.79	0.19
East Winds	.95	0.15

An attempt was made to compare winds at Barrow with a closer station: Oliktok Point (approximately 200 km from Barrow). We found that for our purposes there was insufficient data. However, the following general observations can be made:

1. When winds at Barrow are westerly (255-270°), the winds at Oliktok Point are northwesterly (280-300°). Wind speed at both stations is similar.

2. When winds at Barrow are easterly (70-100°), the winds at Oliktok are also easterly but are more erratic in direction.

Our recourse here is to subjectively interpret the limited wind data (such as in Figure 5) and make conservative predictions of the expected character of the wind field along the coast. For this paper we will consider the winds at Barrow representative of the north coast as far east as 152°W. From 152°W to Demarcation Point the winds at Barter Island will be considered as representative.

3.3 Storms

The primary storm track for low pressure systems follows the Siberian coast eastward across the Chukchi Sea and then along the Alaskan north coast. During an average summer six or seven storm systems follow this track. The secondary track follows the Alaskan coast from the Bering Sea northward to Point Barrow and turns eastward following the north coast.

Those storms which produce westerly winds can cause a rise in sea level along the shore. Sea level records from Barrow (Matthews, 1970) show that meteorologically induced tides cause the greatest variations in sea level. Westerly storms can cause a rise in sea level of over 3 meters (Reimnitz, et. al, 1972). These storm surges can force an oil spill on the water into low-lying coastal regions. Selmann, et. al (1972) indicate that 75 percent of the north Alaskan coast has a relief of 5 m or less.

To predict winds during a typical storm system moving along the Alaskan north coast, a wind field generating model has been developed. The model can be used to determine at a given set of positions the wind speed and direction of the storm as it moves through the area (for a more detailed description of the model, see Miller, et. al (1975)). The following assumptions are made in the model:

1. Direction and speed of the storm movement is constant over the time interval considered.

2. The storm is considered circular with the isobars arranged symmetrically about the minimum pressure at the center.

3. The model computes geostrophic wind at the indicated position from the storm. Values are corrected for friction over the ocean.

The model was tested using actual storm conditions. For this discussion a comparison between model-generated winds and actual winds at Barrow for a storm that occurred in August 1972 is given in Figure 9. The similarity between the winds is good, except for wind speed at the end of the storm where the model-generated winds are consistently greater in magnitude than the observed winds. The poorer agreement of the winds near the end of a storm appeared in all comparisons made between actual storms and the simulated data. However, the overall agreement of the model winds with actual winds is sufficient to utilize the model to determine the drift of an object during a storm condition.

3.4 Circulation

The surface circulation of the shelf waters along the north Alaskan coast is not well known. The U. S. Navy Hydrographic Office (1958) has produced a generalized chart of the surface circulation derived from scattered, short, direct current measurements, ship and ice movements, and the distribution of observed water properties. The chart (Figure 10) indicates that in the summer the surface water flows westward at speeds of less than 15 cm sec^{-1}. The highest surface currents (> 20 cm sec^{-1}) occur near Point Barrow. The movement of the surface water is apparently the result of the general wind pattern. (A select list of direct surface current measurements is given in the appendix.)

Recent surface current observations reveal a more complex pattern in surface flow than the chart discussed above. The U. S. Geological Survey (Barnes and Garlow, unpublished manuscript) has released 4200 surface drift cards along the North Alaskan coast during August-September 1972. The drifter release and recovery data are summarized in Table 7. The low rate of return (1.8%) is expected for this remote area.

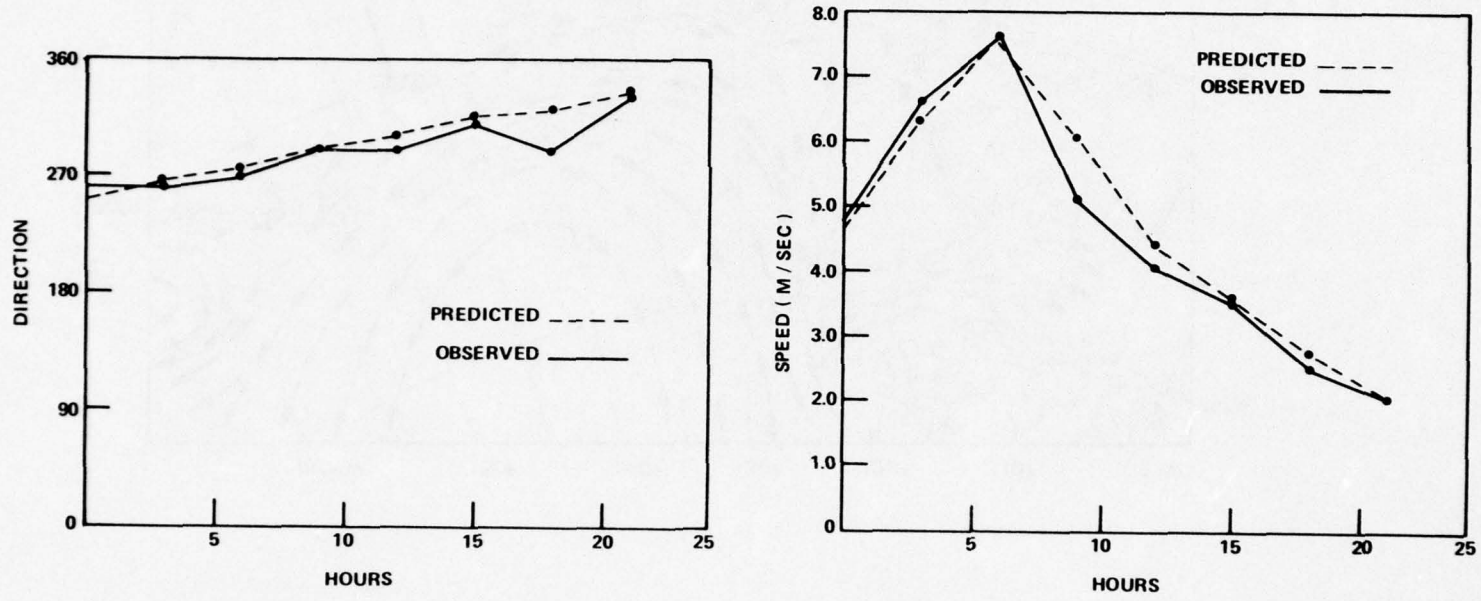

Figure 9. Comparison of actual wind data to model wind data for a storm, 11 August 1972.

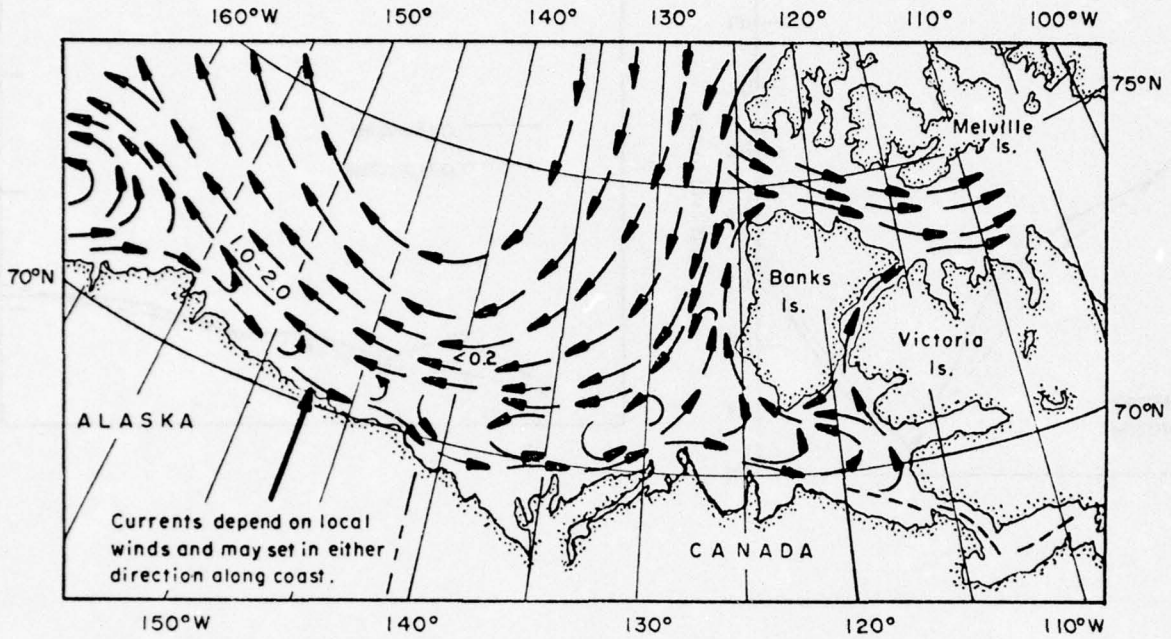

Figure 10. General summer surface water circulation (from U.S. Navy Hydrographic Office, 1958).

TABLE 7

DRIFTER RELEASE AND RECOVERY DATA

DATE RELEASED	NUMBER RELEASED	NUMBER RECOVERED	PERCENT RECOVERED
8 Aug - 11 Sep 1972	2925 (released from ice breaker in waters deeper than 20 meters)	9	0.3%
21 Aug - 6 Sep 1972	1275 (released from coastal vessel in water depths less than 20 meters)	66	5.2%
TOTALS	4200	75	1.8%

The late summer (September) release of many of the drifters limited the time for transit to the beaches prior to freezeup when surface water motion ceases and the drifters could have been incorporated into the coastal ice of the polar pack. Although cards have been found and returned for three conseutive summers, there is no data suggesting drifters were not already ashore before freezeup in 1972.

The direction of drifter movement is summarized in Table 8 and on Figure 11. The result is a dominance (79%) of westerly movement. About half of the recovery points were onshore from their release points (distance to shore $\geq$ half distances traveled parallel to shore). If the onshore movements are not considered as part of the directional data, the ratio of west to east drifters remains about the same with about 80 percent of the drifters moving west.

TABLE 8

SUMMARY OF DRIFTER MOVEMENTS

DIRECTION OF MOVEMENT	NUMBER	PERCENT
Easterly	16	21
Westerly	59	79
East along coast	8	11 (22%)
Onshore	38	50 (-)
West along coast	29	39 (78%)

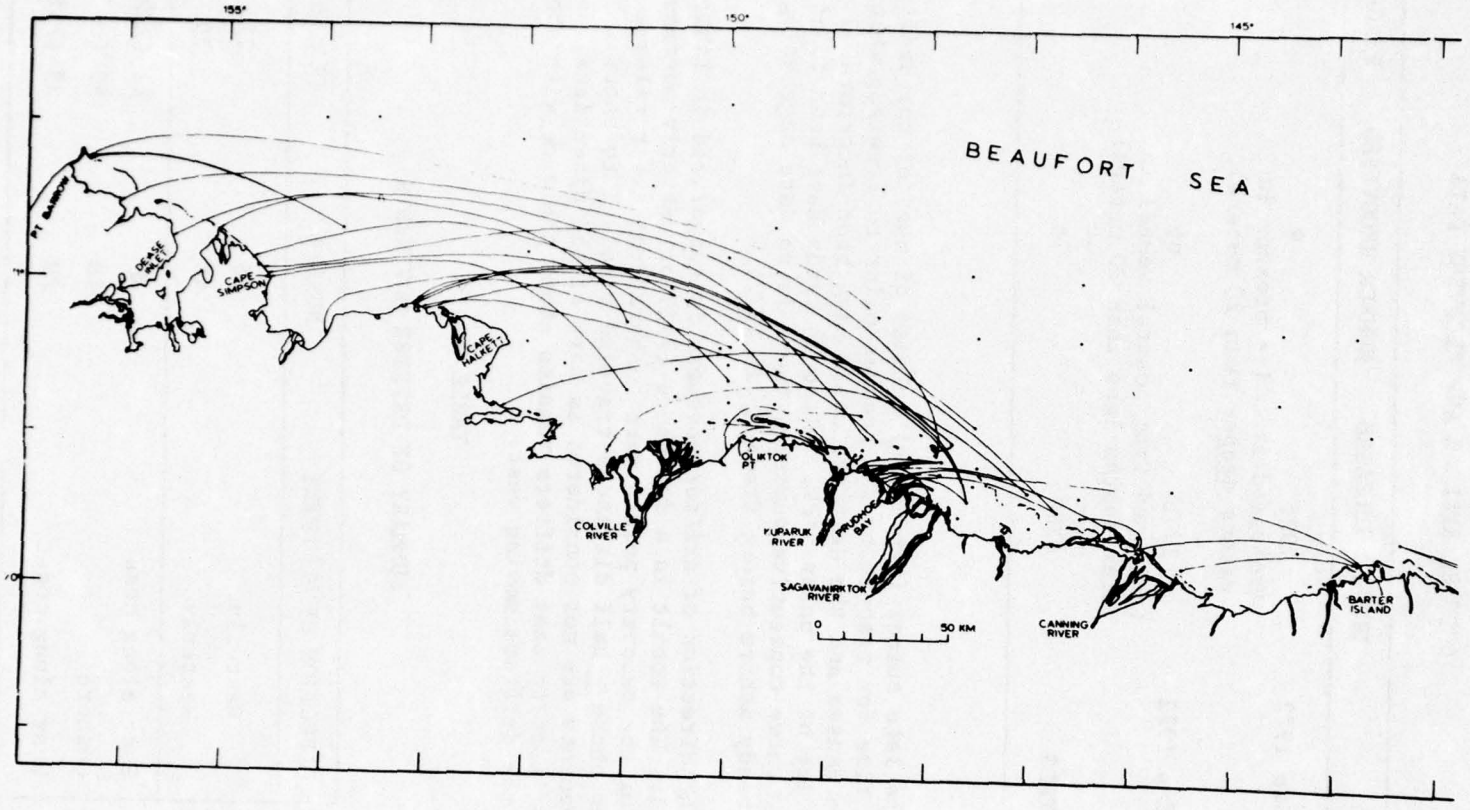

Figure 11. Paths of drifter cards released summer of 1972 along the north Alaskan coast.

TABLE 9

DRIFTER SPEED COMPARISON AND DATA - 1972

RELEASE DATE	RECOVERY DATE	DAYS ADRIFT	DISTANCE (MILES)	RATE (MI/DAY)	RATE (CM/SEC)	DIRECTION	RECOVERY LOCATION
21 Aug	22 Aug	1±	15	15±	32.0±	West	Lagoon
21 Aug	27 Aug	6	17.5	2.9	6.3	West	Lagoon
21 Aug	27 Aug	6	24	4	8.6	West	Oliktok
23 Aug	26 Aug	3	17	5.7	12.0	West	Kup. R.
23 Aug	28 Aug	5	8	0.62	1.3	South (onshore)	Prudhoe Bay
23 Aug	9 Sep	16	7	0.44	0.9	South (onshore)	Prudhoe Bay
29 Aug	19 Sep	21	73	3.5	7.5	East	Barter
3 Sep	11 Sep	8	107	13.3	29.0	West	Cape Simpson
6 Sep	9 Sep	3	53	17.7	38.0	West	Barrow

Velocity data are sparse, with only nine useable recoveries occurring prior to freezeup in 1972 (Table 9). Rates of drift range from less than 1 cm/sec to almost 38 cm/sec. The lowest velocities were seen in those two cards which drifted onshore. Drifters traveled westerly at the highest velocities with an average drift rate of 18 cm/sec (1/3 knot). The one rate of drift calculated for an easterly direction (7.5 cm/sec) was less than 1/2 the average westerly rate.

Hufford, et. al (1974) have measured velocities of near zero to 50 cm sec^{-1} along the outer shelf. The observed currents do appear to be wind driven. The current direction normally falls within the same quadrant as the wind direction (predominantly to the west) unless wind speeds are less than 2 m sec^{-1}. Then the current, especially near Point Barrow flows to the east (Hufford, et. al, 1974). Near the shore, the surface current is generated by local winds and the flow is generally parallel with the shore (Kinney, et. al, 1972; Hufford and Bowman, 1974). Current velocities of 0-37 cm sec^{-1} were observed under wind regimes of 0-8 m sec^{-1}.

Additional evidence that the surface currents are wind driven, at least on the eastern Alaskan north coast, is the presence of upwelling near Barter Island (Figure 12) (Hufford, 1974a, 1974b). Hufford concluded that the easterly winds present throughout the summer in the area create an offshore Ekman transport in the surface layer which in turn leads to upwelling of the deeper offshore water onto the shelf. Table 10 contains estimates of the Ekman transport and associated wind stress using values of the mean easterly wind speed from past data.

TABLE 10

ESTIMATED EKMAN TRANSPORT ASSOCIATED WITH
AVERAGE EAST WINDS NEAR BARTER ISLAND

TIME	AVERAGE WIND SPEED (m/sec)	WIND DIRECTION	WIND STRESS (dynes/cm^2)	EKMAN TRANS. (g/cm sec)
Jul	5.7	E	0.63	4.60×10^3
Aug	7.0	E	0.95	6.93×10^3
Sep	7.1	E	0.98	7.15×10^3

The two-layer model of upwelling by O'Brien and Hurlburt (1972) predicts that for a wind stress of 0.8 dynes cm^{-2} the interface between the layers will rise 30-40 meters in 10 days depending upon the assumed shelf bathymetry. The model also predicts that the upwelling region will

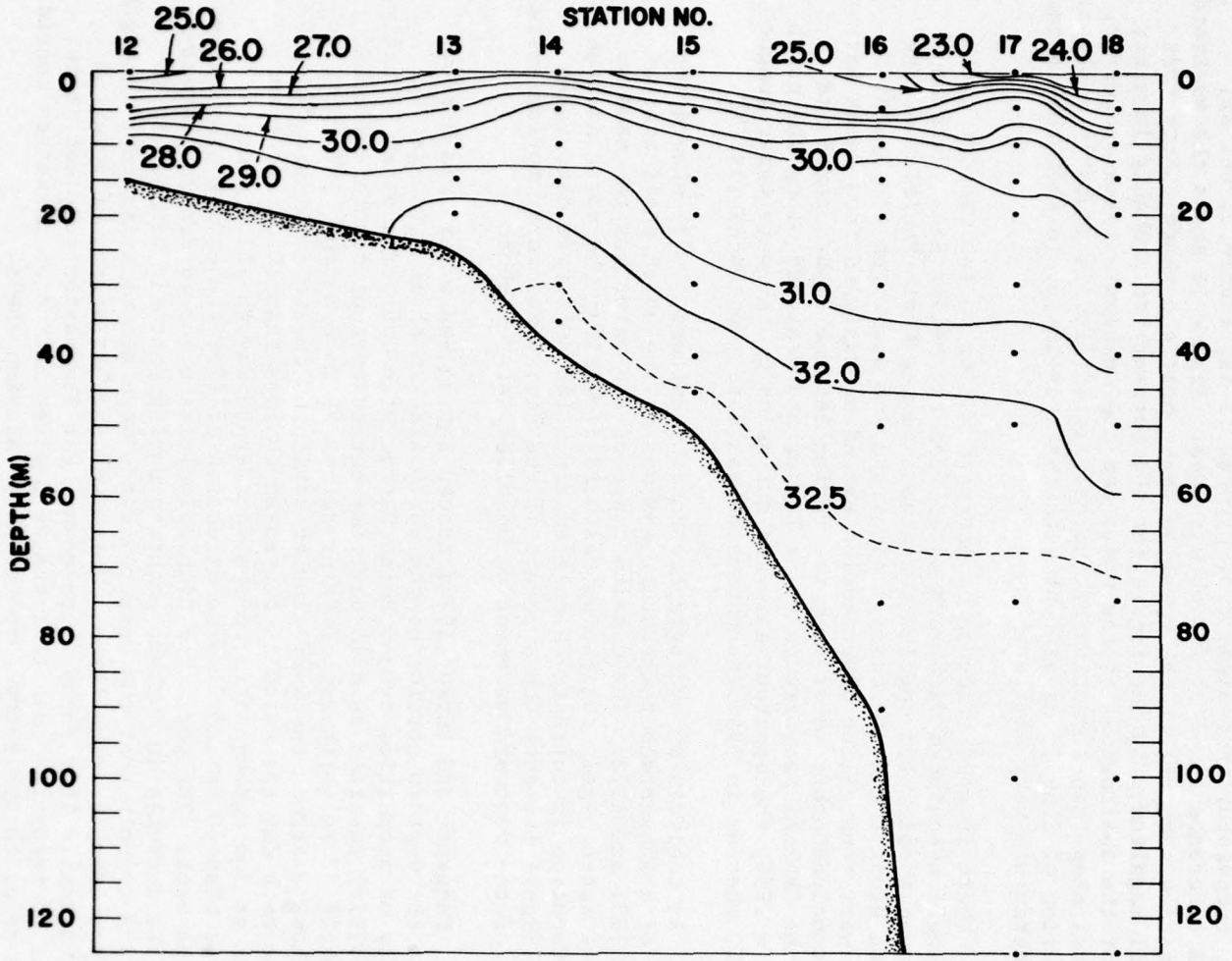

Figure 12. Vertical profile of salinity (o/oo) along 145°W during August 1972.

be located within 30 km of the coast and be characterized by a baroclinic coastal jet parallel to the shoreline and moving to the west. Observations by Hufford (1973) agree very well with the model. Evidence of the coastal jet appears in the area off Prudhoe Bay (148°W) in the 1972 data. Geostrophic currents were calculated from a line of observations along 148°30'W (using salinity, temperature and sigma t of Figures 13-15) (Hufford, et. al, 1974). A reference level of 100 db was used. Figure 16 shows the westward flow (negative numbers) of the upwelled water near the shore. Note that the actual magnitudes in the figure for the current are probably in error because of the shallowness of the water and the reference level. However, the general shape and direction of the calculated flow is probably realistic: the direction of flow is consistent with the hydrography in that the isotacs and isotherms are very similar.

There is good evidence of eastward motion on the western north Alaskan shelf associated with warm water from the Bering Sea. Johnson (1956) found zooplankton species indigenous to the North Pacific and the Bering Sea along the north coast. Also, the surface water temperatures showed a warm tongue-like distribution extending eastward from Point Barrow. Johnson concluded that water from the Bering Sea had flowed northward through the Chukchi Sea, around Point Barrow and eastward along the north coast. In 1950, the apparent eastward extension of the warm water tongue was 151°W, whereas in 1951 the extension was more pronounced (143°W).

An analysis of hydrographic data by Hufford (1973) showed the presence of a subsurface temperature maximum on the north shelf east of 154°W in 1971 and 1972. The density range of the water was the same as Bering Sea water, again suggesting eastward flow along the north Alaskan coast. Geostrophic currents calculated along 148°30'W from data taken in 1972 (Figure 16) show the presence of the Bering Sea water moving eastward offshore of the westward movement of upwelled water inshore.

Paquette and Burke (1974) traced Bering Sea water from Barrow Canyon to the western portion of the north Alaskan shelf establishing continuity of properties around Point Barrow with Hufford's data. Finally, Hufford (1975) reported on a 15-day time series current record collected on the shelf 83 km northeast of Point Barrow at 25 m depth. The current record shows a strong eastward flow averaging 60 cm sec^{-1} for six days. On the seventh day the velocity decreased to less than 10 cm sec^{-1} and persisted at low speeds until on the fourteenth day the flow increased to greater than 40 cm sec^{-1}. The direction of flow the entire time series was to the east. The period of high velocities occurred during westerly winds. The decrease in current occurred during easterly winds. It is interesting to note that the westerly winds were not of sufficient strength to be the primary driving force. There was another source of momentum for the current. That force is unknown. For discussion purposes it is important to recognize only that the warm water intrusion possesses considerable momentum prior to its entry onto the north Alaskan shelf.

The existing data indicate two modes of circulation on the north Alaskan shelf; a wind-driven system with upwelling and advection. To understand the possible causes and what mode might dominate, the dynamics controlling these modes should be examined.

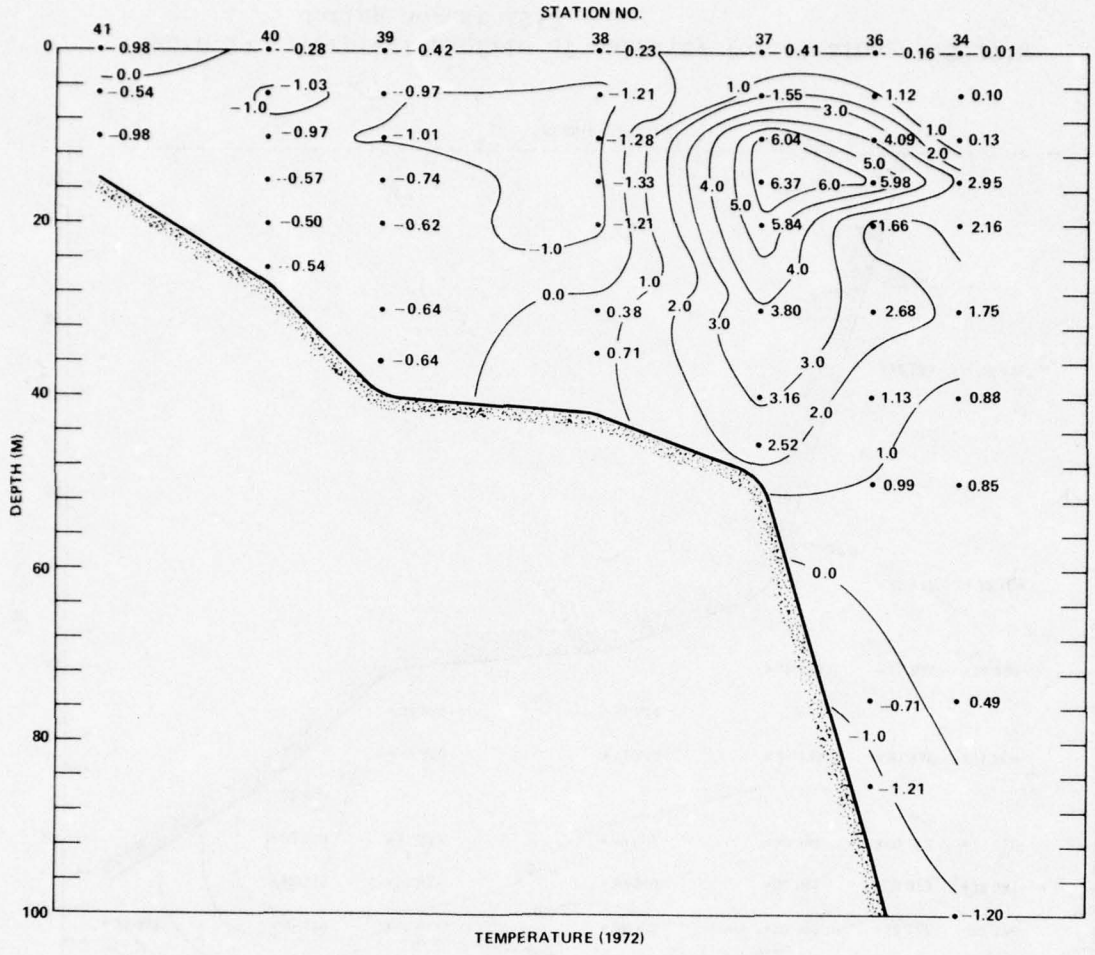

Figure 13. Vertical profile of temperature (°C) along 148°30'W during August 1972.

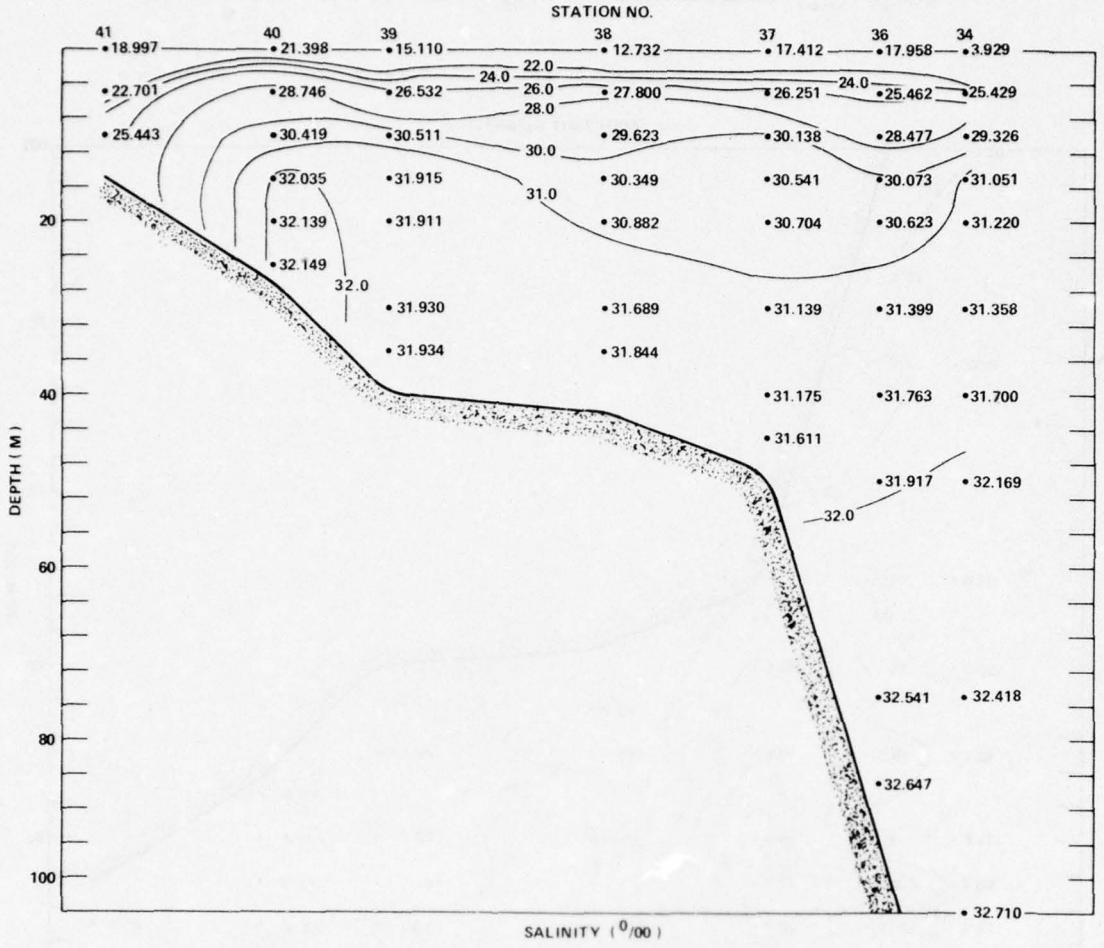

Figure 14. Vertical profile of salinity (o/oo) along 148°30'W during August 1972.

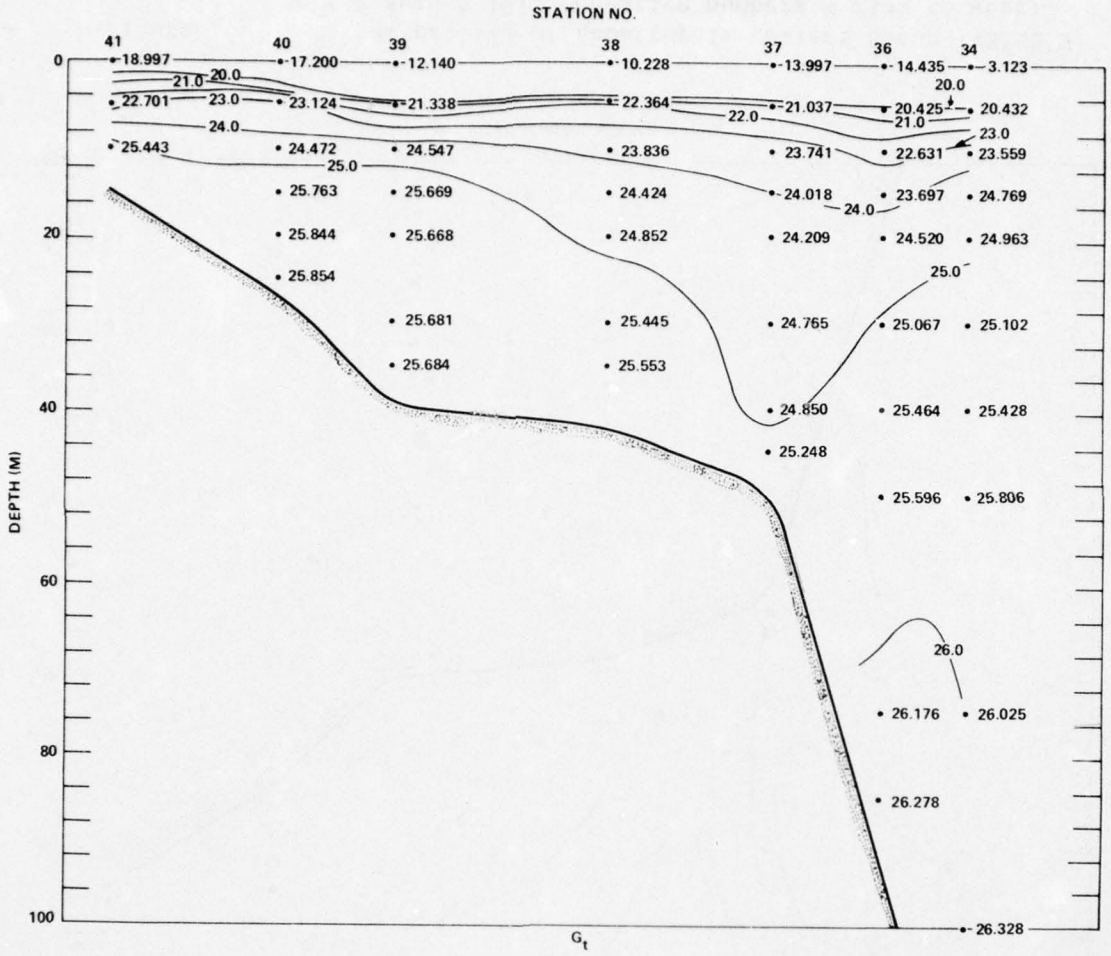

Figure 15. Vertical profile of sigma-t along 148°30'W during August 1972.

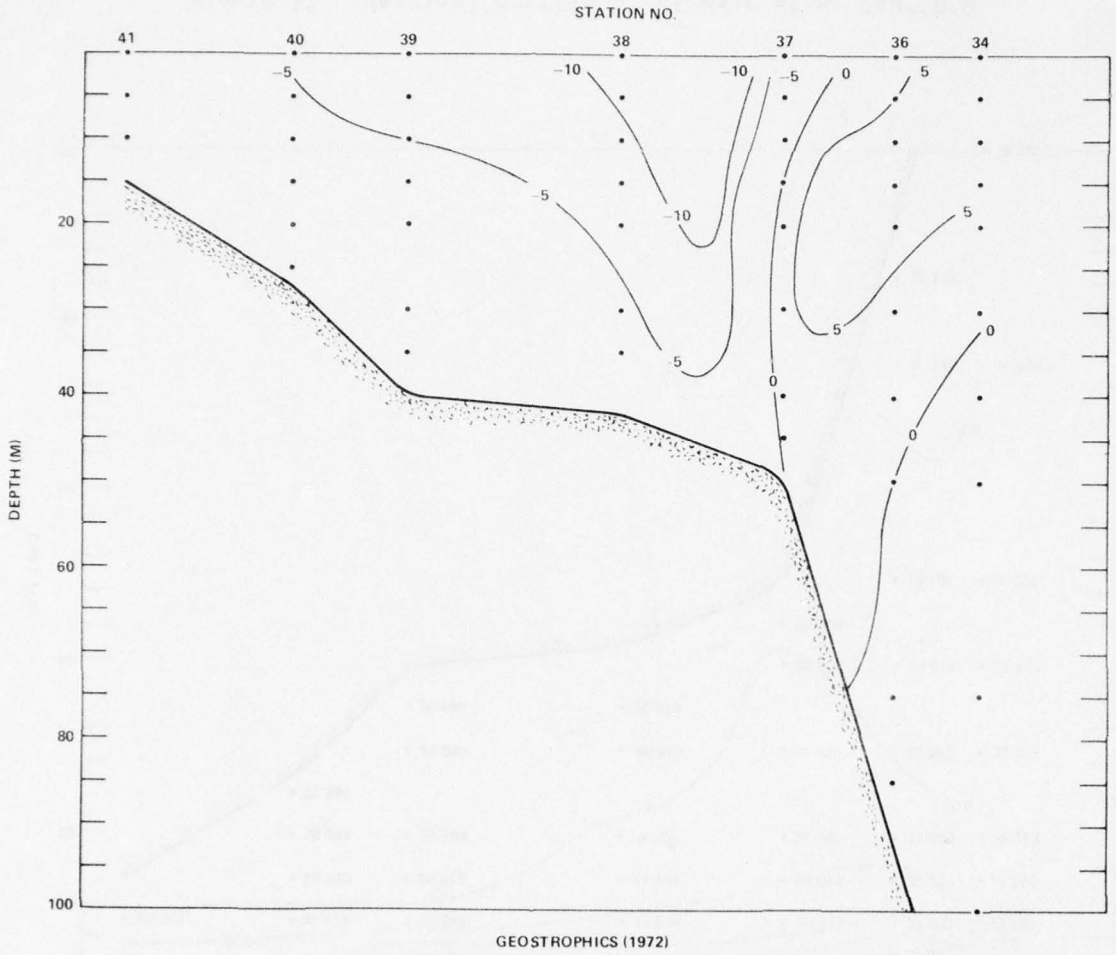

Figure 16. Vertical profile of geostrophic current along 148°30'W during August 1972 (negative numbers = flow to west).

The two terms advective acceleration and wind stress can be scaled to estimate their individual magnitudes:

$$U \frac{U}{L} \quad \text{and} \quad 1/\rho \frac{\tau}{H}$$

where L is the horizontal length scale and H is the depth of frictional influence. The rate of momentum transfer is:

$$U\,(UH) = \tau \cdot L$$

The two sources of momentum, wind stress and advection, will at times be additive (during westerly winds) but most of the time will be opposed (winds are primarily easterly). For the wind stress to stop or prevent the eastward flow of Bering Sea water onto the shelf, the wind stress must be applied over a distance greater than L. If the wind stress is applied at a distance less than L from the advection source, the water motion would be controlled by advection. On the north Alaskan shelf a water depth of 40 m is chosen. Analysis of the wind data (last section) shows that the wind field at Barrow can be applied to the coastal region as far as Harrison Bay (220 km). The wind stress is determined from the quadratic equation:

$$\tau = \rho C U^2$$

where C is the dimensionless drag coefficient (= 1.5×10^{-3}). Table 11 contains different advection velocities, wind stresses, and associated length scales. The average monthly easterly wind stress during the summer is sufficient to prevent the eastward flow of Bering Sea water to less than 100 km east of Point Barrow when the average water flow is 40 cm sec^{-1}.

TABLE 11

HORIZONTAL LENGTH SCALE VALUES FOR PENETRATION OF BERING SEA WATER ON THE NORTH ALASKAN SHELF

CURRENT SPEED (cm sec^{-1})	TIME	WIND STRESS (dynes cm^{-2})*	LENGTH (km)
60	Jul	0.90	160
	Aug	1.21	119
	Sep	1.09	132
40	Jul	0.90	71
	Aug	1.21	53
	Sep	1.09	59
30	Jul	0.90	40
	Aug	1.21	30
	Sep	1.09	33

*Calculated from data of Searby and Hunter (1971.

For water motions in shallow water friction should be included in the consideration of the dynamics. To estimate its importance, bottom stress is determined using the equation:

$$\tau_b = \rho_o C_d U_w^2$$

where ρ_o is the density of the water, U_w is the velocity of the water, and C_d is 3.3×10^{-3} (Sternberg, 1965). Assuming a bottom velocity of 10 cm sec^{-1}, τ_b would be 0.33 dynes cm^{-2}. Friction alone would limit the advection of momentum to less than 300 km.

Past data (Johnson, 1956; Hufford, 1973) show that Bering Sea water can penetrate as far east as 450 km but usually as a subsurface flow. Just where the Bering Sea water sinks from the surface and becomes a subsurface flow is not known. Data from 1971 and 1972 indicated that the warm layer comes around Point Barrow as a surface flow and disappeared from the surface around 154°W in 1971 and 150°W in 1972. This is about the same distance from Barrow as the length scale calculated from the wind stress and advection of momentum. For the surface layer, it is assumed that the eastward flow of Bering Sea water is limited to less than 150 km east of Point Barrow.

The hydrographic data and direct current measurements show the presence of two modes of circulation on the north Alaskan shelf: warm water from the Bering Sea intruding eastward along the outer portion of the shelf; and the wind-driven circulation on the eastern half of the shelf with upwelling and its associated western jet of water moving westward. The upwelling is in response to the easterly winds which predominate in the summer. The absence of upwelling further to the west is probably due to the influence of the eastward-moving Bering Sea water. Nearshore, the currents are not steady state and are influenced by the local winds. The currents show dominant longshore components, moving either east or west. The average direction is to the west because of the predominance of easterly winds.

3.5 Tides

Periodic phenomena were estimated from the current record of Hufford (1975) recognizing the restrictions of a short record. Amplitudes of about 1 cm sec^{-1} were observed for the diurnal and semi-diurnal components of the record. These small amplitudes indicate that temporal forcing of the shelf current by the tide is insignificant on the Beaufort Sea shelf.

Wiseman, et. al (1974), have also observed a similar absence of a strong current signal at the tidal periods on a short current record obtained near Point Lay, southwest of Barrow. A semi-diurnal component was present and had an amplitude of only 1 cm sec^{-1}.

3.6 Waves

Because of the presence of the pack ice usually only a few kilometers from shore, wave action along the north Alaskan coast is much reduced. The pack ice reduces the open water fetch, and floating ice in open water areas inhibits wave development. The prevailing direction of the seas coincides with that of the surface winds: the swell tends to be from the northeast in the summer.

The most severe wave conditions occur during the passage of rapidly moving storms in the summer (provided ice conditions permit an appreciable fetch across open water). The largest waves recorded offshore were greater than 9 m (Lewellen, 1969). Near Point Barrow waves of 6 m height occurred during a storm in August 1951 (Carsola, 1952). However, tabulation of sea height versus direction for the vicinity of Point Barrow shows that about 90 percent of the time sea height is less than 1 m (Table 12). Wiseman, et. al (1974) found that the most common nearshore wave field at Pingok Island had an energy peak at periods between 2 and 3 seconds and a significant wave height of 20 to 30 cm.

TABLE 12

SEA HEIGHT VERSUS WAVE DIRECTION FOR NEARSHORE AREAS BETWEEN POINT BARROR AND PITT POINT, ALASKA

DATA TAKEN JULY TO NOVEMBER (From Sellmann, et. al 1972)

WAVE DIRECTION	SEA HEIGHT, m					TOTAL OBS	% OF TOTAL
	<1	1	1-2	2-3	>3		
NNE-NE	146	25	2	2	1	176	7.3
ENE-E	317	57	7	2	2	385	15.9
ESE-SE	68	6		1		75	3.1
SSE-S	22	3				25	1.0
SSW-SW	23	7				30	1.2
WSW-W	102	20	7	4		133	5.5
WNW-NW	63	29	28	12	1	133	5.7
NNW-N	68	20				88	3.6
CALM	1370					1370	56.7
TOTAL	2178	168	44	21	4	2415	
%	90.2	7.0	1.8	.9	.1		

The wave-induced drift along the north Alaskan coast can on occasion become important. The equation for the surface Stokes transport is:

$$V_w = \left(\frac{\pi H}{L}\right)^2 C$$

where H is the wave height, L, the wave length, and C, the wave velocity. Table 13 contains values of V_w for typical values of H, L, and C at different wind speeds. The estimated transport is roughly 10 percent of the total surface drift current, assuming the total current is 3.5 percent of the wind.

TABLE 13

SURFACE DRIFT CURRENT DUE TO WAVE TRANSPORT

WIND SPEED ($m\ sec^{-1}$)	TRANSPORT CURRENT ($cm\ sec^{-1}$)
5	2
10	5
15	9
20	13
25	17

The estimated Stokes transport for the common wave conditions for the north Alaskan coast given in Table 12 is only 2 cm sec^{-1}. The only time that wave-induced drift will be important along the North Slope will be during the infrequent summer storms.

4.0 FORECAST MODEL

The oil spill forecasting model presented here is based on the following:

1. It is assumed that the movement of the oil slick can be computed as the vectorial sum of the permanent current vector, tidal current vector, and the wind-induced drift vector.

2. The permanent and tidal current vectors for the north Alaskan shelf are ignored based on evidence in the previous sections.

3. The wind-induced drift vector for the oil slick is assumed to be in the same direction as the wind vector and has a magnitude of 3.5 percent of the wind speed. This treatment assumes the wind drift current is at fully developed conditions, i.e., the current has reached its maximum attainable speed. The drift angle for the distances and for the latitudes of interest in this study is expected to be small and hence will be neglected.

4. The state of the local winds is described by one of sixteen directions (N, NNE, NE, ENE, etc.) with an associated mean monthly speed for each direction.

5. The wave-induced surface drift vector will be neglected except during storm conditions.

Oil spreading can be accounted for by the Fay-Hoult spreading description (Fay and Hoult, 1971) which treats the oil as a fluid of homogenous density, viscosity and surface tension. Recent studies by Glaeser and Vance (1971) and by Hoult, et. al (1975) indicate that the crude oil does not spread as readily in cold waters. Using the Fay-Hoult spreading represents a "worst case" situation. However, for purposes of this paper the spreading of the oil will be omitted. If necessary, for environmental risk assessment, one can calculate the maximum slick area as equal to the volume of the spill divided by the spill thickness ($\sim$1 cm).

There are natural processes that, given a sufficient time, tend to mitigate the effect of a spill beaching upon a coast. These processes are evaporation of lighter fractions into the atmosphere, the dissolution of the soluble fraction into the water, and the breakdown of the larger slick into numerous smaller slicks by the action of the ambient turbulence and presence of floating ice. Unfortunately the importance of these processes on the north Alaskan coast are unknown. These processes, therefore, will be ignored in the following discussion.

4.1 Results - Using Historical Wind

To forecast impact locations along the north Alaskan coast, oil spill movement from fifteen arbitrarily chosen spill sites is generated using the environmental data discussed in previous sections. Figures 17-31 are summer composites of potential impact areas along the north Alaskan coast. Each figure contains a wind rose with percent frequency for each individual sector. For example, in Figure 17, the 20.7 value is the percent frequency of an easterly wind which would move an oil spill in a westerly direction during the summer.

The data from Figures 17-31 was used to determine the minimum impact time and the probability of impact for the 15 different areas (Table 14). The wind was presumed to stay within the same sector throughout the drift period. This assumption of constant wind probably gives artificially low values of minimum impact time. However, as a worst case estimate of minimum impact time, the time can be a valuable tool for environmental risk assessment. The probability of impact is determined by adding all the percent frequency values of those sectors of the wind rose which intersect the shoreline and is expressed as a percent where 100 percent is a certain impact.

The predominant wind directions which cause minimum impact times are ENE and E. These are the most frequent directions of the wind along the North Slope in the summer, as shown in Table 14. The minimum impact times for the fifteen spill sites vary between 6 and 53 hours and the probability of impact from 40 to 96 percent.

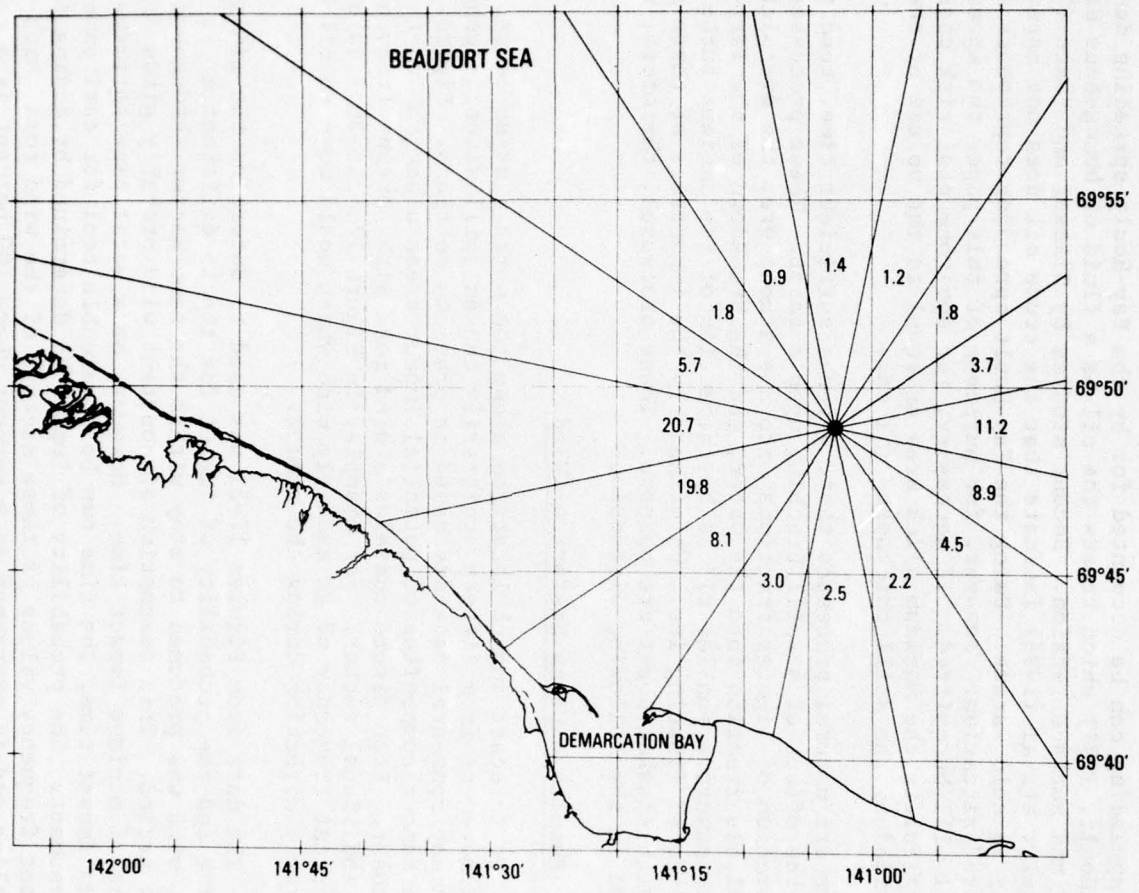

Figure 17. Potential impact areas near Demarcation Bay for a spill site 8.5 nm offshore.

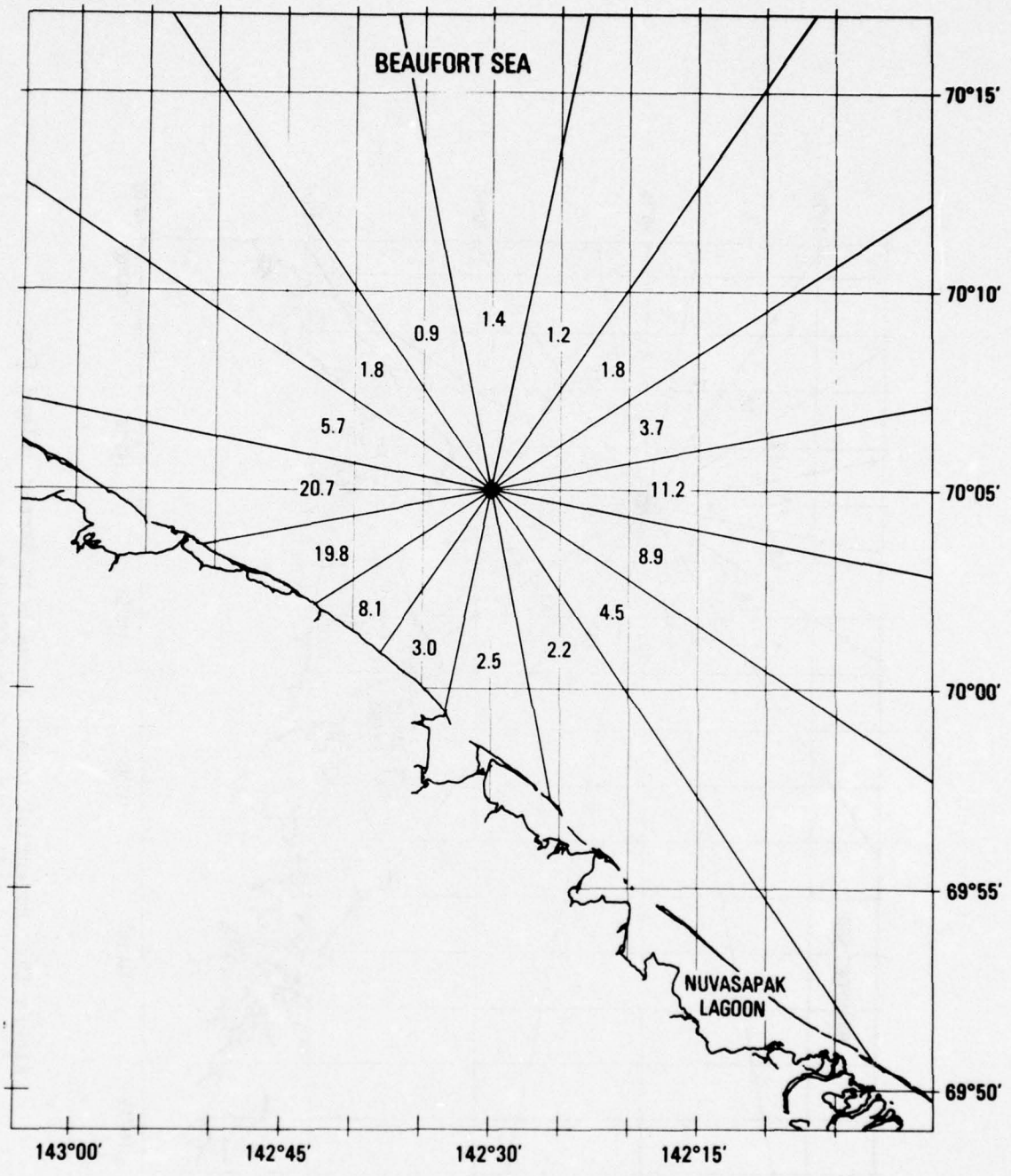

Figure 18. Potential impact areas near Nuvasapak Lagoon for a spill site 5.0 nm offshore.

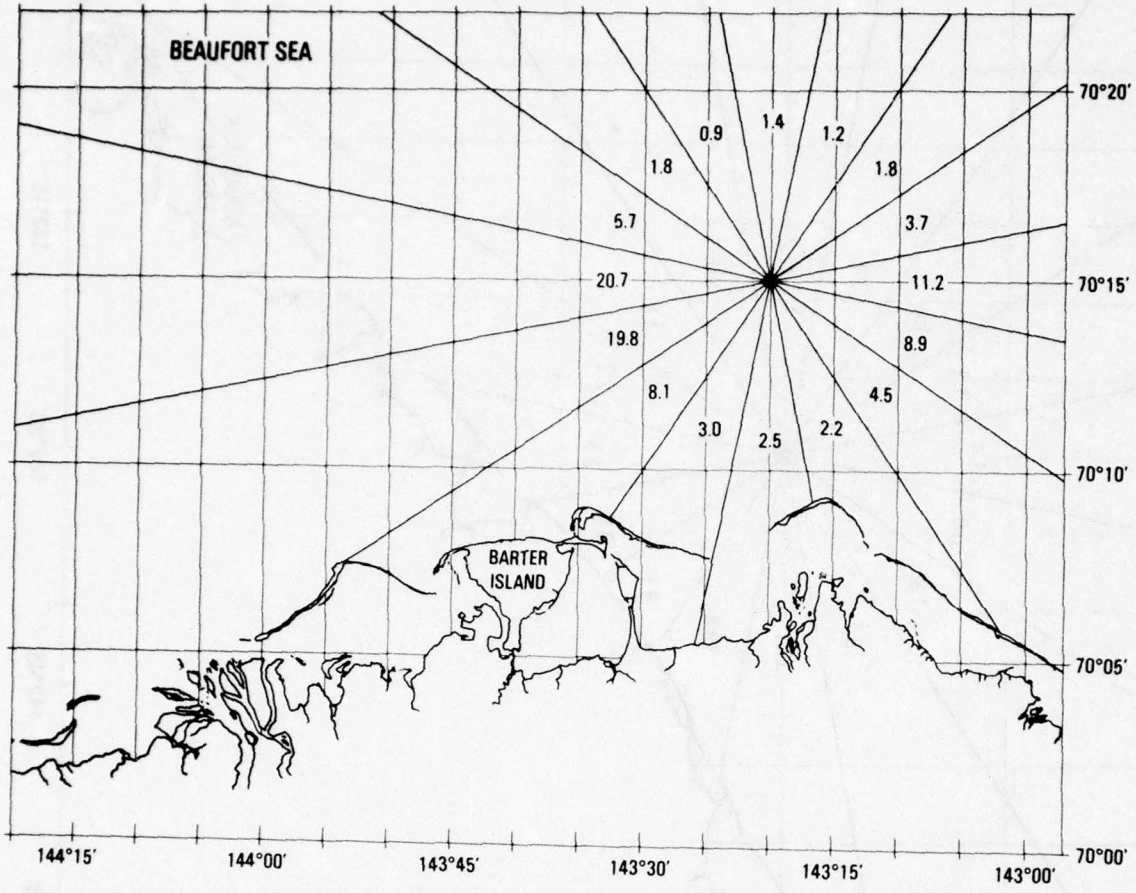

Figure 19. Potential impact areas near Barter Island for a spill site 6.0 nm offshore.

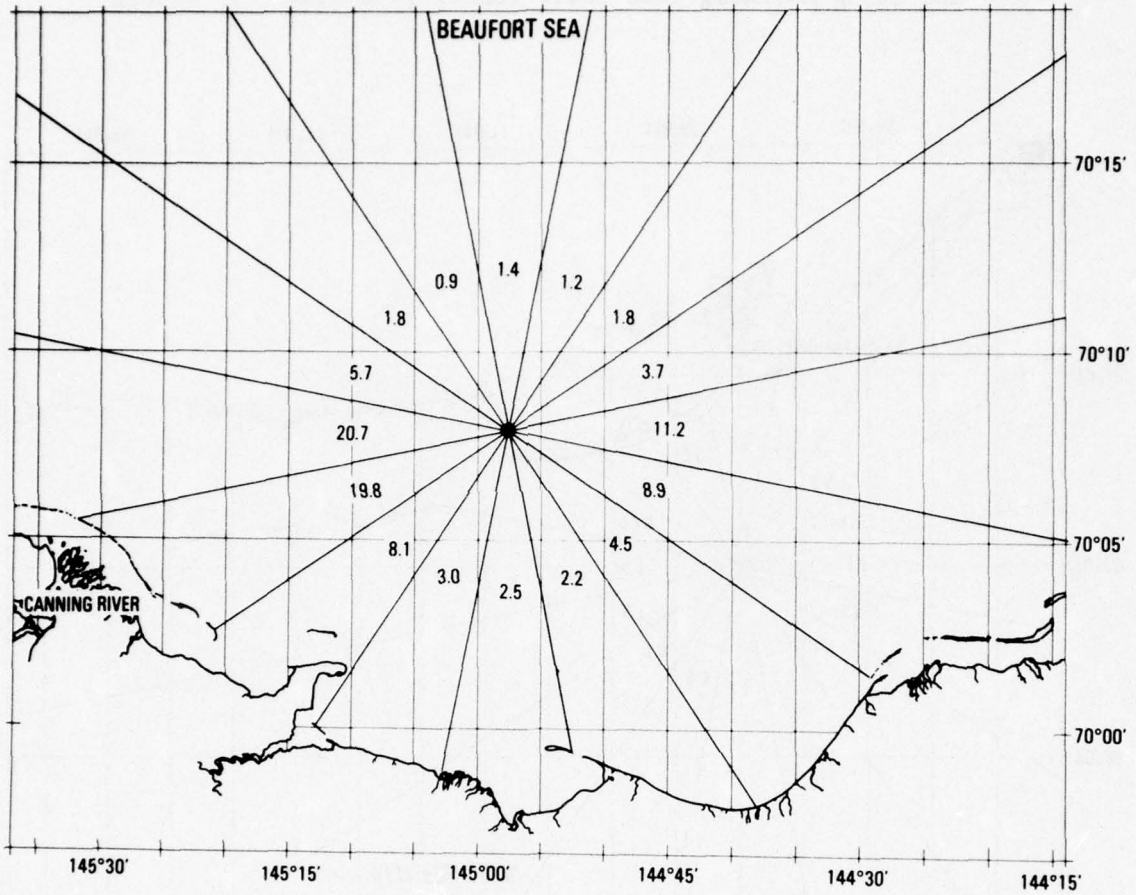

Figure 20. Potential impact areas near the Canning River for a spill site 7.3 nm offshore.

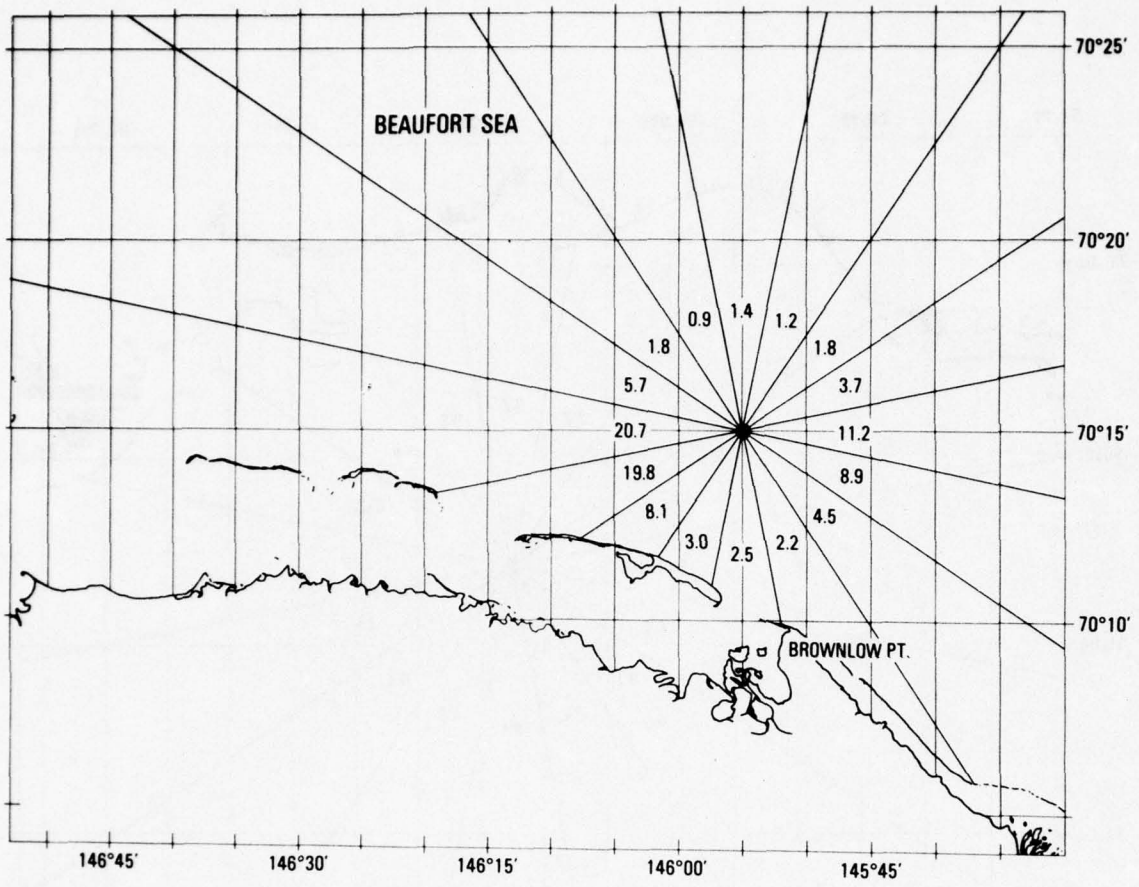

Figure 21. Potential impact areas near Brownlow Point for a spill site 7.2 nm offshore.

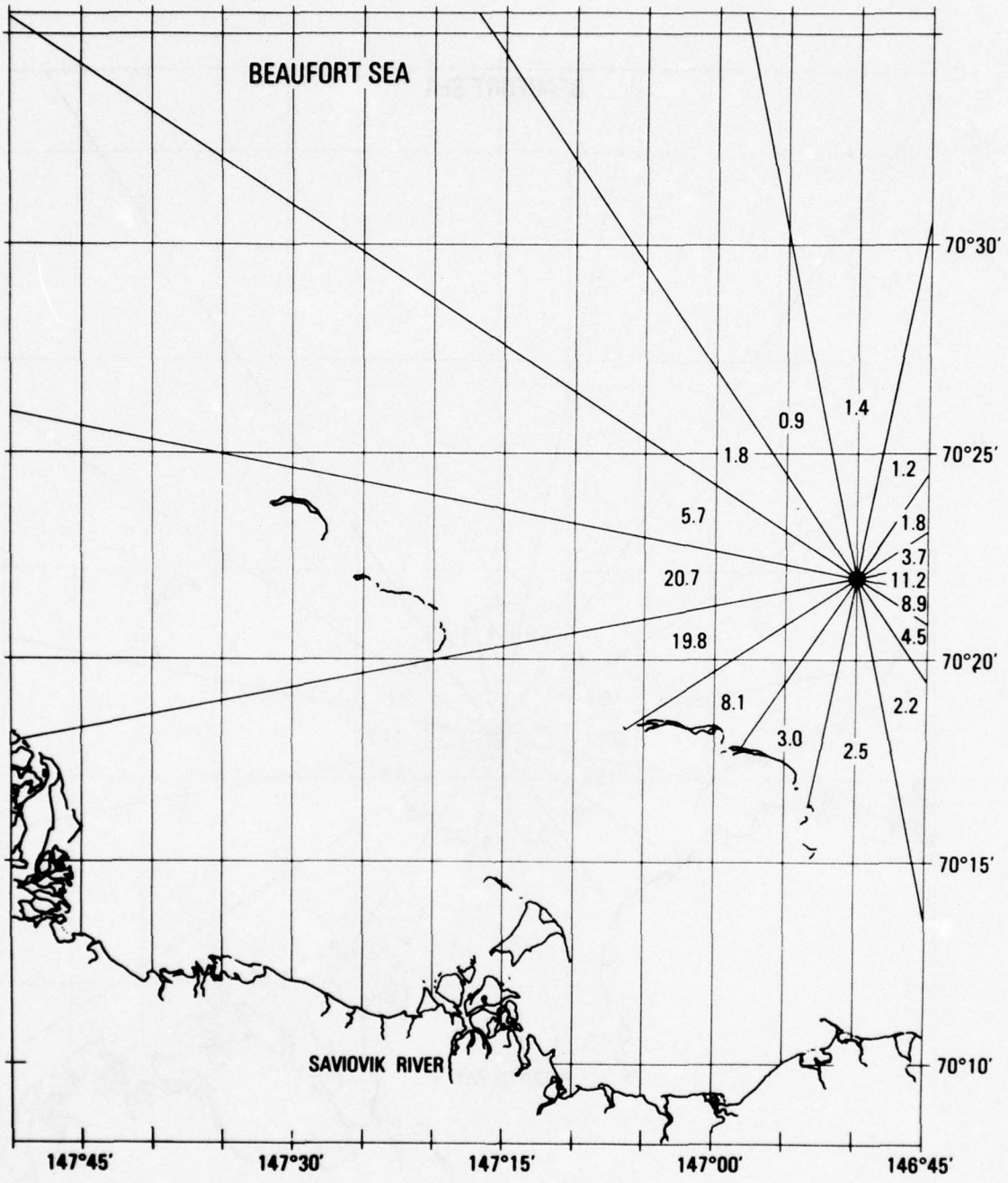

Figure 22. Potential impact areas near Saviovik River for a spill site 5.0 nm offshore.

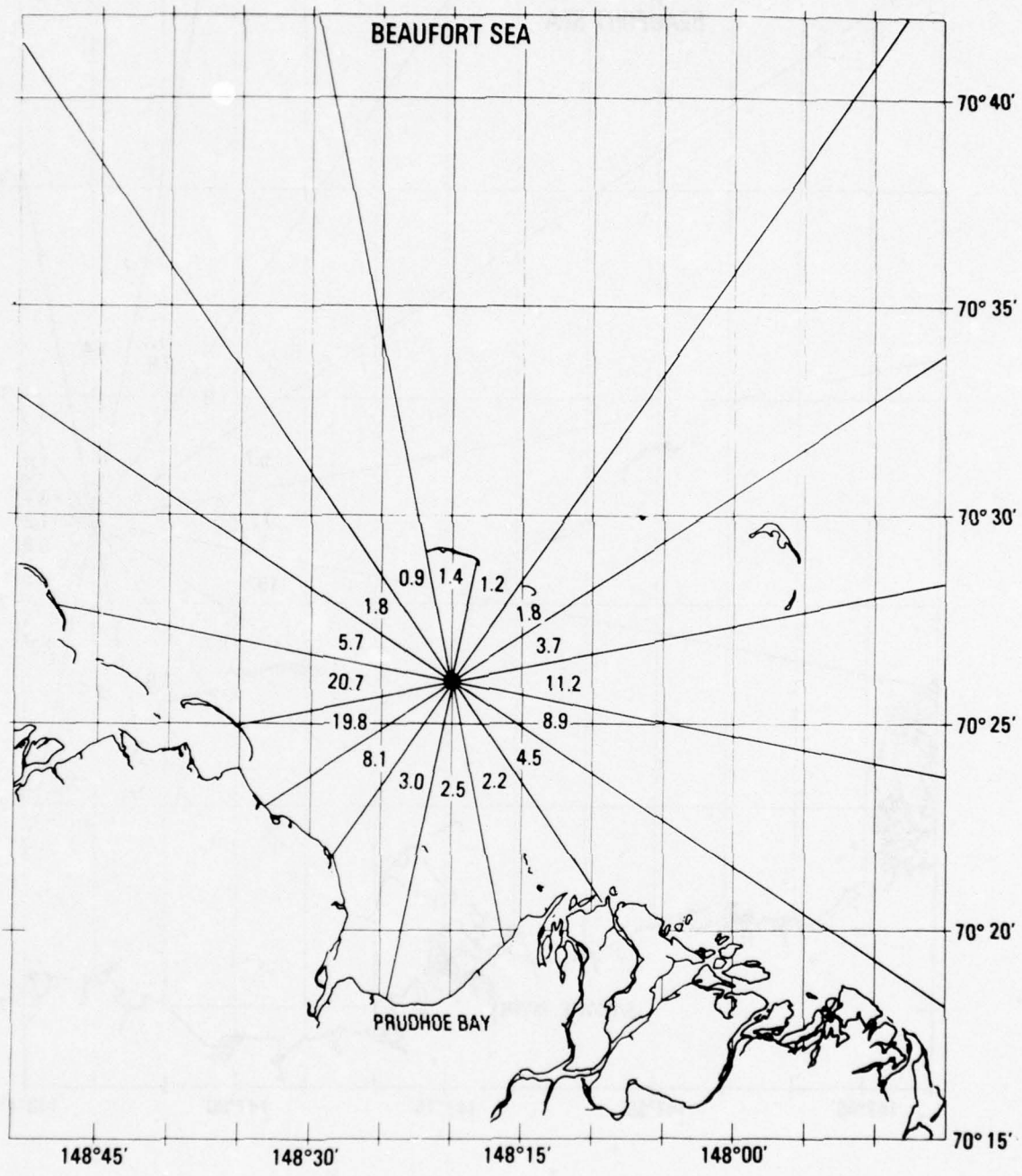

Figure 23. Potential impact areas near Prudhoe Bay for a spill site 5.2 nm offshore.

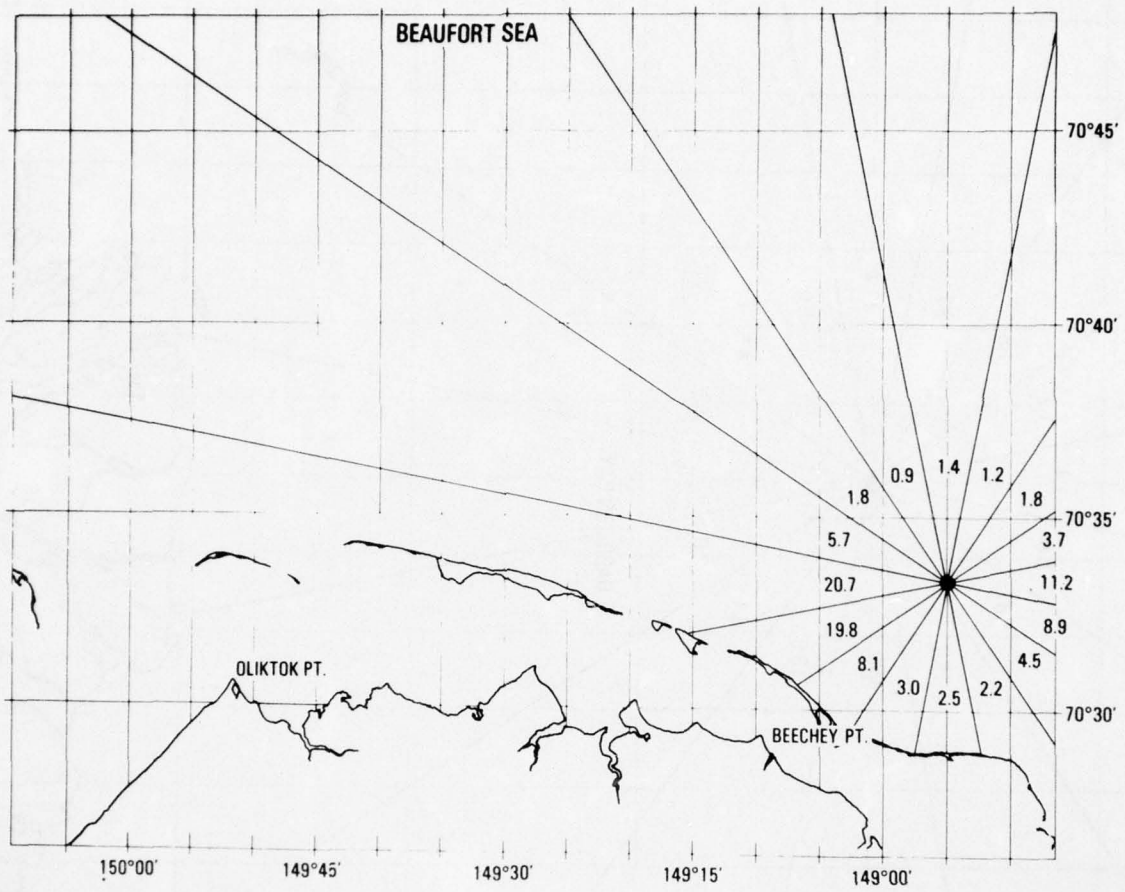

Figure 24. Potential impact areas near Beechey Point for a spill site 4.7 nm offshore.

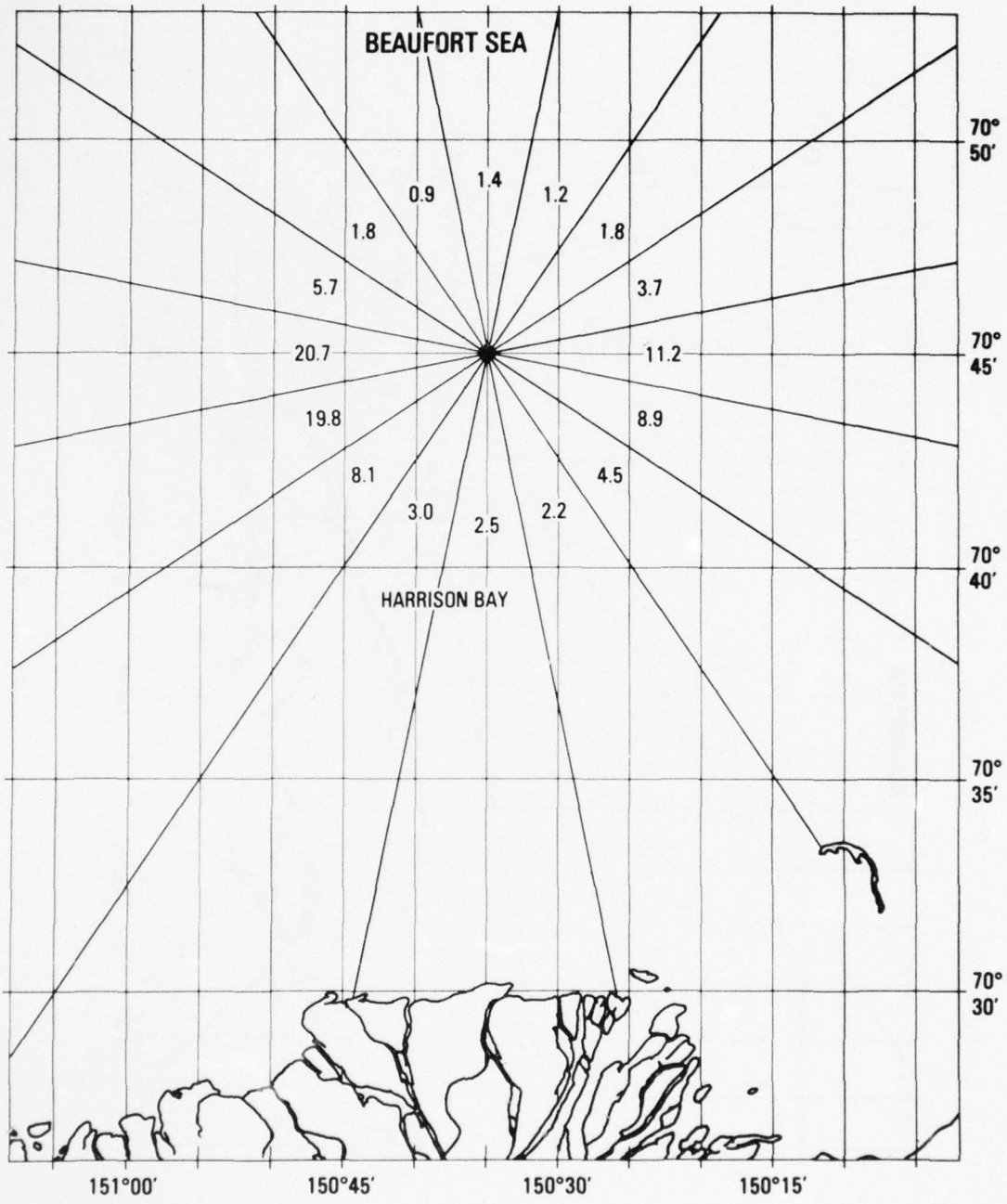

Figure 25. Potential impact areas near the Colville River for a spill site 14.7 nm offshore.

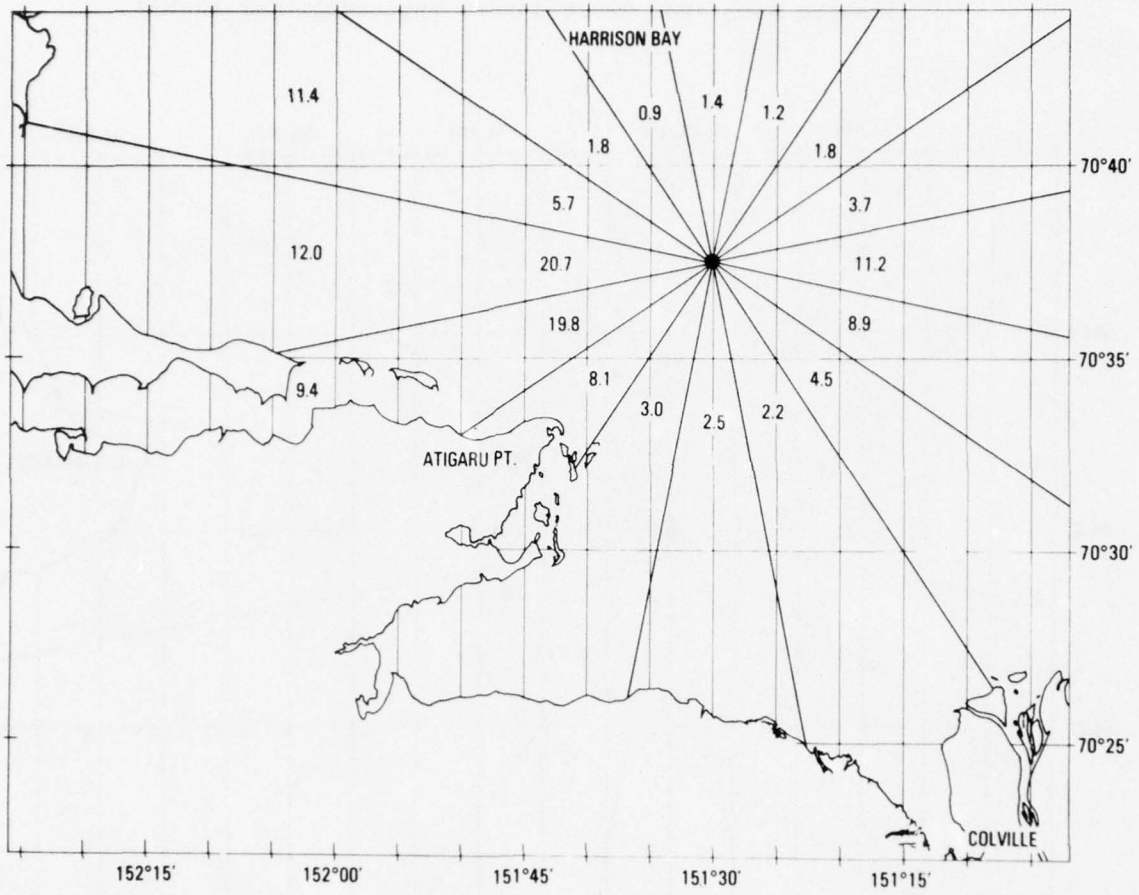

Figure 26. Potential impact areas near Atigaru Point for a spill site 5.9 nm offshore.

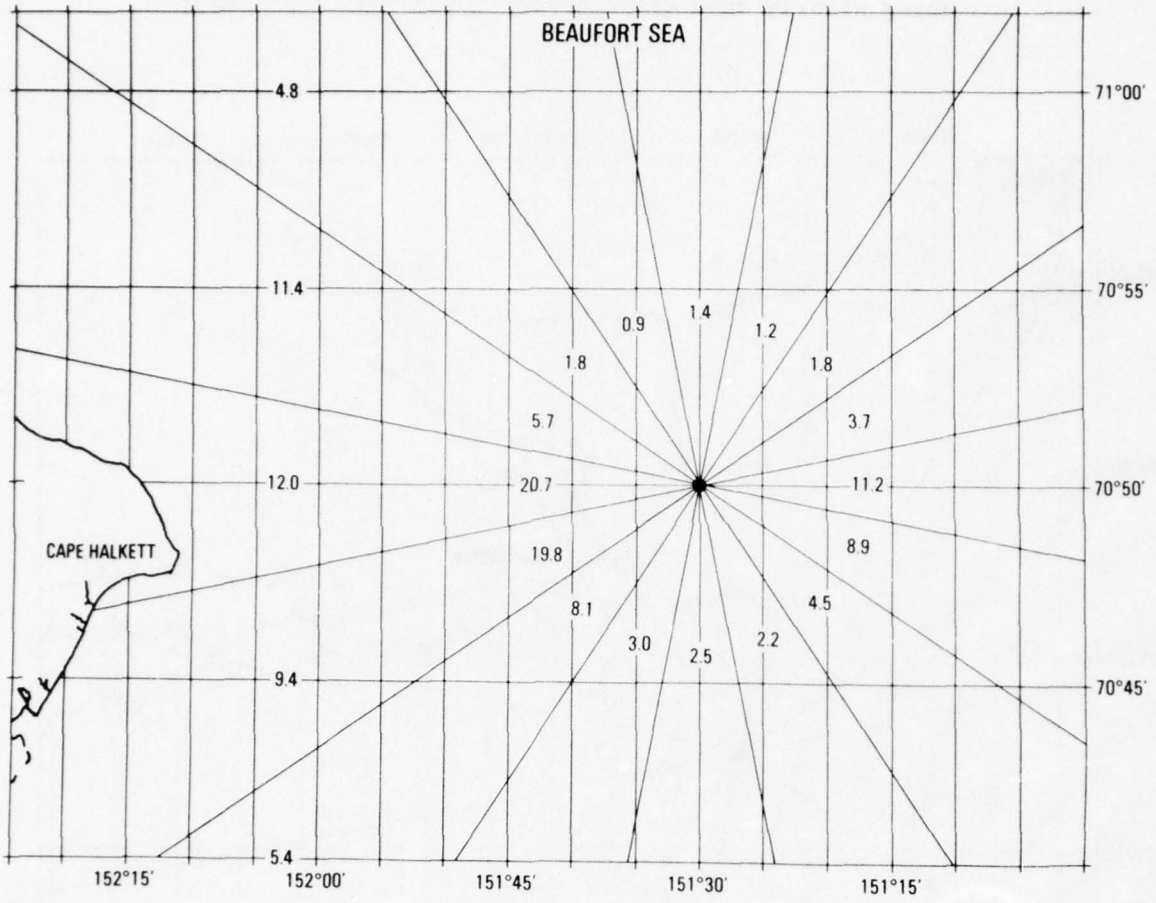

Figure 27. Potential impact areas near Cape Halkett for a spill site 14.5 nm offshore.

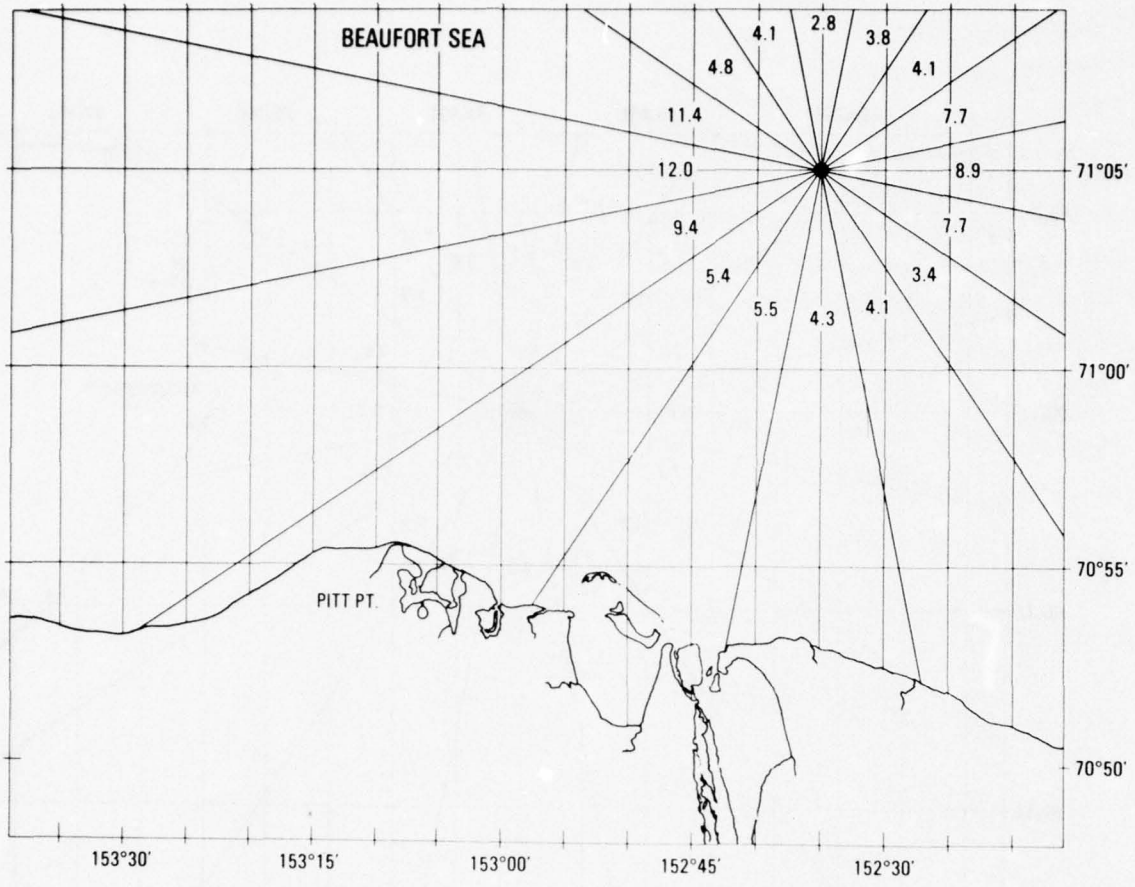

Figure 28. Potential impact areas near Pitt Point for a spill site 12.3 nm offshore.

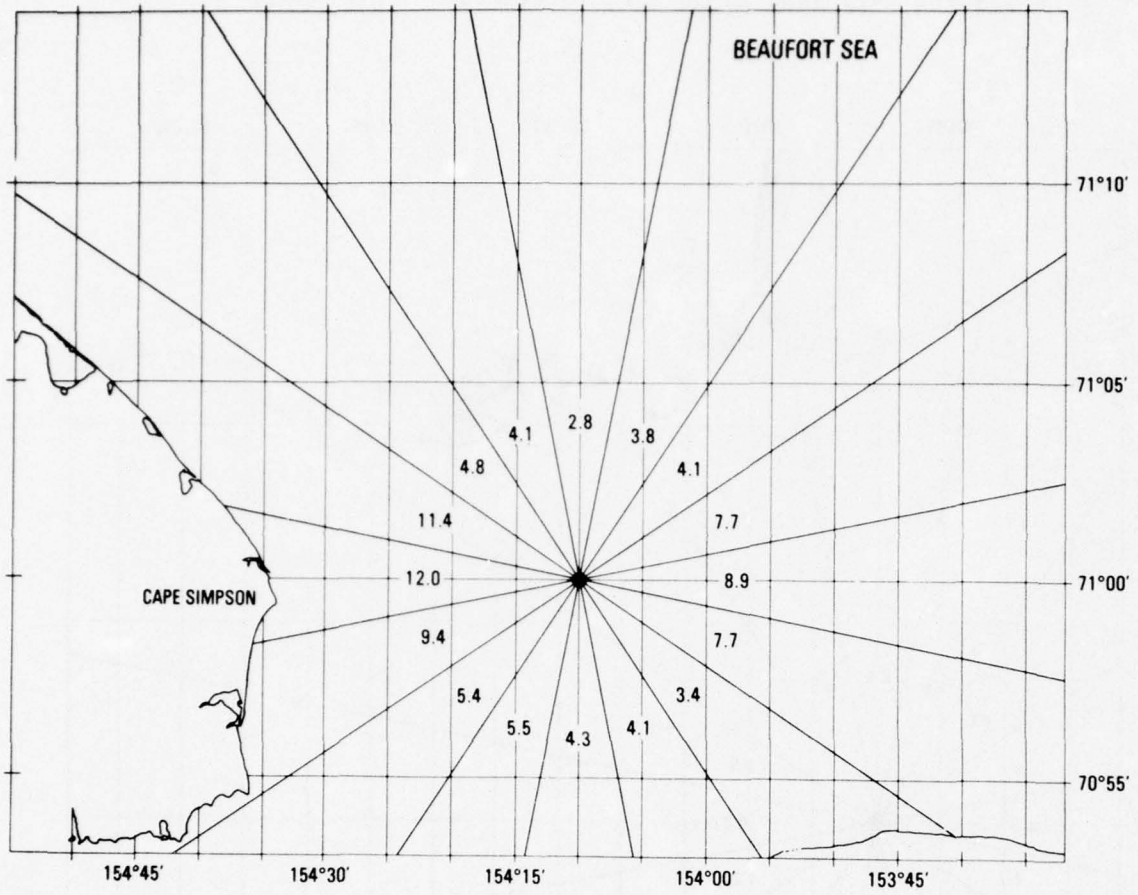

Figure 29. Potential impact areas near Cape Simpson for a spill site 7.7 nm offshore.

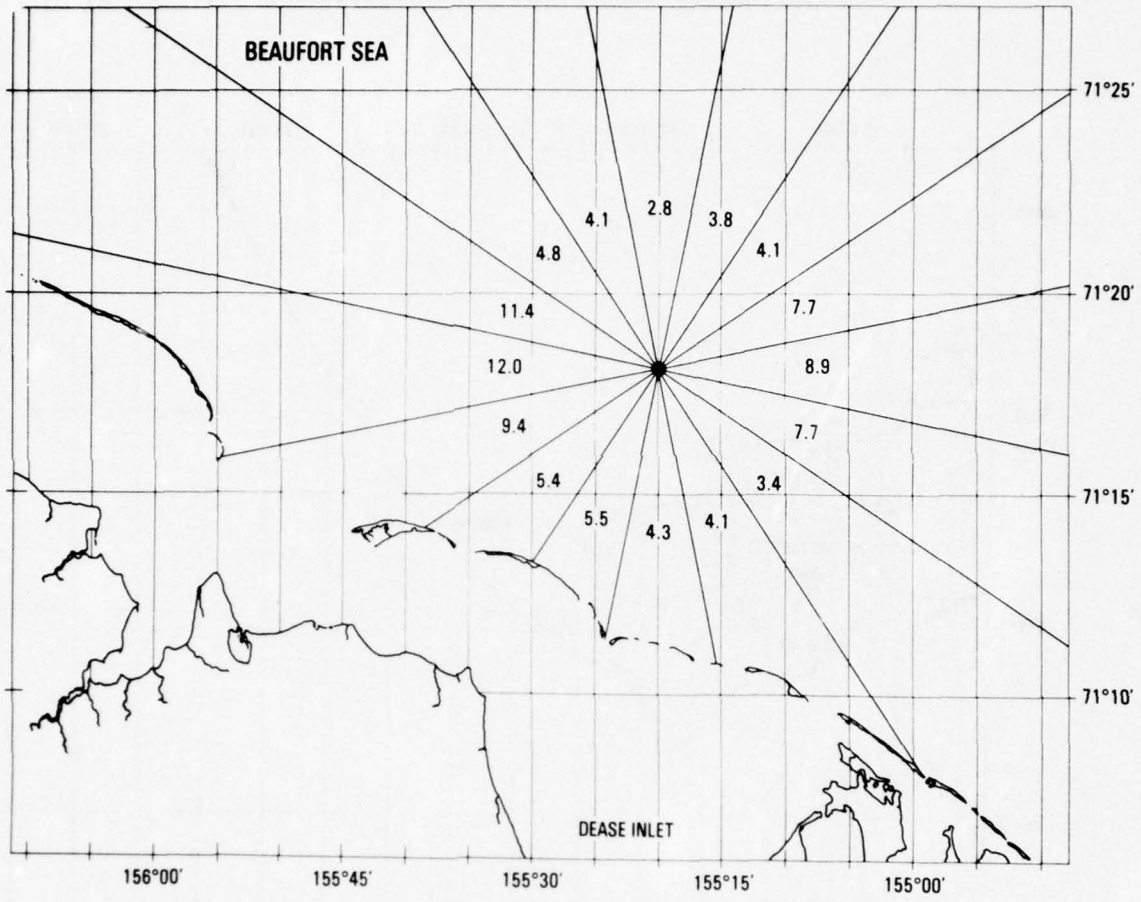

Figure 30. Potential impact areas near Dease Inlet for a spill site 5.5 nm offshore.

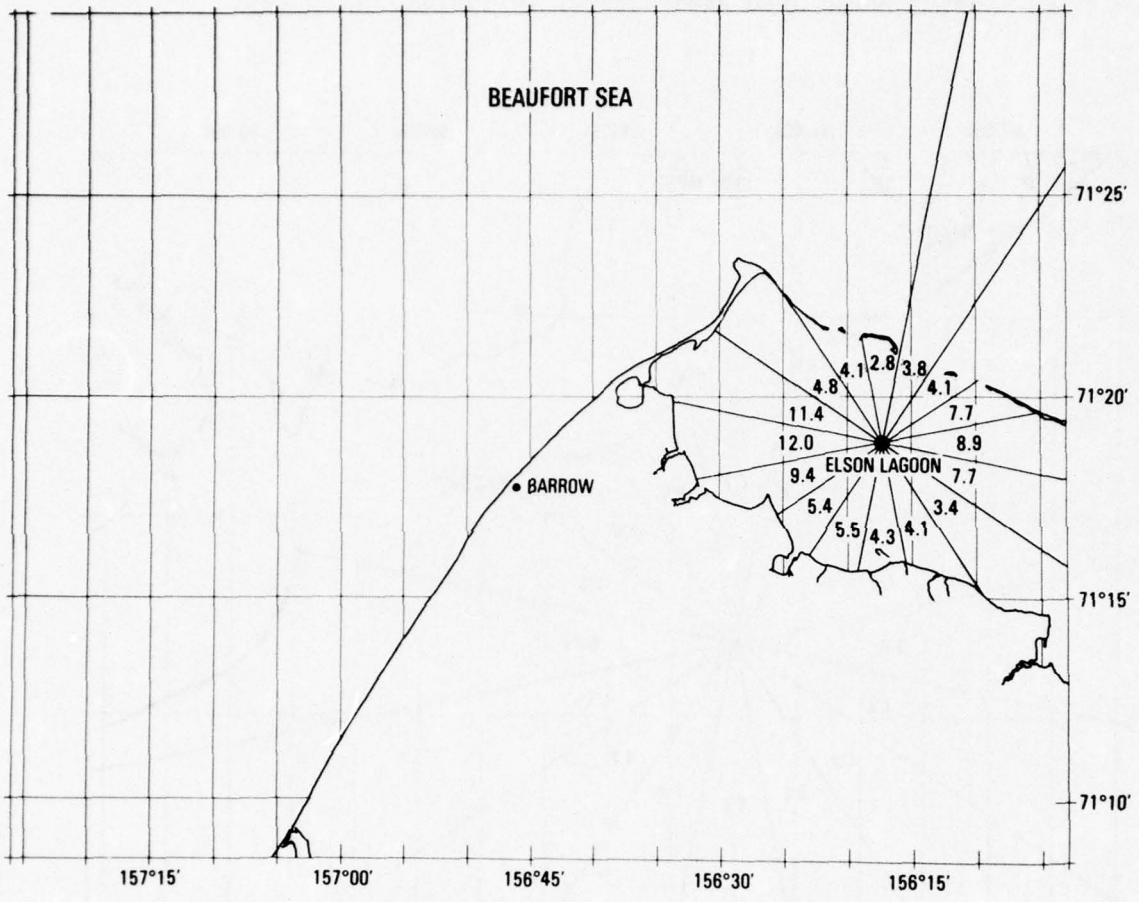

Figure 31. Potential impact areas near Elson Lagoon for a spill site 2.3 nm offshore.

TABLE 14

MINIMUM IMPACT TIME AND PROBABILITY OF IMPACT
FOR EACH OF THE FIFTEEN SELECTED SPILL SITES

FIGURE	DISTANCE TO SHORE (MILES)	MINIMUM IMPACT TIME (HOURS)	CONSTANT WIND DIRECTION FOR MINIMUM IMPACT TIME	PROBABILITY OF IMPACT (%)
17	8.5	25	ENE	60
18	5.0	12	ENE	56
19	6.0	27	NE	40
20	7.3	22	ENE	72
21	4.2	12	ENE	61
22	5.0	15	ENE	61
23	4.2	11	E	67
24	4.7	12	ENE	61
25	14.7	53	ENE	75
26	5.9	19	ENE	68
27	14.5	30	E	61
28	12.3	34	NNE	41
29	7.7	14	ENE	63
30	5.7	13	ENE	63
31	2.3	6	E	96

A graph was constructed of impact time versus distance offshore, using the data in Table 14, to assist in assessing environmental risk along the entire north Alaskan coastline. A best fit curve was calculated and fitted to the data and is shown in Figure 32. The equation of the curve is:

$$y = -6.54 + 4.81 \text{ x } -0.10x^2$$

where x is the distance offshore (in nautical miles) and y is the impact time (in hours). The equation can be used for computing minimum impact time for a spill to reach the coastline from any site offshore.

A map was developed (Figure 33) to show the probability of impact along the north Alaskan coastline. The 70 percent line in Figure 33 indicates that an oil spill occurring shoreward of the line has a 70 percent or greater probability of impacting the coastline. Likewise, a spill occurring shoreward of the 40 percent line has a 40 percent or greater probability of impacting the shoreline.

The map for impact probability (Figure 33) was developed as follows:

Fifteen transects were drawn from the shore through the fifteen arbitrarily selected spill sites. These transects are shown in Figure 33. The wind rose centers were placed along these lines and the probability of impact was computed for one, five, ten, fifteen, twenty, twenty-five and thirty miles offshore. As before, the probability of impact for each distance offshore was determined for each transect by adding all the wind frequency values of those sectors which intersected the shoreline. Two constraints on this method were used. First, if only one side of a sector intersected the coastline, half the frequency value was used in computing the total probability. Second, if the distance to the shoreline from the center of the wind rose for a particular sector was greater than fifty miles, that sector was omitted from the total probability computation. The results of these computations of impact probability versus distance offshore for each of the fifteen transects are shown in Figures 34 to 48. We arbitrarily selected the 40 percent and 70 percent probabilities in Figure 33. However, using Figures 34 to 48, any probability line can be computed and mapped.

Figures 17 through 48 indicate that drilling offshore of the North Slope could cause environmental risk to barrier islands and the coastline itself. For a discussion of the ecological impact of the oil, we refer the reader to Isakson, et. al (1975).

It is important when using Figures 17-31 that the user be aware of processes that can alter the predicted spill track. Along the eastern north Alaskan coast upwelling can occur. The oil spill model assumes lateral homogeneity along the coast. However, we know that inhomogeneity exists with respect to upwelling. These areas of convergence known to occur parallel to the coast may serve as traps and collectors for oil spilled near them.

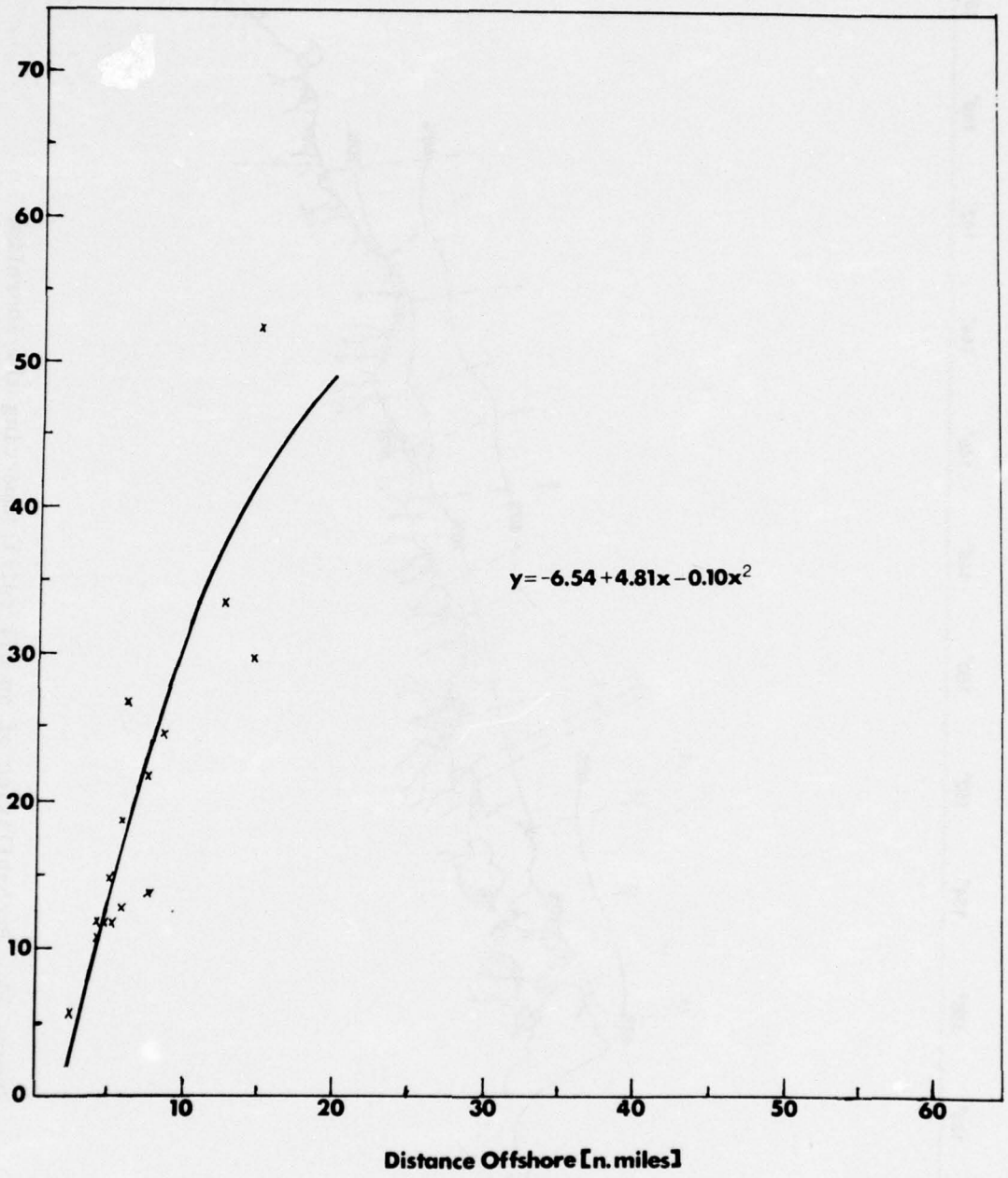

Figure 32. Impact time (hours) of an oil spill offshore to reach the coastline. (Distance in nautical miles.)

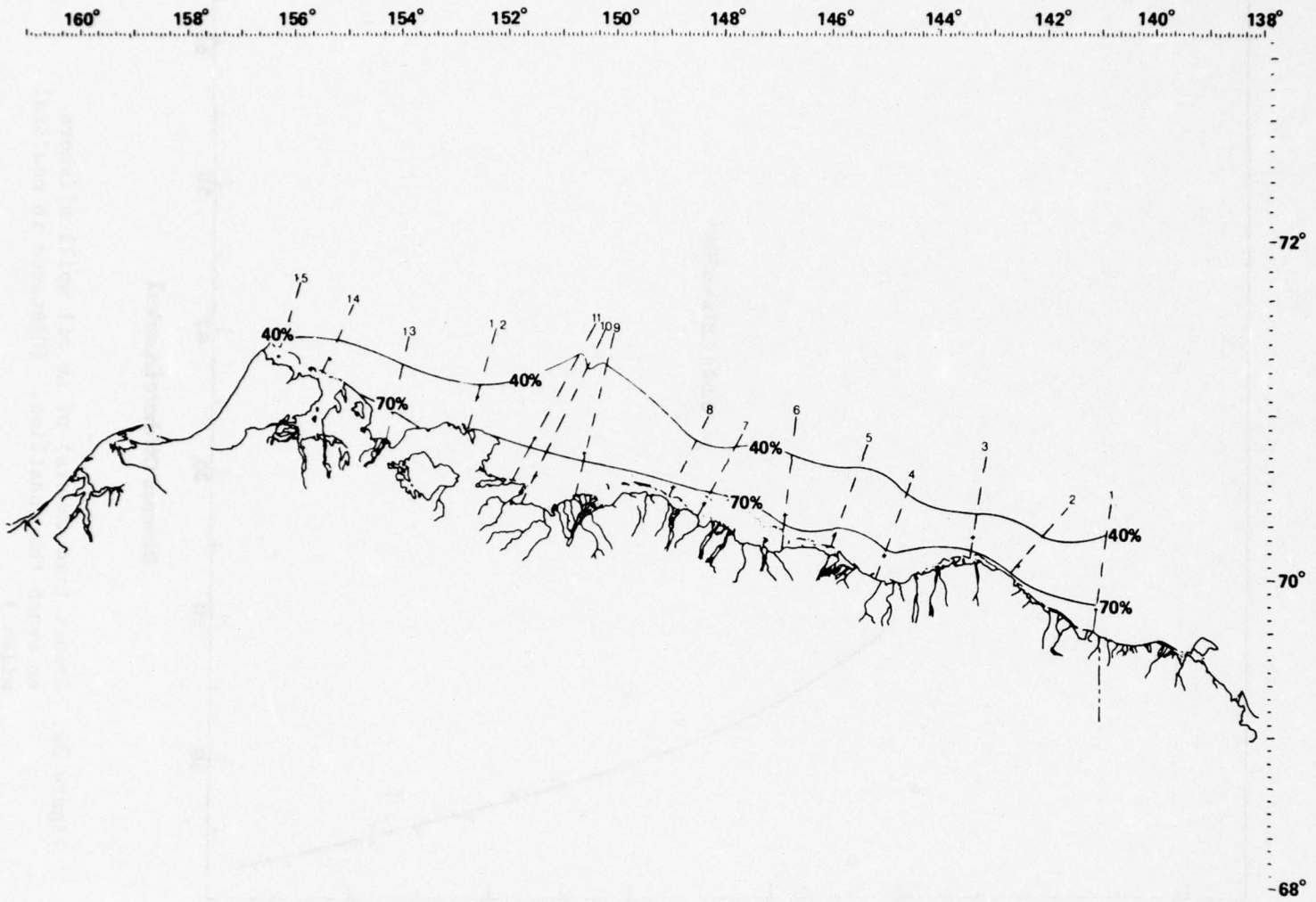

Figure 33. Probabilities of an oil spill impacting the shoreline for the entire Alaskan north coast.

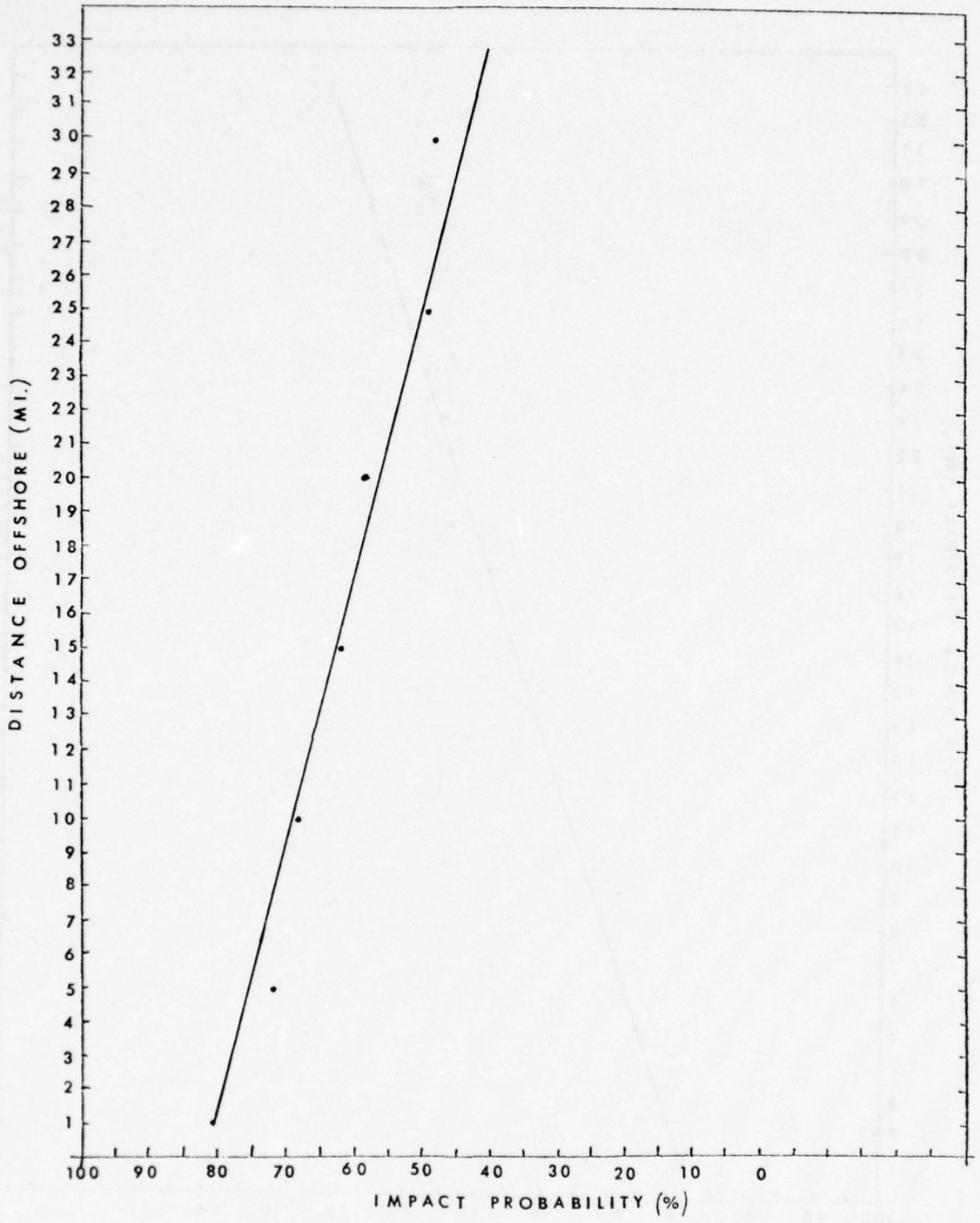

Figure 34. Impact probability as a function of distance offshore for area near Demarcation Bay.

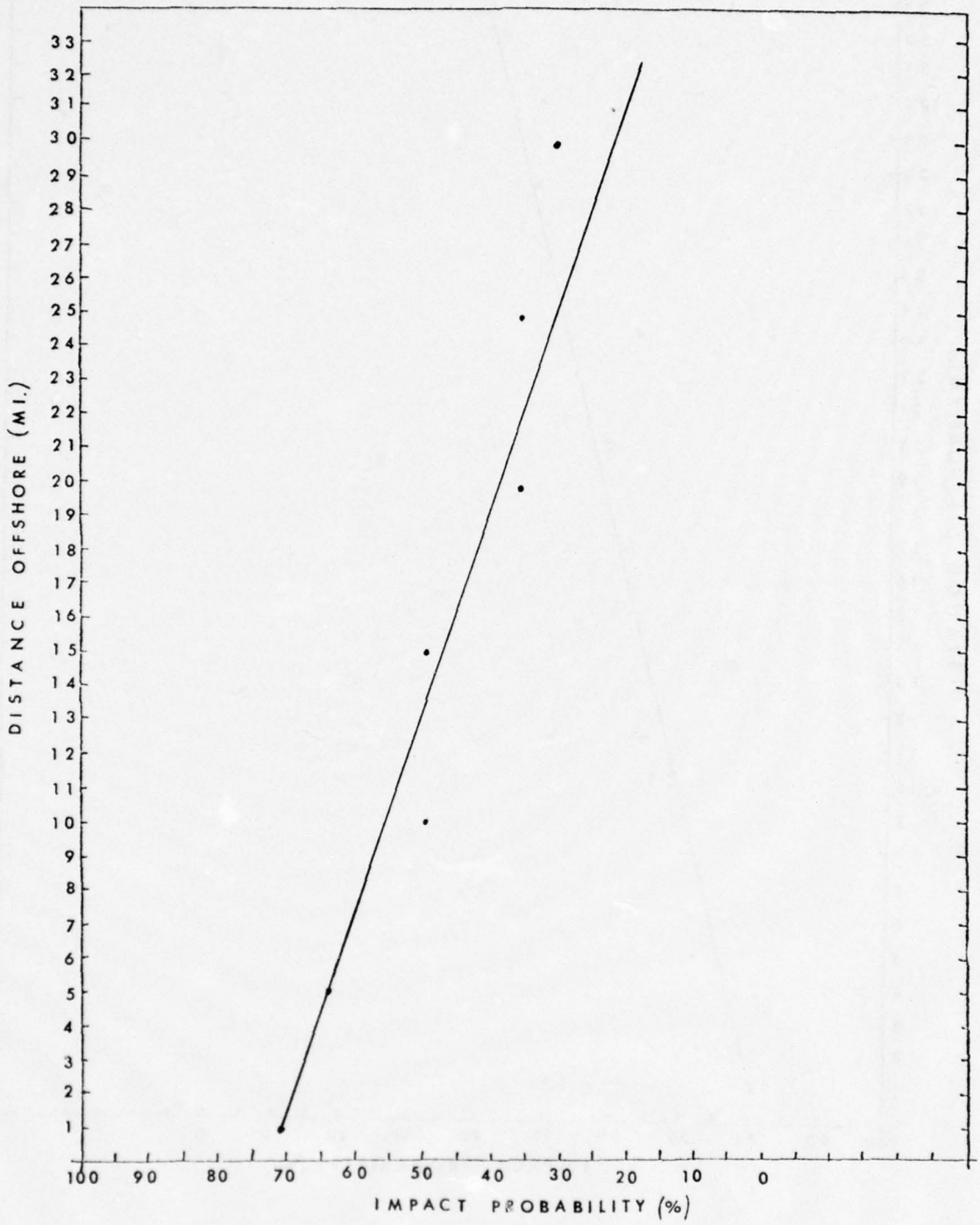

Figure 35. Impact probability as a function of distance offshore for area near Nuvasapak Lagoon.

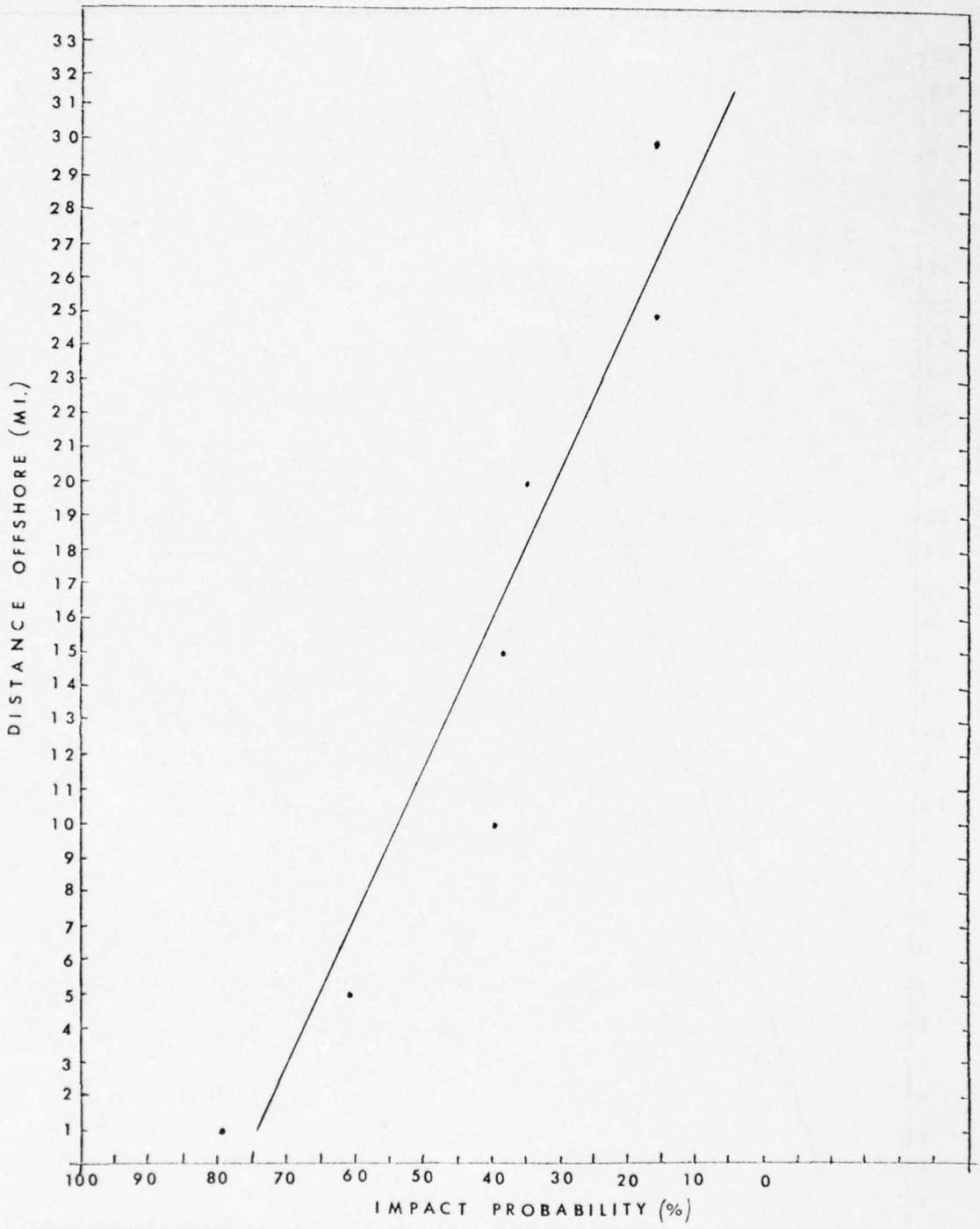

Figure 36. Impact probability as a function of distance offshore for area near Barter Island.

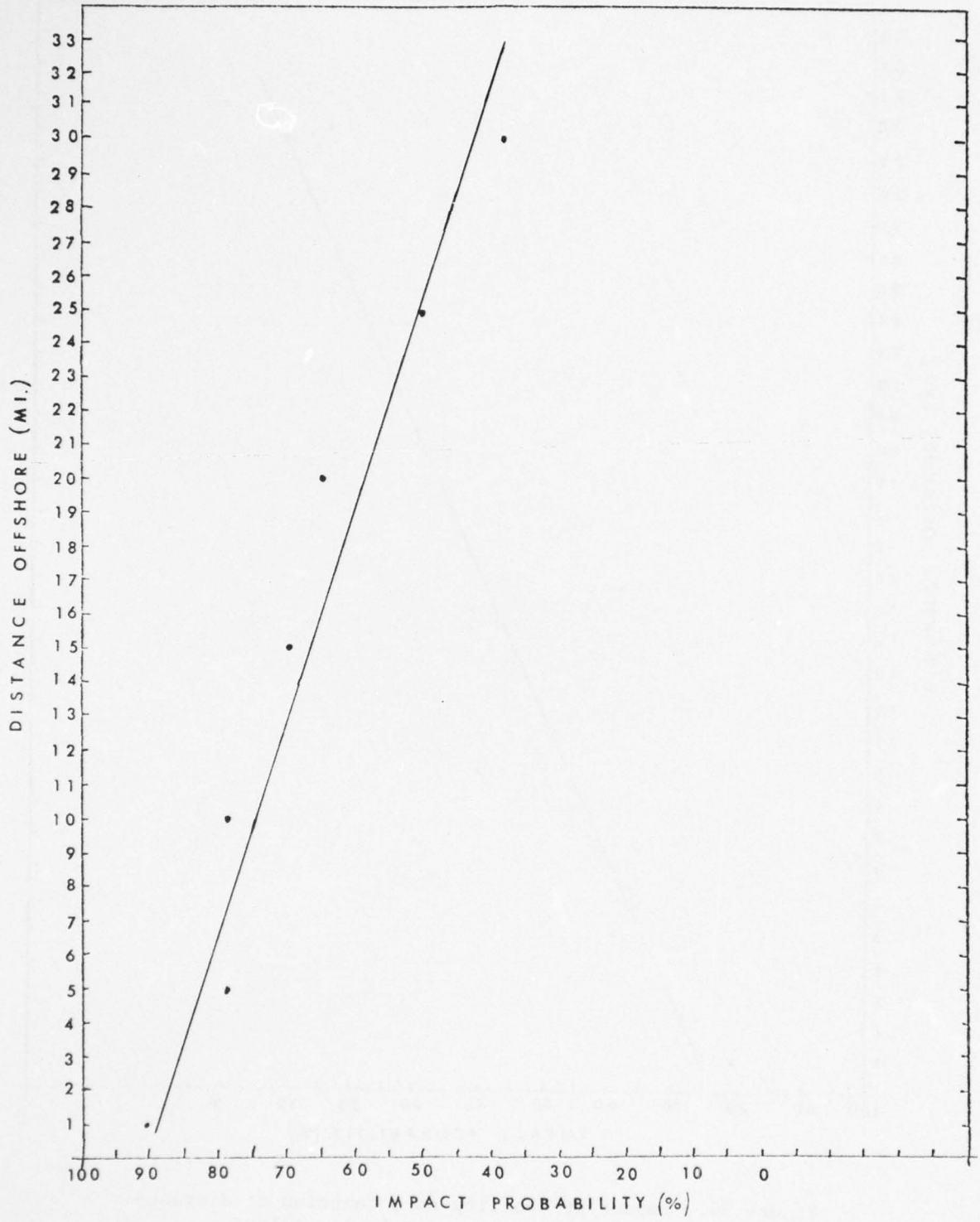

Figure 37. Impact probability as a function of distance offshore for area near Canning River.

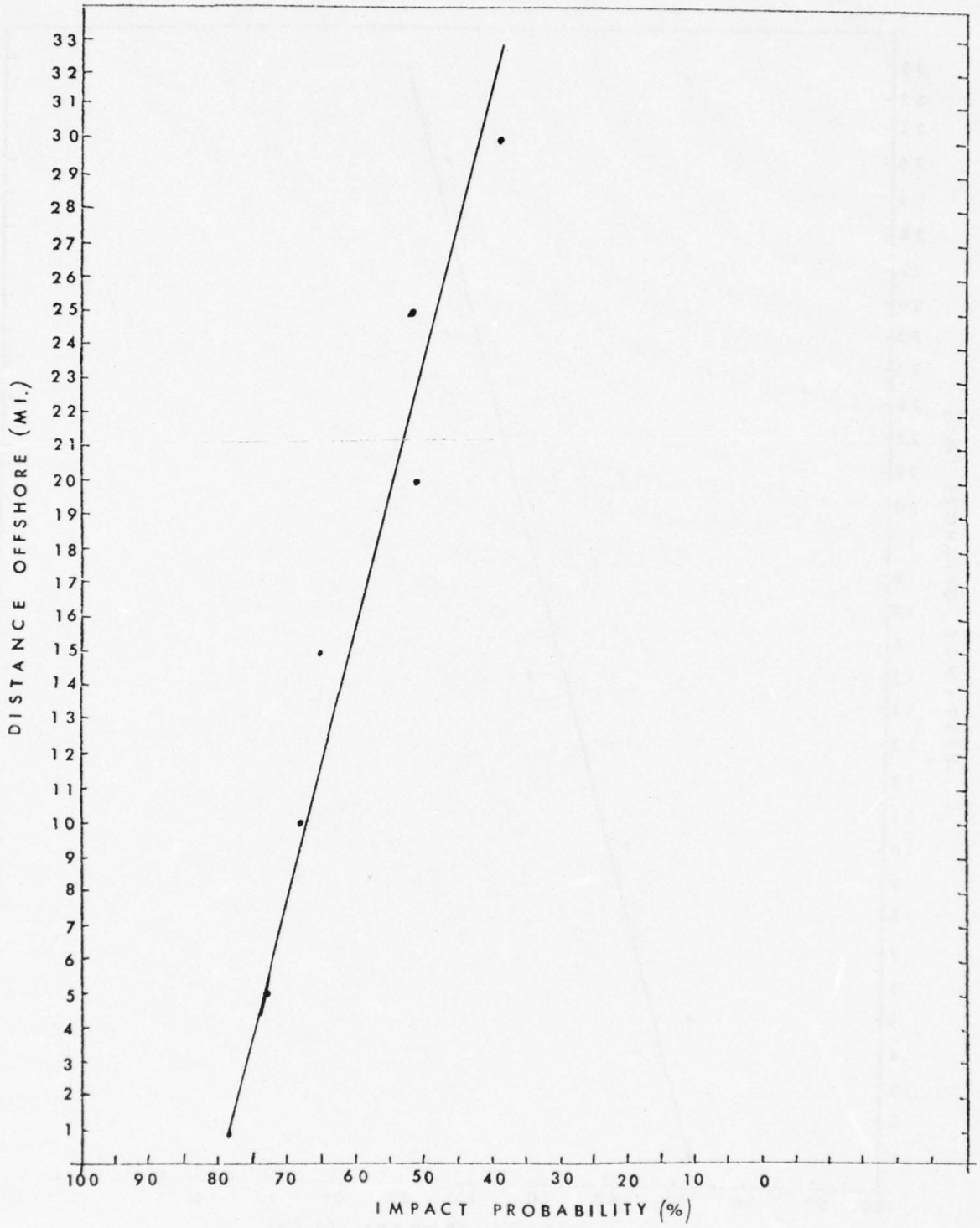

Figure 38. Impact probability as a function of distance offshore for area near Brownlow Point.

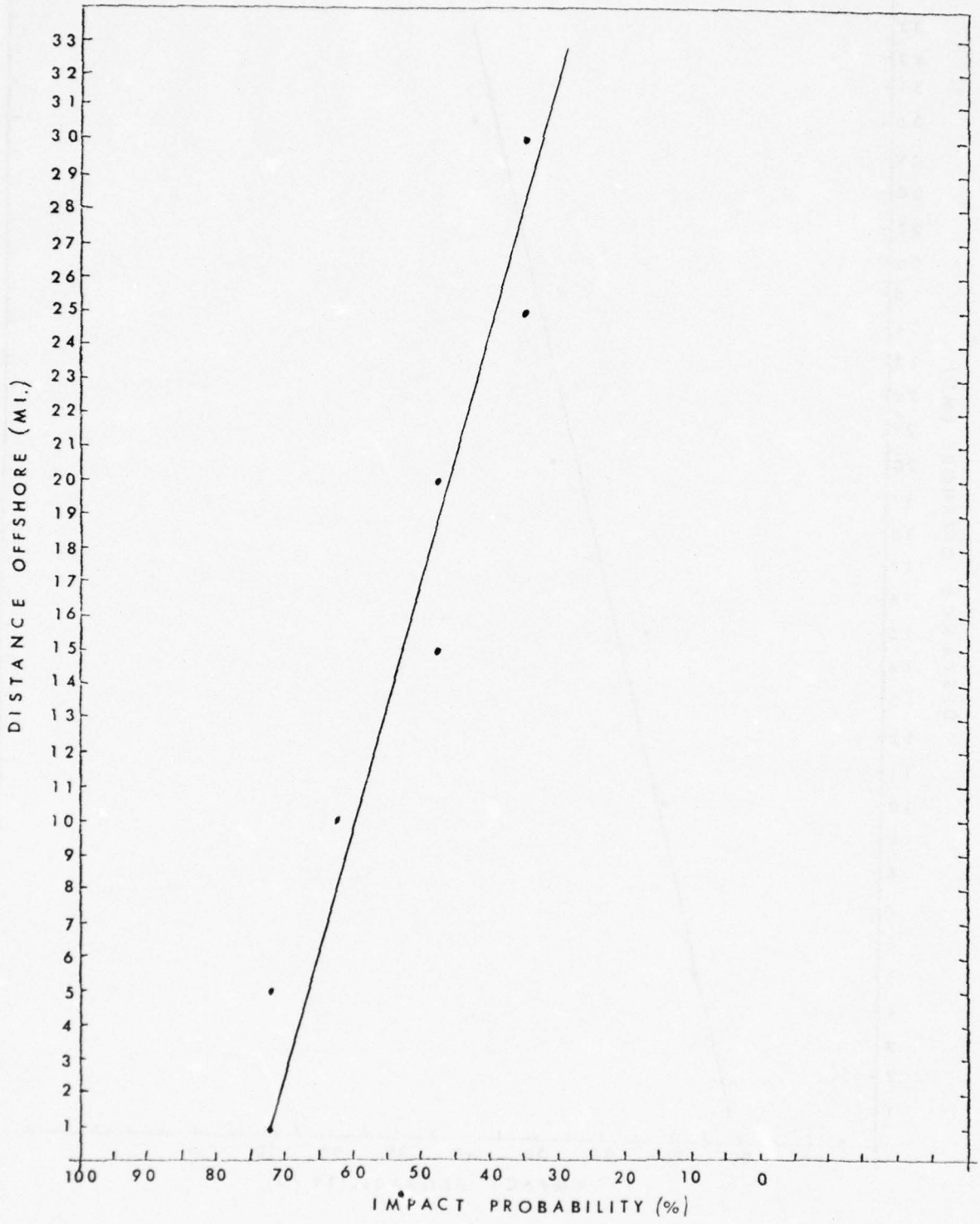

Figure 39. Impact probability as a function of distance offshore for area near Saviovik River.

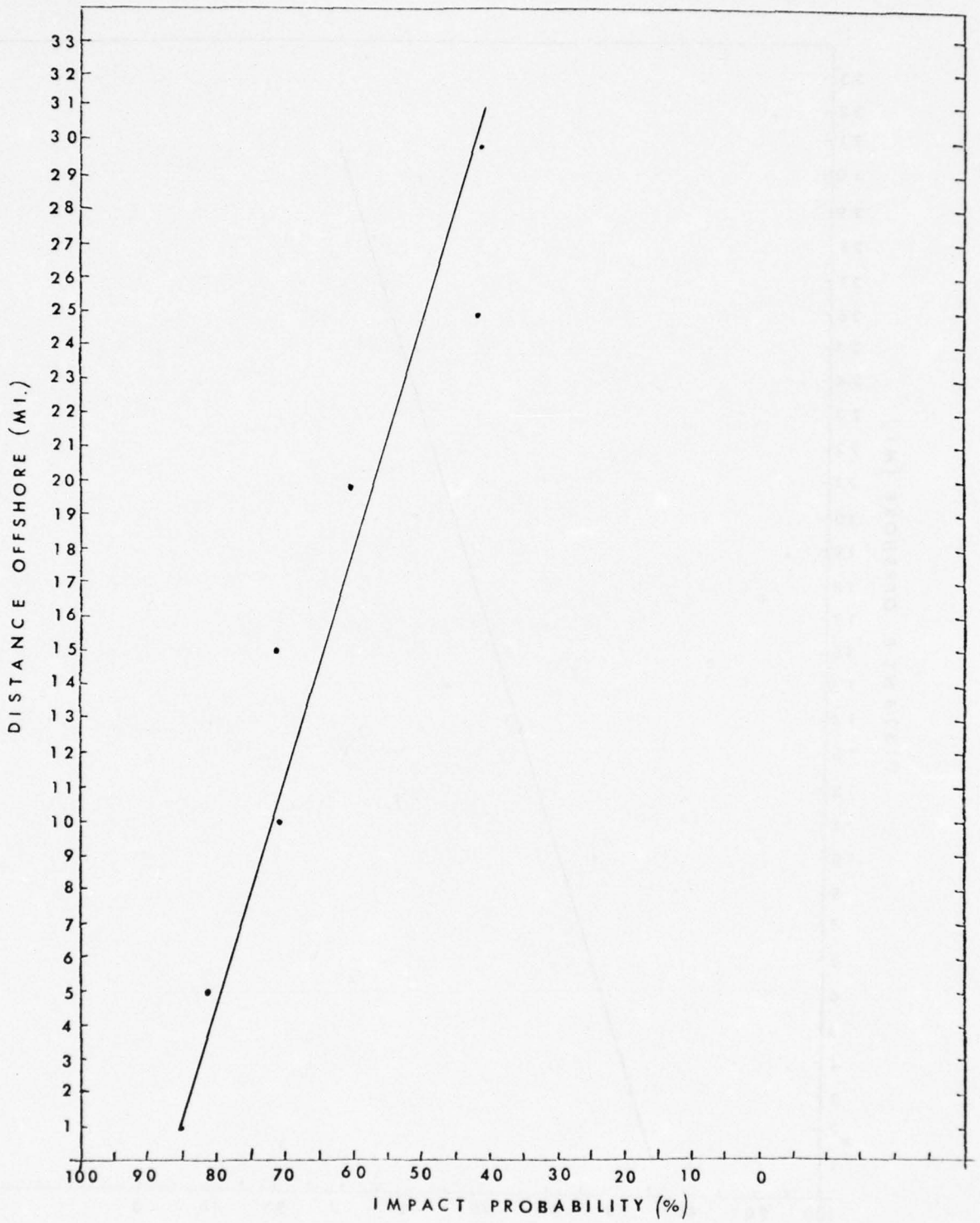

Figure 40. Impact probability as a function of distance offshore for area near Prudhoe Bay.

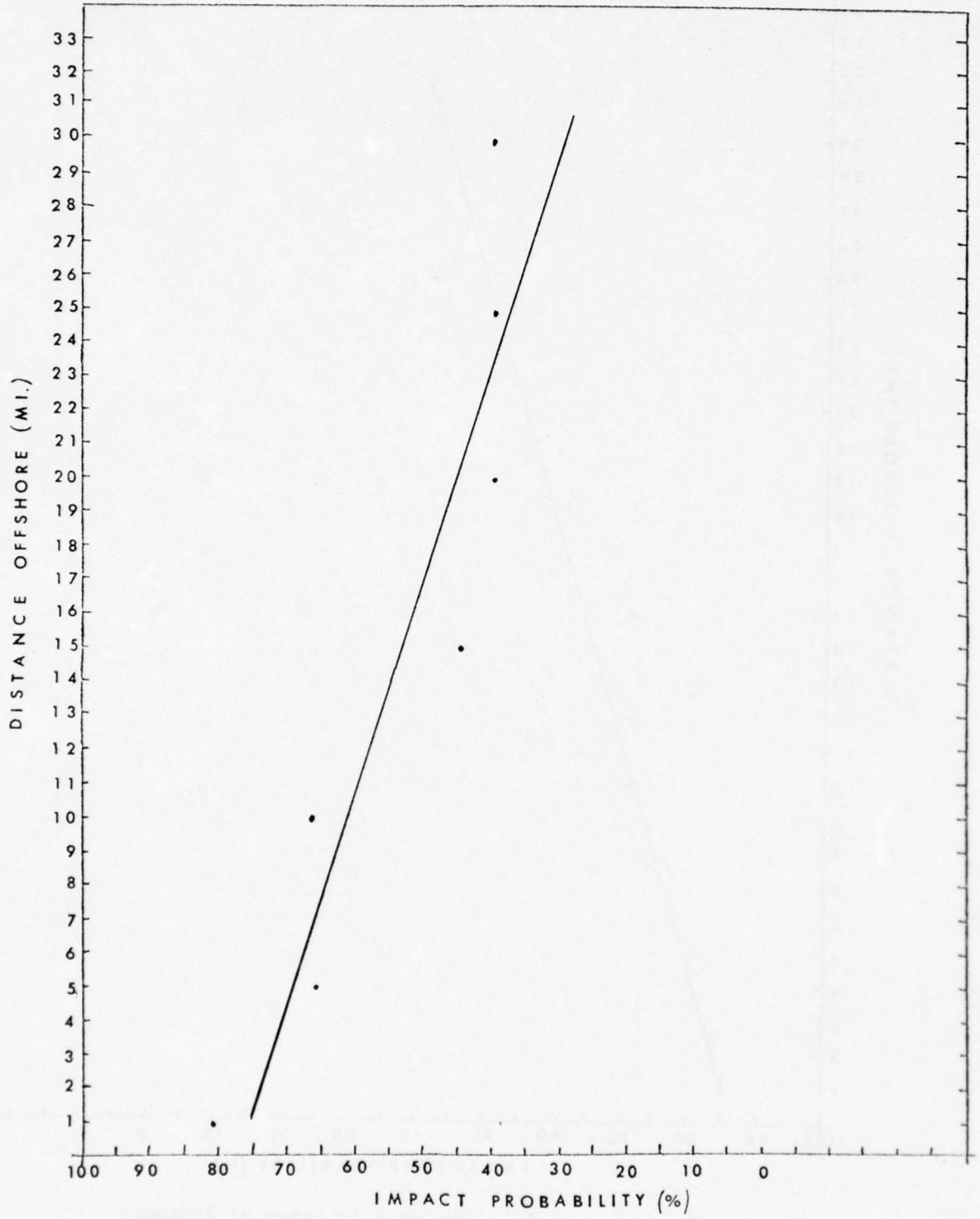

Figure 41. Impact probability as a function of distance offshore for area near Beechey Point.

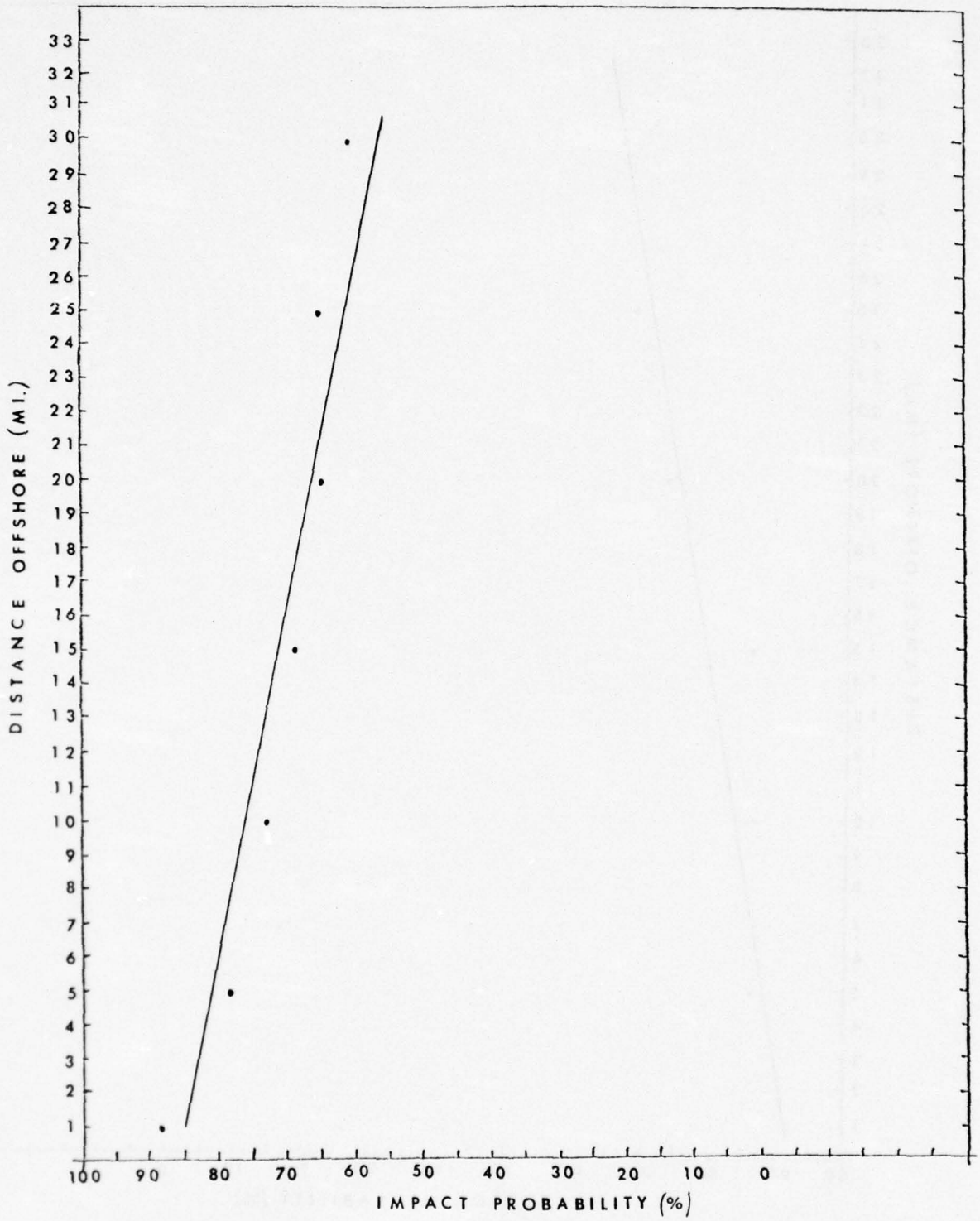

Figure 42. Impact probability as a function of distance offshore for area near Calville River.

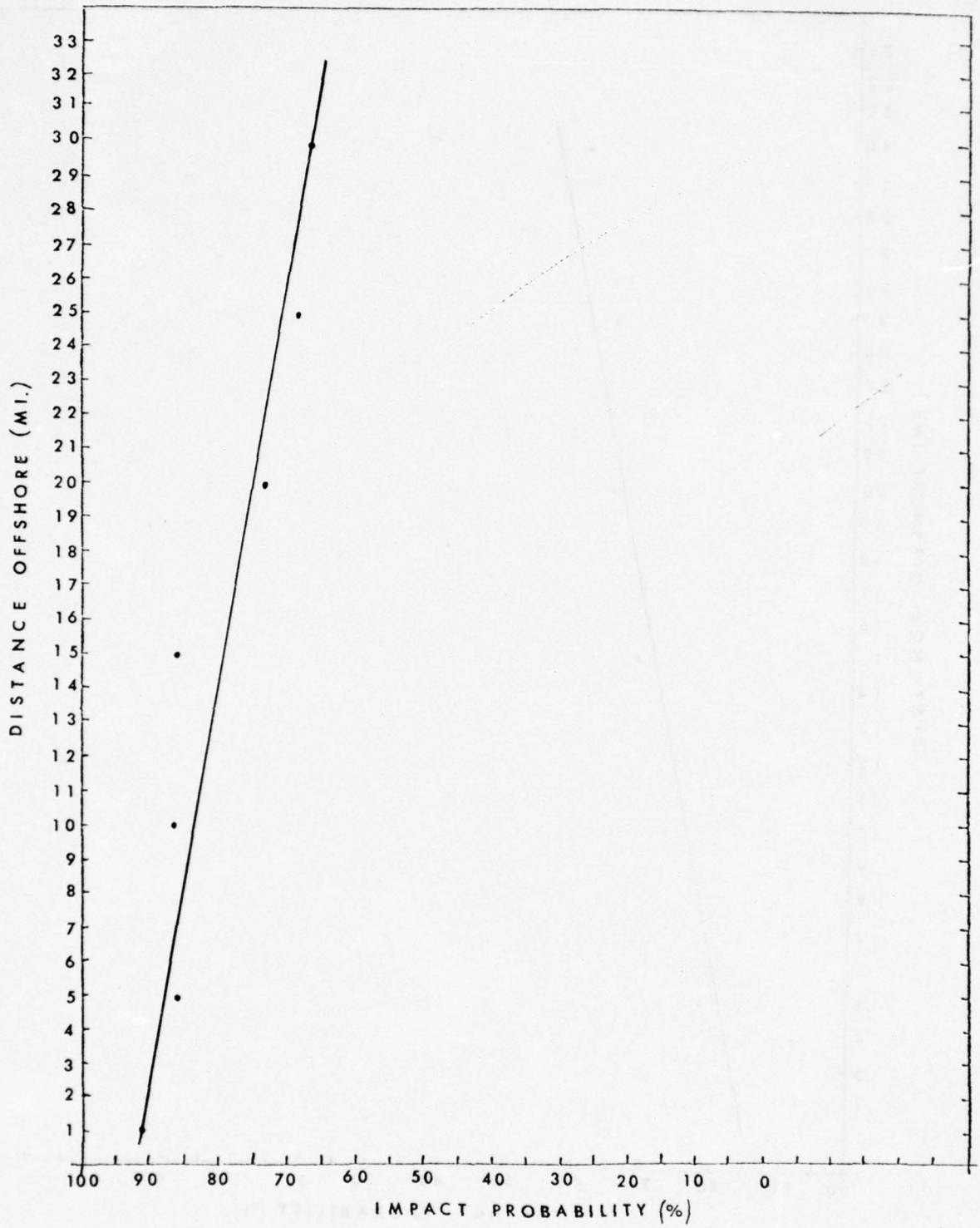

Figure 43. Impact probability as a function of distance offshore for area near Atigaru Point.

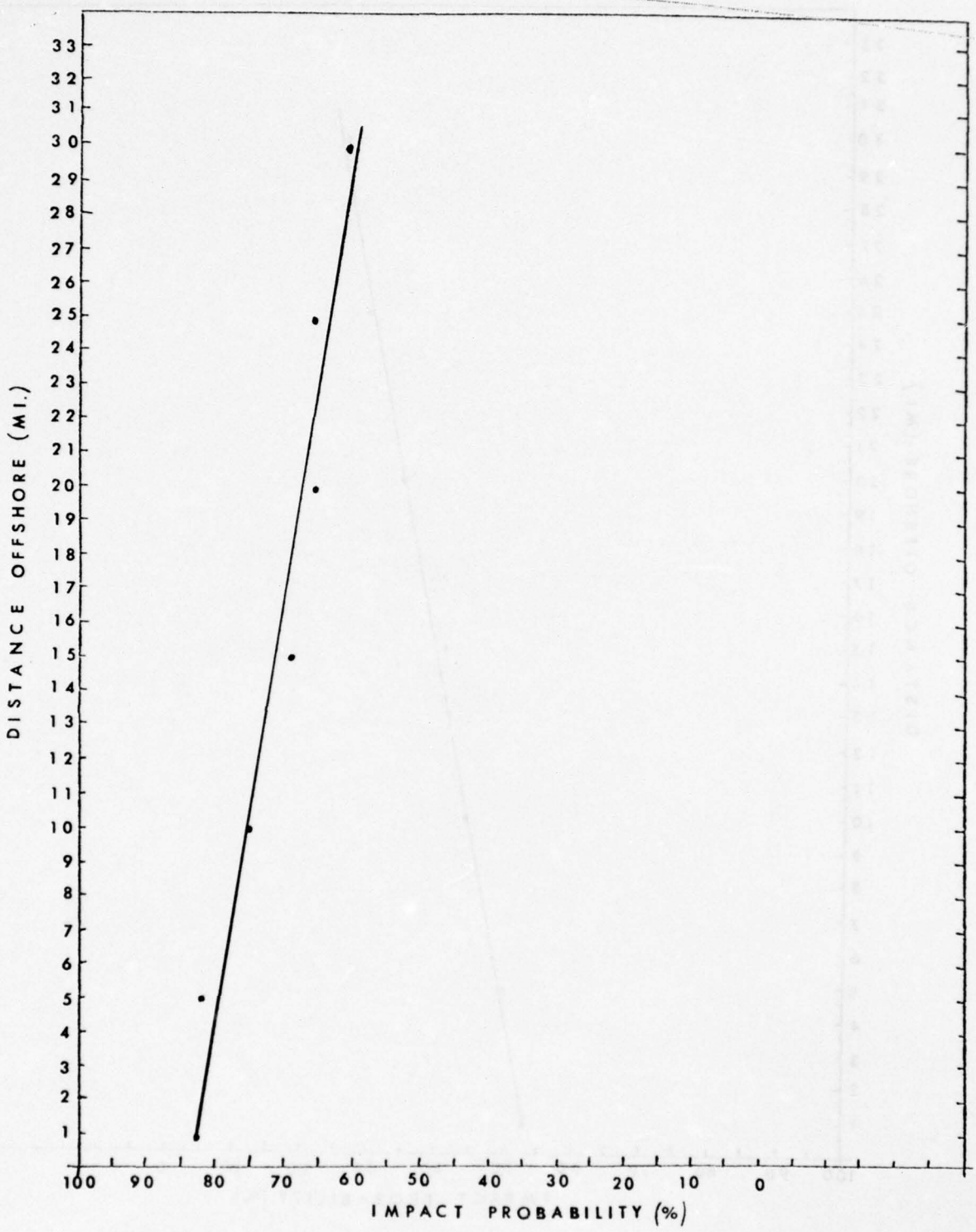

Figure 44. Impact probability as a function of distance offshore for area near Cape Halkett.

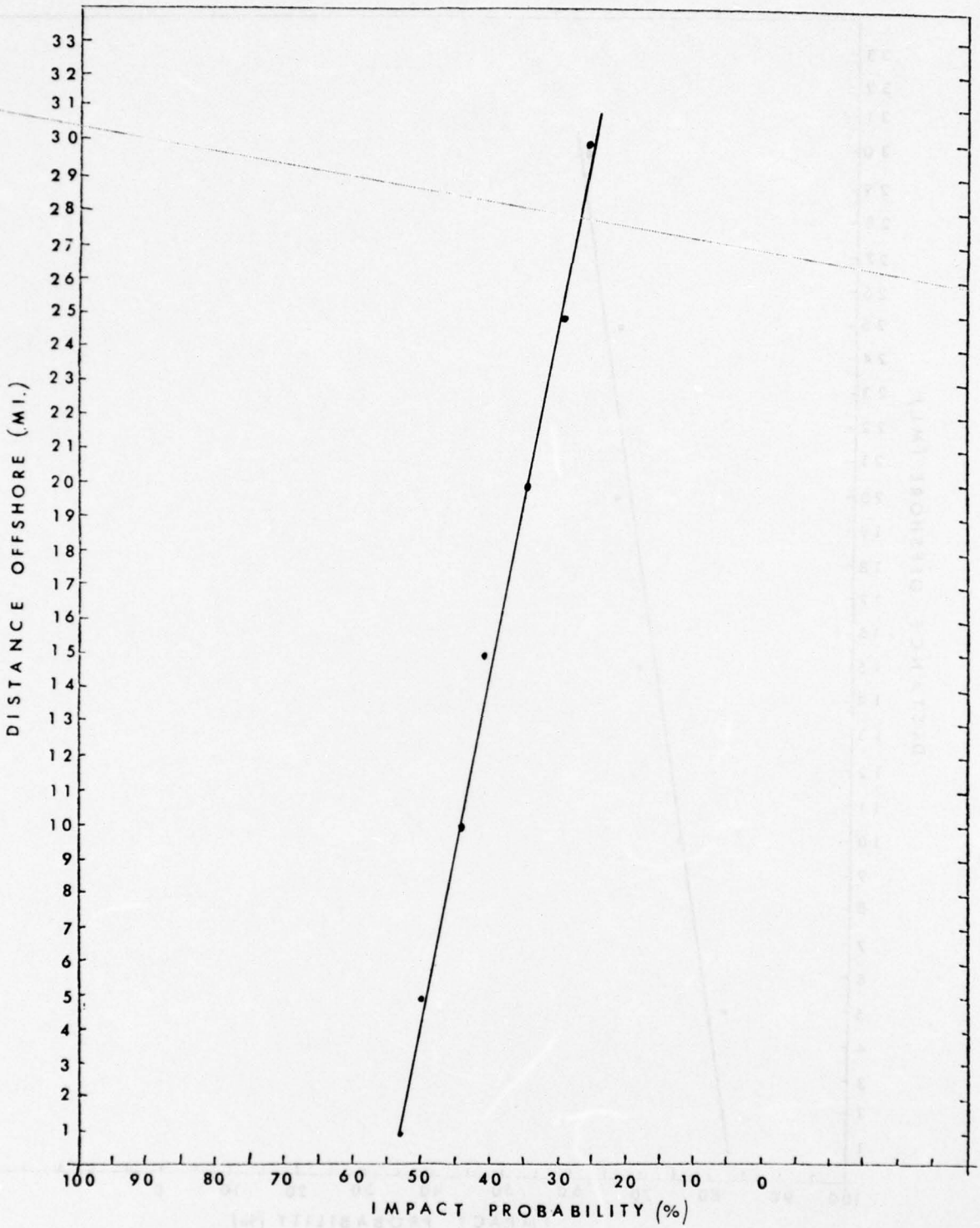

Figure 45. Impact probability as a function of distance offshore for area near Pitt Point.

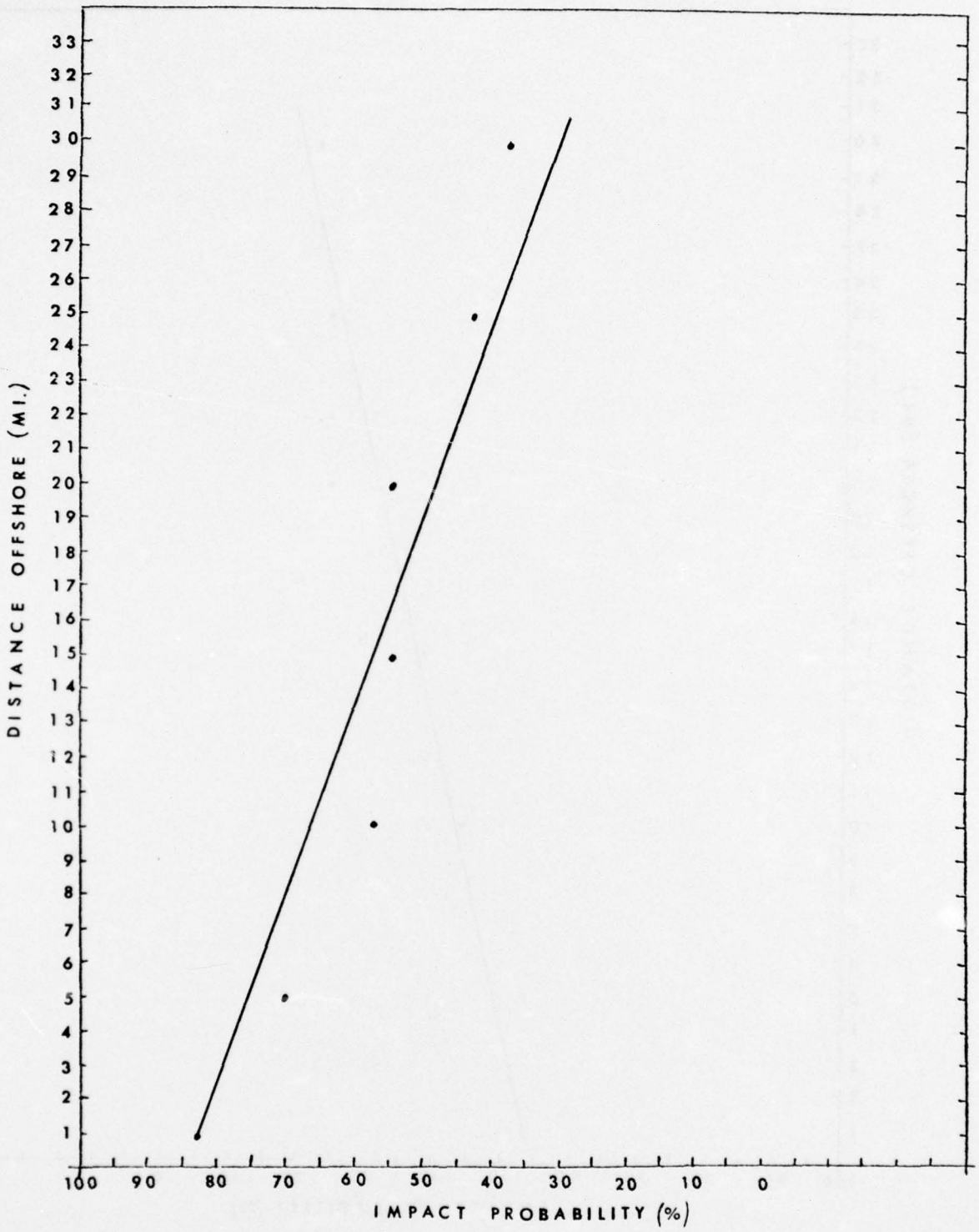

Figure 46. Impact probability as a function of distance offshore for area near Cape Simpson.

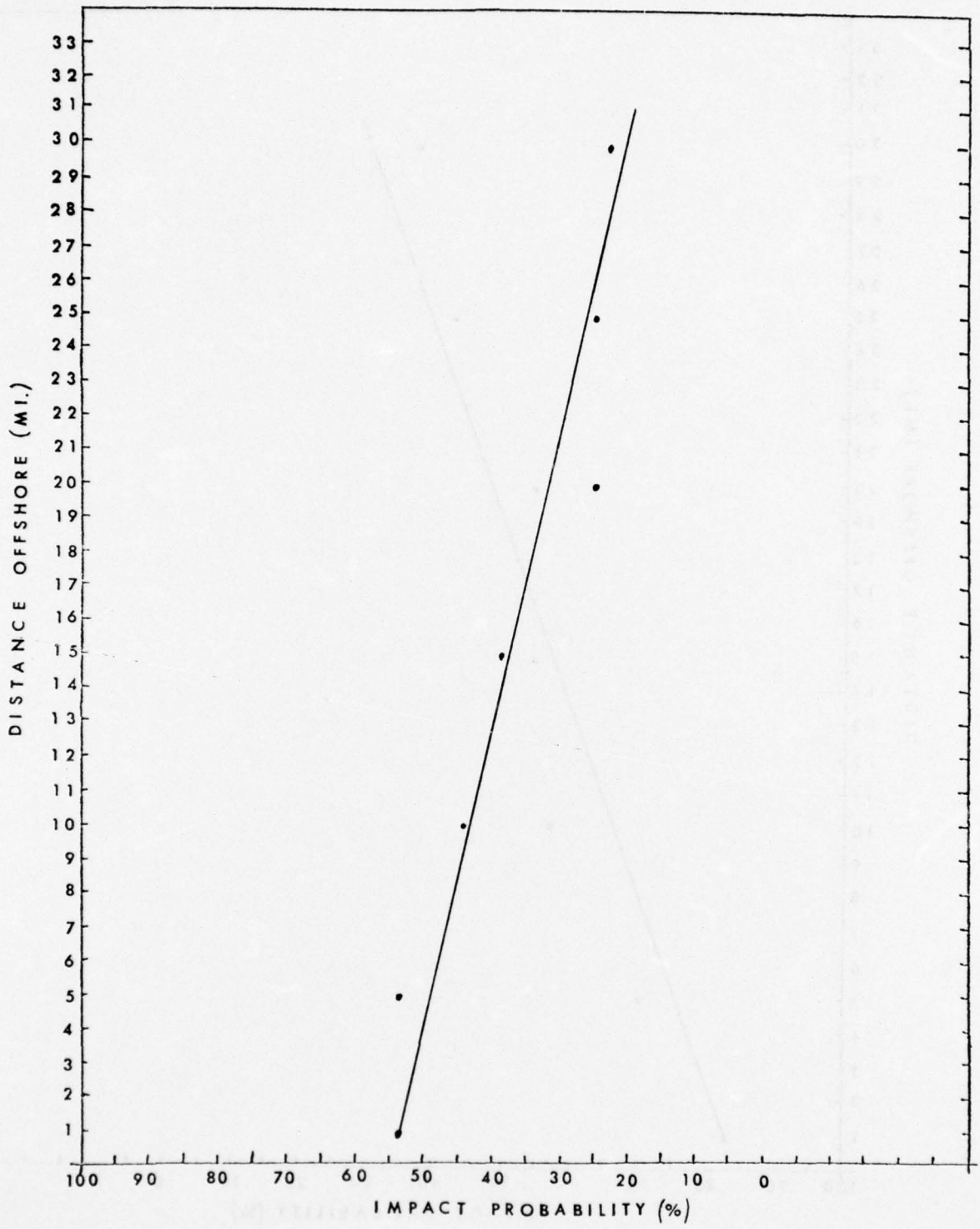

Figure 47. Impact probability as a function of distance offshore for area near Dease Inlet.

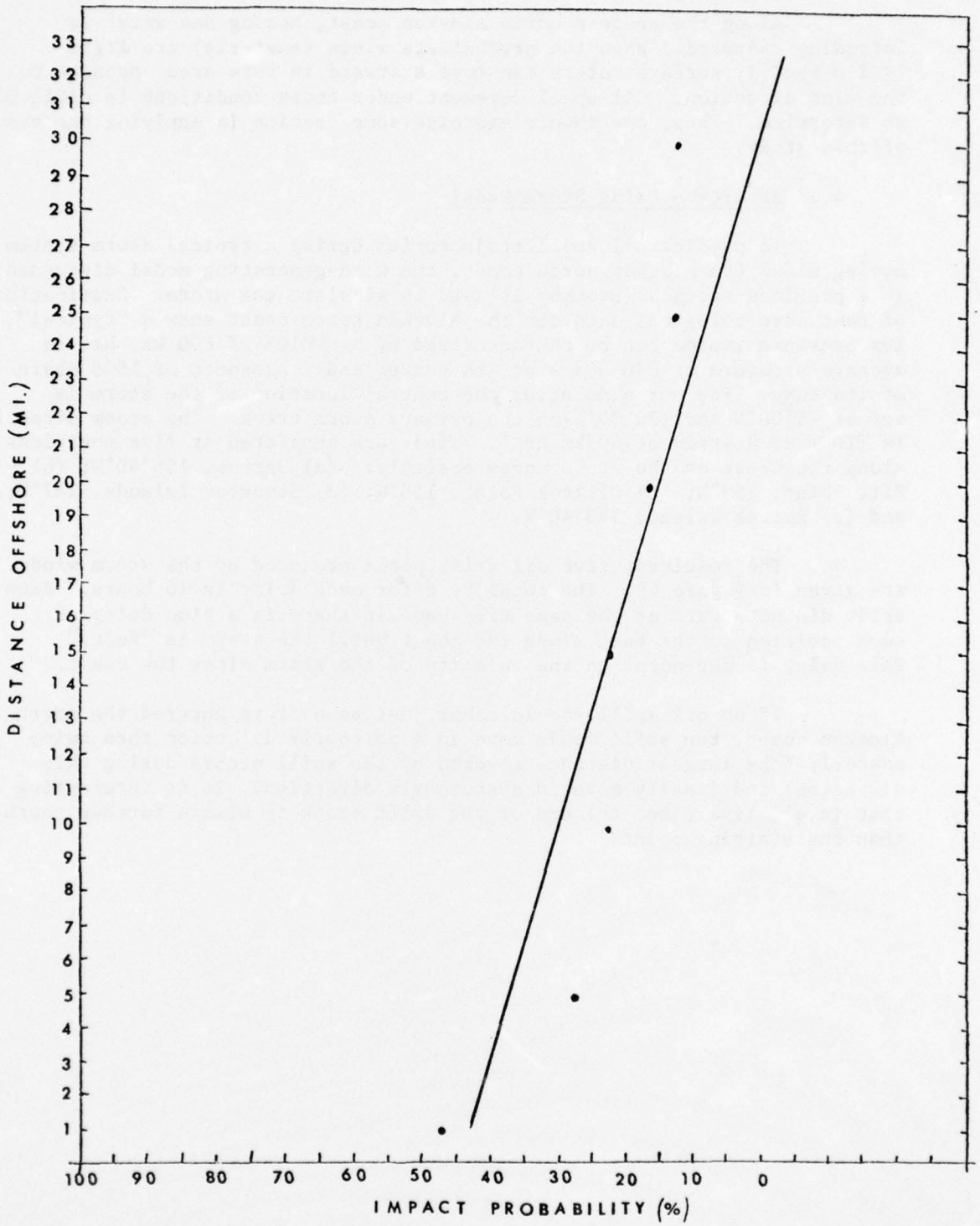

Figure 48. Impact probability as a function of distance offshore for area near Elson Lagoon.

Along the western north Alaskan coast, Bering Sea water is intruding eastward. When the predominate winds (easterly) are light (< 2 m sec^{-1}), surface waters can move eastward in this area opposite to the wind direction. Oil spill movement under these conditions is difficult to determine. Thus, one should exercise some caution in applying the results of this study.

4.2 Results - Using Storm Model

To predict oil spill trajectories during a typical storm system moving along the Alaskan north coast, the wind-generating model discussed in a previous section (Storms) is used to simulate the storm. Examination of past meteorological data for the Alaskan north coast show a "typical" low pressure system can be characterized by a radius of 600 km, has an average pressure of 996 mbars at its center and a pressure of 1008 mbars at its edge. For our simulation the central location of the storm is set at 75°00'N and 170°00'W on the primary storm track. The storm direction is 110°T at a speed of 40 km hr^{-1}. Winds are generated at five positions along the coast as the storm moves easterly: (a) Barrow, 156°40'W; (b) Pitt Point, 153°W; (c) Oliktok Point, 150°W; (d) Stockton Islands, 147°W; and (e) Barter Island, 143°40'W.

The resultant five oil drift paths produced by the storm winds are given in Figure 49. The total time for each drift is 16 hours. Each drift did not start at the same time because there is a time delay at each position to the east along the coast until the storm is "felt." This delay is dependent on the velocity of the storm along the coast.

If an oil spill should occur just as a storm entered the north Alaskan coast, the spill would move in a northerly direction then swing easterly (the largest distance covered by the spill occurs during this direction) and finally move in a southerly direction. It is interesting that in all five cases the end of the drift track is always farther south than the starting point.

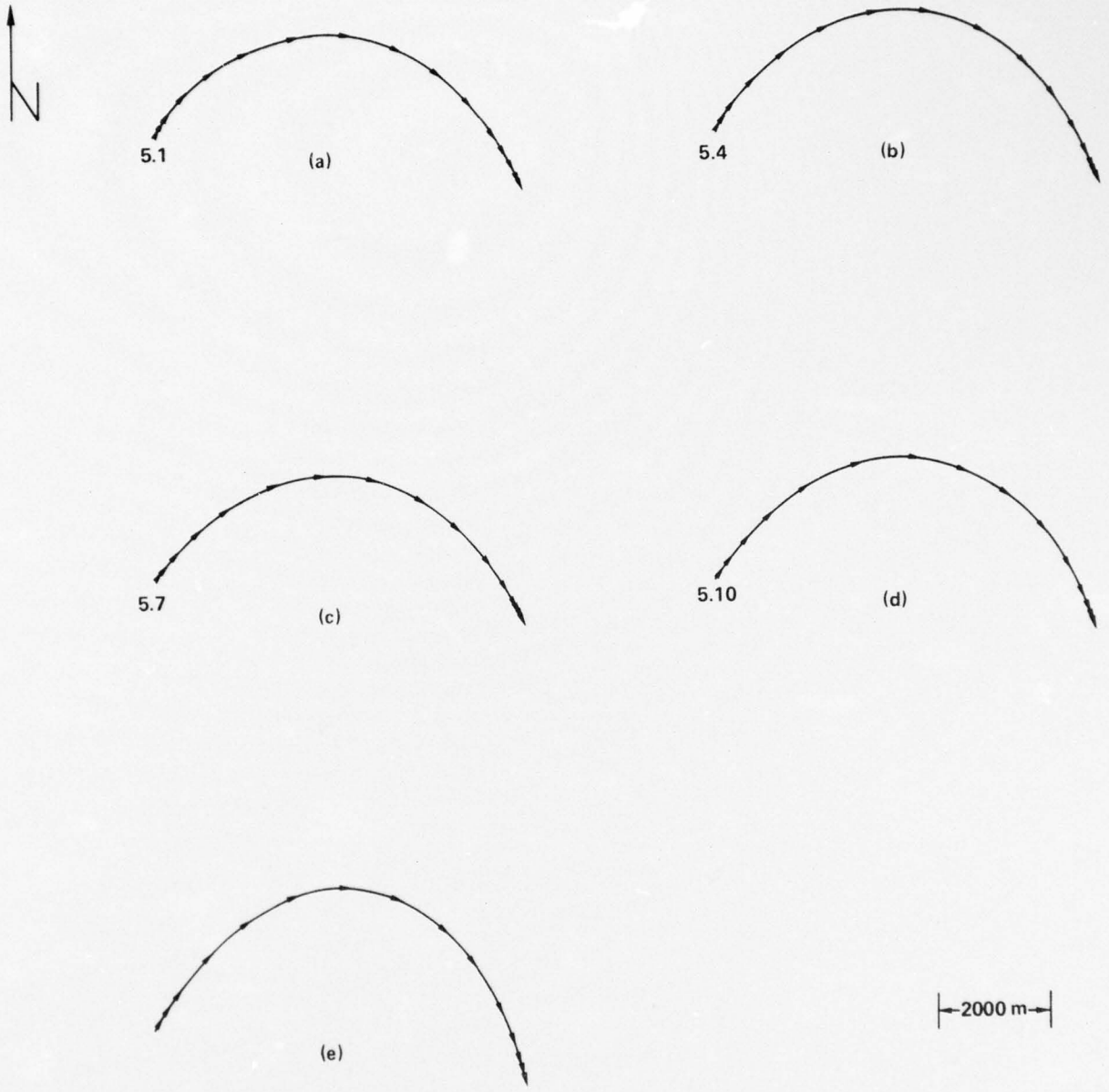

Figure 49. Drift tracks due to a low pressure system moving on the primary storm track across the Alaskan north coast: (a) 156°40'W, (b) 153°W, (c) 150°W, (d) 147°W, and (3) 143°40'W.

APPENDIX 1

POSITION	DATE	LOCAL TIME	SURFACE (Kn) SPEED	SURFACE (°T) DIR	SHIP
	1956				USS ELDORADO
71°21'N	17 Aug	1030	0.9	118	
156°44'W	17 Aug	1410	1.1	127	
	18 Aug	1015	0.5	083	
		1410	0.6	065	
	19 Aug	1600	0.3	103	
	20 Aug	1030	0.6	049	
		1600	0.2	023	
	21 Aug	1145	1.3	105	
	22 Aug	1410	0	0	
		2200	0	0	
	23 Aug	1100	0.8	054	
		1140	0.6	060	
		1450	0.8	053	
	24 Aug	1400	0	0	
	25 Aug	1030	0	0	
		1405	0.3	260	
	26 Aug	0815	1.2	118	
		1400	0	0	
	27 Aug	0900	0	0	
	1956				USS REQUISITE
71°21.9'N	22 Jul	2135	1.1	161	
146°43'W	23 Jul	0001	1.3	166	
		0435	1.4	179	

APPENDIX 1 (cont.)

POSITION	DATE	LOCAL TIME	SURFACE (Kn) SPEED	SURFACE (°T) DIR	SHIP
	1957				USS ELDORADO
71°21'N	6 Aug	0255	1.5	058	
156°46'W	6 Aug	0500	1.5	075	
	7 Aug	1816	1.5	104	
71°21'N	7 Aug	2246	1.8	026	
156°42'W	8 Aug	2240	2.2	021	
71°26'N	9 Aug	1805	2.1	040	
156°44'W	9 Aug	2145	2.1	025	
	10 Aug	0210	2.2	120	
		0502	2.0	046	
	12 Aug	1930	2.3	122	
	14 Aug	0220	2.3	122	
		1812	2.3	122	
	16 Aug	1755	2.3	134	
	1957	*	**		USS ATKA
70°23'N	1 Aug	0950	0.2	079	
144°46'W					
69°51'N	1 Aug	2230	0.4	019	
141°09'W					
70°25'N	7 Aug	2215	0	0	
148°28'W					
71°10'N	8 Aug	1110	0.6	129	
154°00'W					

APPENDIX 1 (cont.)

POSITION	DATE	LOCAL TIME	SURFACE (Kn) SPEED	SURFACE (°T) DIR	SHIP
	1957	*	**		USS ATKA
69°03'N 166°37'W	10 Aug	1040	1.1	035	
69°16'N 167°33'W	10 Aug	1440	0.7	050	
60°53'N 151°31'W	21 Aug	2210	0.1	099	
	1958		**		USS BURTON ISLAND
70°30'N 143°32'W	1 Sep	0000	0.1	249	
69°55'N 140°58'W	3 Sep	1915	0.1	089	
70°30'N 145°00'W	4 Sep	0530	0.1	047	
70°46'N 148°30'W	4 Sep	1215	0	173	
71°07'N 151°08'W	4 Sep	2040	0.1	221	
71°20'N 154°00'W	5 Sep	0245	0.0	176	

APPENDIX 1 (cont.)

POSITION	DATE	LOCAL TIME	SURFACE (Kn) SPEED	SURFACE (°T) DIR	SHIP
	1958		**		USS BURTON ISLAND
71°31'N 156°47'W	6 Sep	0650	0.2	236	
71°45'N 155°30'W	6 Sep	1020	0.4	256	
	1971				CGC GLACIER
70°38.4'N	28 Aug	0100-0330	0.15	161	
148°04.0'W	28 Aug	0330-0600	0.04	181	
		0600-0920	0.08	162	
70°39'N	8 Sep	0334-0604	0.04	267	
148°21'W	8 Sep	0604-1016	0.17	303	
		1016-1300	0.07	312	
		1300-1400	0.18	007	
70°41.2'N	8 Sep	2046-2436	0.09	287	
148°22.3'W	9 Sep	0036-0445	0.1	172	
		0445-0630	0.1	295	

APPENDIX 1 (cont.)

POSITION	DATE	LOCAL TIME	SURFACE (Kn) SPEED	SURFACE (°T) DIR	SHIP
	1971				CGC GLACIER
71°07.5'N 153°00.0'W	16 Sep	0245-1245	0.4	317	
71°23.8'N 154°31.5'W	17 Sep	0050-0420	0.26	095	

REFERENCES

Bilello, M. A. (1973), Prevailing Wind Directions in the Arctic Ocean. U. S. Army Corps of Engineers, CRREL Res. Report No. 306.

Campbell, W. J. (1965), The Wind Driven Circulation of Ice and Water in a Polar Ocean. Jour. Geophy. Res., 70(14): 3279-3301.

Carsola, A. J. (1952), Marine Geology of the Arctic Ocean and Adjacent Seas off Alaska and Northwestern Canada. Unpublished Ph.D dissertation, University of California, Los Angeles, CA.

Carsola, A. J. (1954), Extent of Glaciation on the Continental Shelf in the Beaufort Sea. American Jour. Sci., 252: 366-371.

Carsola, A. J.; Fisher, R. L.; Shipek, C. J.; and Shumay, G. (1961), Bathymetry of the Beaufort Sea. In: Geology of the Arctic, University of Toronto Press, Toronto, Canada, pp. 678-689.

Coachman, L. K. and Barnes, C. A. (1961), The Contribution of Bering Sea Water to the Arctic Ocean. Arctic, 14: 145-161.

Coachman, L. K. (1963), Water Masses of the Arctic. In: Proceedings of the Arctic Basin Symposium, October 1962, Arctic Institute of North America, pp. 143-167.

Coachman, L. K.; Aagaard, K.; and Tripp, R. B. (1975), Bering Strait: The Regional Physical Oceanography. University of Washington Press, Seattle, WA.

Defant, A. (1961), Physical Oceanography. Pergamon Press, London, England, Vol. 1: 134.

Dickey, W. W. (1961), A Study of a Topographic Effect on Wind in the Arctic. Jour. Meteor., 18: 790-803.

Fay, J. A. and Hoult, D. P. (1971), Physical Processes in the Spread of Oil on a Water Surface. U. S. Coast Guard Research and Development Tech. Report No. 714107/A/001.

Fletcher, J. O. (1965), The Heat Budget of the Arctic Basin and Its Relation to Climate. Rand Corp., R-444-PR, pp. 179.

Glaesar, J. L. and Vance, G. D. (1971), A Study of the Behavior of Oil Spills in the Arctic. U. S. Coast Guard Research and Development Tech. Report No. 714108/A/001,002.

Houlf, D. P.; Wolfe, S.; O'Dea, S.; and Patureau, J. P. (1975), Oil in the Arctic. U. S. Coast Guard Research and Development Tech. Report No. CG-D-96-75.

Hufford, G. L. (1973), Warm Water Advection in the Southern Beaufort Sea, August-September 1971. Jour. Geophy. Res., 78: 2702-2707.

Hufford, G. L.; Fortier, S. H.; Wolfe, D. E.; Doster, J. F.; and Noble, D.L. (1974), Physical Oceanography of the Western Beaufort Sea. In: Marine Ecological Survey of the Western Beaufort Sea, U. S. Coast Guard Oceanographic Report No. CG-373-64.

Hufford, G. L. and Bowman, R. D. (1974), Airborne Temperature Survey of Harrison Bay. Arctic, 27: 69-70.

Hufford, G. L. (1974-a), Dissolved Oxygen and Nutrients Along the North Alaskan Shelf. In: The Coast and Shelf of the Beaufort Sea, Arctic Institute of North America, Arlington, VA, pp. 567-588.

Hufford, G. L. (1974-b), On Apparent Upwelling in the Southern Beaufort Sea. Jour. Geophy. Res., 79(9): 1305-1306.

Hufford, G. L. (1975), Some Characteristics of the Beaufort Sea Shelf Current. Jour. Geophy. Res., 80(24): 3465-3468.

Isakson, J. S.; Storie, J. M.; Vagnero, J.; Erickson, G. A.; Kruger, J. F.; and Corlett, R. F. (1975), Comparison of Ecological Impacts of Postulated Oil Spills at Selected Alaskan Locations. U. S. Coast Guard Research and Development Tech. Report.

Johnson, M. W. (1956), The Plankton of the Beaufort and Chukchi Sea Areas of the Arctic and Its Relation to the Hydrography. Arctic Inst. North America Tech. Paper, No. 1, pp. 32.

Kinney, P. J.; Schell, D. M.; Dygas, J.; Nenahlo, R.; and Hall, G. E. (1972), Baseline Study of the Alaskan Arctic Aquatic Environments. University of Alaska, Institute of Marine Science Report No. R72-3, pp. 29-48.

Lewellen, R. I. (1969), Beaufort Sea - Arctic Coast Oceanographic and Climatological Data. Continental Shelf Data Systems, Denver, CO, Vol. 1.

Matthews, J. B. (1970), Tides at Point Barrow. The Northern Engineer, 2(2): 12-13.

Miller, M. C.; Lissauer, I. M.; and Bacon, J. C. (1975), A Computer Simulation Technique for Oil Spills Off the New Jersey-Delaware Coastline. U. S. Coast Guard Research and Development Tech. Report No. CG-D-171-75.

Mountain, D. G. (1974), Preliminary Analysis of Beaufort Shelf Circulation in Summer. In: The Coast and Shelf of the Beaufort Sea, Arctic Institute of North America, Arlington, VA, pp. 27-42.

Paquette, R. G. and Bourke, R. H. (1974), Observations on the Coastal Current of Arctic Alaska. Jour. Mar. Res., 32(2): 195-207.

Reimnitz, E.; Barnes, P. W.; Forgatsch, T. C.; and Rodeick, C. A. (1972), Influence of Grounding Ice on the Arctic Shelf of Alaska. Marine Geology, 13: 323-334.

Searby, H. W. and Hunter, M. (1971), Climate of the North Slope Alaska. NOAA Tech. Memo. NWS AR-4.

Sellmann, P. V.; Carey, K. L.; Keeler, C.; and Hartwell, A. D. (1972), Terrain and Coastal Conditions on the Arctic Alaskan Coastal Plain. U. S. Army Corps of Engineers, CRREL Special Report No. 165.

Sternberg, R. W. (1965), Observations of Boundary Layer Flow in a Tidal Current. Unpublished Ph.D dissertation, University of Washington, Seattle, WA, pp. 71.

U. S. Navy Hydrographic Office (1954), Oceanographic Observations. USS Burton Island, 1950-1953. H. O. Pub. 618-C, pp. 309.

U. S. Navy Hydrographic Office (1958), Oceanographic Atlas of the Polar Seas, 2, Arctic. H. O. Pub. 705, pp. 149.

Walker, H. J. (1974), The Colville River and the Beaufort Sea: Some Interactions. In: The Coast and Shelf of the Beaufort Sea, Arctic Institute of North America, Arlington, VA, pp. 513-539.

Wiseman, W. J.; Suhayda, J. N.; Hsu, S. A.; and Walters, C. D. (1974), Characteristics of Nearshore Oceanographic Environment of Arctic Alaska. In: The Coast and Shelf of the Beaufort Sea, Arctic Institute of North America, Arlington, VA, pp. 49-64.

☆U. S. GOVERNMENT PRINTING OFFICE: 1976--600-492--286